

MASTER THESIS

Thesis submitted in partial fulfillment of the requirements
for the degree of Master of Science in Engineering at the
University of Applied Sciences Technikum Wien
Degree Program: Tissue Engineering and Regenerative
Medicine

Investigation of a newly-identified protein required for mitochondrial protein synthesis

By: Sophie Dürauer, BSc
Student Number: 1810692029

Supervisor 1: Dr. rer. nat. Elisabeth Simböck
Supervisor 2: Evgeni Frenkel, Ph.D.

Cambridge (MA), 30th September 2020



Declaration of Authenticity

“As author and creator of this work to hand, I confirm with my signature knowledge of the relevant copyright regulations governed by higher education acts (see Urheberrechtsgesetz / Austrian copyright law as amended as well as the Statute on Studies Act Provisions / Examination Regulations of the UAS Technikum Wien as amended).

I hereby declare that I completed the present work independently and that any ideas, whether written by others or by myself, have been fully sourced and referenced. I am aware of any consequences I may face on the part of the degree program director if there should be evidence of missing autonomy and independence or evidence of any intent to fraudulently achieve a pass mark for this work (see Statute on Studies Act Provisions / Examination Regulations of the UAS Technikum Wien as amended).

I further declare that up to this date I have not published the work to hand nor have I presented it to another examination board in the same or similar form. I affirm that the version submitted matches the version in the upload tool.”

Cambridge (MA), 30th September 2020

Signature

Abstract

GTPases are important regulators of many cellular processes. Among others, they play an, in some cases, essential role in mitochondrial protein biosynthesis, a process still not completely understood. Especially steps of mitoribosome assembly, translation initiation and ribosome splitting are still subject of intensive research.

In the David M. Sabatini Laboratory, a mitochondrial GTPase, referred to as mitochondrial GTPase X (MGPX), of unknown function was identified. MGPX was proven to be essential for mitochondrial translation.

In the presented project we aimed to investigate MGPX's biochemical activity and related function in mitochondria.

Focusing on three main approaches to answer this question, we analyzed (1) mitoribosome sedimentation profiles using sucrose density gradients, (2) identified potential binding partners of MGPX by immunoprecipitation combined with immunoblotting and mass spectrometry and (3) investigated the influence of MGPX's individual protein domains on its activity.

Sucrose gradients indicated that mitoribosome assembly is defective in cells where MGPX is genetically knocked out, and add-back of MGPX rescued this defect. Immunoprecipitation experiments suggest that MGPX binds the mitoribosome and additional proteins involved in mitochondrial translation, including TRMT61B and DDX28. MGPX with mutations in the GTPase domain did not rescue respiration in cells with native MGPX knocked-out, suggesting that GTP hydrolysis is essential for the function of MGPX in mitochondrial translation.

Our preliminary findings suggest MGPX is essential for mitoribosomal assembly but its precise role remains to be elucidated. In contrast, MGPX orthologs are known to be dispensable for translation in bacteria and absent entirely in fungi. This evolutionary divergence suggests that better understanding of MGPX could aid development of antibiotics, many of which target bacterial translation but have toxicity stemming from inhibition of mitochondrial translation as well.

Keywords: Mitochondrial translation, GTPase, Mitoribosomes, Sedimentation profile, Immunoprecipitation

Kurzfassung

GTPasen sind wichtige Regulatoren vieler zellulärer Prozesse, unter anderem mitochondrialer Proteinbiosynthese, ein Prozess, der noch nicht vollständig beschrieben ist. Insbesondere die Formierung und Spaltung des Mitoribosoms und die Initiation der Translation sind noch nicht ganz verstanden.

Eine bisher nicht beschriebene mitochondriale GTPase, hier genannt mitochondriale GTPase X (MGPX), wurde im Labor von Dr. David M. Sabatini identifiziert. MGPX erwies sich als essentiell für Proteinbiosynthese in Mitochondrien.

Die präsentierte Arbeit beschäftigte sich mit der Frage, welche Rolle MGPX in Mitochondrien spielt und welche biochemischen Eigenschaften darin involviert sind.

In drei verschiedenen Ansätzen wurde versucht diese Frage zu beantworten: (1) Evaluierung des mitoribosomalen Sedimentationsprofils mit Hilfe von Dichtegradientenzentrifugation, (2) Identifizierung von potenziellen Bindungspartnern von MGPX durch Kombination von Immunopräzipitation gefolgt von Immunoblotting und Massenspektrometrie und (3) Untersuchung der individuellen Proteindomänen von MGPX und deren Einfluss auf seine Aktivität.

Mitoribosomale Sedimentationsprofile zeigten, dass Mitoribosomformierung stark von der Verfügbarkeit von MGPX in Zellen abhängt. Immunpräzipitationsexperimente zeigten Bindungen zwischen MGPX und Proteinen, welche mit dem Mitoribosom assoziiert und in mitochondriale Translation involviert sind, einschließlich TRMT61B und DDX28. Untersuchte Mutationen in der GTPase-Domäne von MGPX verloren die Fähigkeit Zellatmung in nativen MGPX knock-out Zellen wiederherzustellen, was darauf hindeutet, dass die GTP-Hydrolyse für die Funktion von MGPX in der Proteinbiosynthese von Mitochondrien essentiell ist.

Die präsentierten Ergebnisse legen nahe, dass MGPX für die Formierung des Mitoribosoms essentiell ist. Das Ortholog von MGPX in Bakterien ist, im Gegensatz dazu nicht essentiell, darüber hinaus wird in Fungi kein Ortholog exprimiert. Dieser evolutionäre Unterschied deutet darauf hin, dass ein verbessertes Verständnis von MGPX und seiner Aktivität in Mitochondrien sich auch in der Entwicklung von Antibiotika als nützlich erweisen könnte. Viele geläufige Antibiotika zielen auf bakterielle Translation ab, weisen jedoch Toxizität durch gleichzeitige Hemmung mitochondrialer Translation in humanen Zellen auf.

Keywords: Mitochondriale Translation, GTPasen, Mitoribosom, Sedimentationsprofile, Immunopräzipitation

Acknowledgements

First of all, I would like to thank my external supervisor Dr. Evgeni Frenkel at the Sabatini lab at the Whitehead Institute for Biomedical Research (Massachusetts Institute of Technology, Cambridge, MA). He guided me through the whole process of my thesis project: from planning experiments over performing them to interpreting the final results. I was able to learn many new techniques and gained a lot of practical experience in the lab. He always took the time to answer my questions and was focused on my complete understanding of used methods, performed experiments and obtained data.

I also want to thank Dr. David M. Sabatini for giving me the opportunity to come to the United States (US) and do an internship in his lab. It was an exceptional experience to work in a research group like this. The whole lab was very well organized enabling all the passionate scientists working there, to completely focus on performing biomedical research at the highest standards. At this point I want to thank all the members of the Sabatini lab for warmly welcoming me to the lab and helping me out whenever I needed a helping hand or professional advice. Within this group I want to highlight all the other Master's and Undergraduate students in the lab, who became my closest friends in the US and kept me sane, even in times of social distancing and quarantine due to COVID-19.

In addition to the Sabatini lab, I want to thank Dr. L. Stirling Churchman and her lab at Harvard Medical School, especially Dr. Iliana Soto, for their support and guidance concerning sucrose density gradients for mitoribosome sedimentation profiles. We would not have been able to get the results presented here without their help in optimizing our protocol. I hope the collaboration between the two labs will remain.

Furthermore, I would like to acknowledge my internal supervisor at the University of Applied Sciences Technikum Wien, Dr. Elisabeth Simböck, who has helped me even before the start of my internship. I am grateful for her guidance and her valuable comments on my work.

I would also like to thank the Austrian Marshall Plan Foundation for their financial support for my stay in the US.

Finally, I must express my very profound gratitude to my family and friends in Austria for providing me with unfailing support and continuous encouragement throughout the years of my studies and through the process of researching and writing this thesis. This accomplishment would not have been possible without them. Thank you!

Disclaimer

This master thesis documents several important results of an ongoing project, which revealed novel protein functions in mitochondrial protein biosynthesis. Therefore, the Whitehead Institute for Biomedical Research classified this thesis in part. Some protein names are pseudonymized.

Table of Contents

1	Introduction	9
1.1	Mitochondria.....	9
1.1.1	Mitoribosomes	10
	Subunit assembly	13
1.1.2	Mitochondrial protein biosynthesis	19
	Initiation.....	20
	Elongation	23
	Termination.....	25
	Recycling.....	27
	Rescue of stalled ribosomes.....	29
1.2	GTPases	31
1.2.1	BGPX.....	32
1.3	Aim.....	34
2	Materials and Methods	35
2.1	Cell culture	35
2.2	Cloning plasmids	35
2.2.1	Fragment generation PCR	36
2.2.2	Backbone generation	38
2.2.3	Gibson assembly	38
2.2.4	Bacterial transformation	39
2.2.5	Virus production	40
2.2.6	Viral Spinfection	41
2.3	Transfection.....	42
2.4	Western blot	42
2.5	Immunofluorescence staining	44
2.6	Seahorse assay.....	45
2.7	Mitochondria Isolation.....	46
2.8	Sucrose gradient analysis of mitochondrial ribosomes	47
2.9	Immunoprecipitation	48
2.10	Statistical evaluation and Data processing	49

3	Results	50
3.1	Knock-out of MGPX effects mitoribosome assembly	50
3.2	MGPX binds MRPs when mitoribosomes are disassembled.....	54
3.3	TRMT61B is a potential binding partner of MGPX	57
3.4	MGPX is essential for mitochondrial translation and mutations in its G-domain affect its ability to restore cellular respiration	60
4	Discussion	68

1 Introduction

Genetic screens and bioinformatic analyses performed in the David M. Sabatini Laboratory identified a new GTPase, evidently important in mitochondrial function. Recent unpublished work by the supervisor has revealed this GTPase, here referred to as mitochondrial GTPase X (MGPX), to be essential for mitochondrial protein biosynthesis. To determine where in the process its function is required, established knowledge of mitochondrial protein biosynthesis from literature, including participating proteins is reviewed here. In addition, general features of GTPases and described functions of the bacterial homolog, referred to as bacterial GTPase X (BGPX) are given.

1.1 Mitochondria

Mitochondria are essential organelles in eukaryotic cells. One of their characteristics is a double membrane with distinct functionality. The outer membrane separates mitochondria from the surrounding cytoplasm. At the inner membrane electron transfer takes place. The electron transfer chain is part of oxidative phosphorylation (OXPHOS), also known as cellular respiration. Through this process mitochondria fulfill their main purpose, the generation of adenosine triphosphate (ATP). ATP is the major source of energy inside the cell and comes predominantly from mitochondria and OXPHOS. Mitochondria are therefore the powerhouse of the cell and essential for several cellular processes, by providing required energy [1].

Inside mitochondria a fully functional gene expression system, including a separate genome and protein synthesis system, is found. This feature is unique among eukaryotic cell organelles and is the result of mitochondria's origin of eubacterial endosymbiosis [2]. The mitochondrial DNA (mtDNA) almost completely consists of coding DNA, encodes 13 proteins, which are all hydrophobic membrane subunits of the OXPHOS [3]. For successful mitochondrial protein synthesis, ribosomal RNA (rRNA), transfer RNA (tRNA) and several other factors are needed. Some proteins, mitochondrial rRNA (mt-rRNA) and mitochondrial tRNA (mt-tRNA), are encoded in the mitochondrial genome, but the remaining required factors, including all proteins of the mitochondrial ribosomes (mitoribosomes), are nuclear encoded proteins and therefore have to be imported from the cytosol [1].

Since the original mitochondrial endosymbiosis event, the host-endosymbiont relationship has changed significantly, leading to remodeled and varying mitochondrial genomes within the eukaryotic lineage. The size/content of mtDNA within mammals is fairly similar and around 20 kb, encoding approximately 13 proteins. In contrast to that, fungi show higher variations in size and coding capacity [1]. In any case, the coding capacity is always under 3,600 genes. 3,600 marks the number of genes necessary for an α -proteobacterium to survive independently, making survival of mitochondria without/outside the eukaryotic cell impossible [4].

1.1.1 Mitoribosomes

In general, ribosomes consist of two different subunits, which when combined, build a large ribonucleoprotein. Their main function is protein translation. mRNA binds to the small ribosomal subunit (SSU), which then selects the corresponding aminoacyl-tRNAs, by translating the genetic sequence of the mRNA. In the peptidyl transferase center (PTC) of the large ribosomal subunit (LSU), peptide bonds between the amino acids are formed. By lining up amino acids in this way, a new polypeptide is formed.

In the assembled monosome the two subunits form three binding sites for tRNAs (A-, P- and E-site), with designated roles in the translation cycle. The aminoacyl-tRNA first interacts with the SSU at the aminoacyl site (A-site). After formation of the peptide bond and a conformational change of the ribosome the tRNA connected to the nascent polypeptide is located at the peptidyl site (P-site). Through this structural change the now deacylated tRNA is shifted to the exit site (E-site) where it leaves the ribosome. The nascent polypeptide exits the ribosome through a tunnel in the LSU after completed translation [5]. At the exit of this tunnel several protein factors are located, which interact with the polypeptide in post-translational processes, like enzymatic processing, targeting and membrane insertion [6], [7].

Together with the mitochondrial genome and the OXPHOS complexes, mitoribosomes have evolved over time, which results in significant differences between human and yeast mitoribosomes and the ancestor bacterial ribosome [8]. The most obvious differences are their variation in size, sedimentation coefficients, protein and RNA proportion as well as the lack of 5S rRNA in mitoribosomes, which is conserved in bacteria and differently replaced in mammalian and fungal mitoribosomes. Table 1 summarizes the molecules, rRNAs and ribosomal proteins (r-proteins)/mitoribosomal proteins (MRPs), forming the different ribosomes and Figure 1 provides a visual comparison of mammalian and yeast mitochondrial ribosomes and the bacterial ribosome. Comparisons made here mainly focus on humans (mammals), *Saccharomyces cerevisiae* (*S. cerevisiae*) (fungi/yeast) and *Escherichia coli* (*E. coli*) (bacteria).

Box 1: Sedimentation coefficient

The sedimentation coefficient (s) is used to describe how fast or how far different particles travel through a fluid during centrifugation. It is defined as: $s = \frac{v_t}{a}$, where v_t = velocity of the particle and a = centrifugal acceleration = $r\omega^2$, where r and ω are the radius and speed of centrifugation. v_t is determined by the balance of centrifugal force $mr\omega^2$, where m = particle mass, and viscous drag, which for a sphere is equal to $v_t \times 6\pi\eta r_0$ (Stokes' Law) in which η = fluid viscosity and r_0 = radius of the sphere. Because mass is proportional to volume ($\frac{4\pi \times r_0^3}{3}$) and density ρ , the sedimentation coefficient can then be written as:

$$S = \frac{\rho \times r_0^2}{\eta} \times \frac{2}{9} \sim \frac{(density) \times (radius)^2}{viscosity}$$

This formula shows that the larger or denser the particle, the faster it will sediment, and the more viscous the fluid, the slower it will sediment. Moreover, it explains why sedimentation coefficients of particles bound together are not the sum of the sedimentation coefficients of the individual particles, as in the case of ribosomal subunits and monosomes. Sedimentation coefficients usually assume η to be the viscosity of pure water and are given in units of time expressed in Svedbergs. One Svedberg is 10^{-13} seconds.

Table 1. Composition of mammalian, bacterial and yeast ribosomes.

Mammalian cytosolic ribosome [9]			
Ribosome	Subunit	rRNAs	r-proteins
80S	60S	28S	49
		5.8S	
		5S	
40S	18S	33	
Mammalian mitochondrial ribosome [10], [11]			
Ribosome	Subunit	mt-rRNAs	MRPs
55S	39S	16S	53
	28S	12S	30
Yeast mitochondrial ribosome (<i>S. cerevisiae</i>) [12]			
Ribosome	Subunit	mt-rRNAs	MRPs
74S	54S	21S	46
	37S	15S	34
Bacterial ribosome (<i>E. coli</i>) [9]			
Ribosome	Subunit	rRNAs	r-proteins
70S	50S	23S	33
		5S	
	30S	16S	21

As mentioned, an important difference between cytosolic and mitochondrial ribosomes is the loss of 5S rRNA in the LSU. 5S rRNA might be the smallest component of bacterial, archaeal and eukaryotic cytosolic ribosomes but still plays a crucial role in ribosomal function. The

protuberance center of the LSU establishes around the 5S rRNA and partially coordinates the movements of the SSU occurring during translation [13]. The tRNA-Val partially replaces 5S rRNA in human mitoribosomes (Figure 1) [1], [14]. The tRNA interacts with the MRP uL18m in a similar way as 5S rRNA does in bacteria during formation of the central protuberance (CP) in the LSU [7]. However, this replacement of mt-tRNA varies between mammalian organisms. The porcine mitochondrial ribosome uses tRNA-Phe instead. This replacement is an example for the reduction in size of mammalian mitoribosomes compared to mitoribosomes in yeast, which compensates the loss of 5S rRNA by expanding already expressed rRNA (Figure 1) [15].

Not far from the tRNA-Val, the guanosine triphosphate (GTP)-binding protein mS29 is found in the 28S subunit of mitoribosomes (Figure 1). This protein is a unique feature of mitochondrial ribosomes, providing them with intrinsic GTPase activity. The mitoribosomes most likely use this activity during ribosome assembly, indicated by the location of mS29 and the fact that mS29 is bound to guanosine diphosphate (GDP) in the assembled monosome. mS29 establishes close to the interface of the two subunits and participates in the coordination of mitochondria-specific intersubunit-bridges [16], [17].

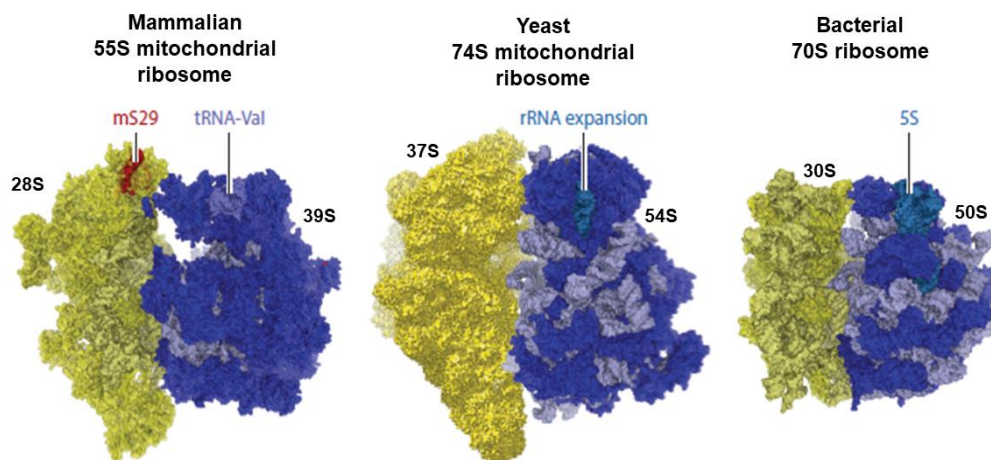


Figure 1. Structural comparison of mammalian and yeast mitochondrial ribosomes and bacterial ribosomes. Mammalian mitochondrial ribosomes are composed of a 28S and a 39S subunit. The missing 5S rRNA is mainly replaced by the mt-tRNA-Val. Moreover, at the interface of the two subunits an intrinsic GTPase (mS29) is found. The yeast 74S mitoribosome consists of a 37S and a 54S subunit and the 5S rRNA seems to be replaced by rRNA expansion. mS29 is also found in yeast (not shown here). In contrast to mitochondrial ribosomes, the bacterial ribosome forms from a 30S and a 50S subunit, including 5S rRNA. In the figure the large subunit (LSU) is shown in blue and the small subunit (SSU) in yellow. The corresponding sedimentation coefficients are noted next to the subunits (modified after Ott *et al.* 2016 [1]).

Interactions between ribosomes and mRNA as well as tRNA are essential during protein synthesis. The main proteins responsible for these interactions in the cytosol, including bL25 and rRNA helix H38 at the A-site (A-site finger) and uL5 and H84 at the P-site, are missing

in mammalian mitochondrial ribosomes [14]. Different mechanisms for the interaction with the conserved parts of tRNA, the CCA-3'-ends and the anticodon containing stem-loop have therefore evolved in mammalian mitoribosomes. The unique P-finger element, including the MRPs mL40, mL48 and mL64, replaces aforementioned missing elements of the A-site finger and uL5 in tRNA-ribosome interactions [15], [18]. This is only one example of multiple structural modifications of mitoribosomes, corresponding to the structure of their mRNAs.

Focusing on mammalian and yeast mitochondrial ribosomes, the large mitoribosomal subunit (mtLSU) shows several differences. Yeast do not use tRNA to compensate the lack of 5S rRNA but show segments of rRNA expansion in the corresponding area (Figure 1). Many of such rRNA expansion segments are found throughout the yeast mitoribosomes. Mammalian mitoribosomes in contrast have reduced amounts of rRNA in the 39S subunit [19]. There is a high chance that a common early mitoribosomal ancestor had an rRNA molecule involved in the formation of the CP in the mtLSU. During evolution, this molecule was lost and partially replaced by rRNA expansion segments [7]. Furthermore, differences in the structure and path of the polypeptide exit tunnel have been described [20].

Mitochondria's origin of endosymbiosis and its evolutionary process led to mammalian mitoribosomes with a set of organelle specific proteins, which still show segments with expanded rRNAs and adapted an exit-tunnel path similar to bacteria. The yeast mitoribosomes contrary maintained a way higher number of rRNA expansion segments and modified the polypeptide tunnel over time [7]. These modifications in RNA and protein content resulted in varying RNA:Protein ratios. Bacterial ribosomes have a ratio of 2:1, whereas rRNA extension and appended mitochondria specific proteins in yeast led to a ratio of 1:1. Mammalian mitochondria even present a 1:2 ratio, due to their reduction in rRNA and further addition of proteins [21]. However, those proteins only replace ~28% of missing rRNAs, compared to the bacterial counterpart. This makes mitoribosomes more porous and explains their sedimentation at lower densities (Box 1) [22].

Subunit assembly

The assembly process of the ribosomal subunits is regulated by several factors, including rRNA modifying enzymes, chaperones, RNA helicases and GTPases. Best studied is the process in bacteria, which is often used as a reference for mitochondria and helped identifying assembly factors with the organelle. Nevertheless, the whole assembly pathway of mitoribosomal subunits in fungi and mammals is still not completely understood. Figure 2 and Figure 3 try to draw alignments for the pathways in mammals and yeast. Bacterial subunit assembly is shown as a reference. Positions for factor interactions are estimated. The assembly takes place at the inner mitochondrial membrane facing towards the matrix. This location is favorable because it enables co-translational insertion of nascently generated proteins and reduces the occurrence of unfunctional protein aggregates related to transportation [23], [24].

Large subunit assembly (Figure 2)

The mtLSU of mammals consists of 16S mt-rRNA and mitoribosomal large-subunit proteins (MRPLs). Its assembly process requires several different types of chemical reactions.

Nucleotide modifications: Some nucleotides within this mt-rRNA undergo modifications during the maturation process. So far five modifications are known. Those modifications are catalyzed by Mrm1/2/3, TRMT61B and RPUSD4. Mrm1 and Mrm2 catalyze the formation of 2'-O-ribose methylations at conserved locations, which is why homologs of both proteins are found in yeast (Mrm1 and Mrm2) [12] as well as in bacteria (RlmB and RrmJ) [25].

The methyltransferase Mrm3 catalyzes the formation of 2'-O-ribose methylation at position 1370 (Gm1370), located in the A-loop. The A-loop directly interacts with aminoacyl mt-tRNA (aa-mt-tRNA) at the A-site during translation and therefore represents an essential component of the PTC. Since the rRNA modification at this site (Gm1370) is exclusive for mammalian mitoribosomes, no homologous proteins are found in yeast mitochondria or bacteria [21].

The enzymes RlmC and RlmD, both methyltransferases, are responsible for two methylations of the 23S rRNA in bacteria [26]. A 1-methyladenosine modification at position 947 is catalyzed by TRMT61B [27], which can be related to the activity of RlmN in bacteria [28]. A single pseudouridylation was found in mitochondrial ribosomes. Its formation is catalyzed in mammalian mitoribosomes by RPUSD4 and by Pus5 in yeast. Bacterial 23S rRNA shows multiple sites with this modification, formed among others by RluC and RluD [29].

Two other proteins that can be included in the group of RNA modifying enzymes are the ATP-dependent protease AFG3L2 (yeast homolog = YTA10) and the ATP-dependent zinc metalloprotease SPG7 (yeast homolog = YTA12). Acting together in a complex these proteins catalyze cleavage of bL32m before its incorporation into the mtLSU [30].

Chaperones and maturation factors: Another group of ribosome assembly factor comprises chaperones and maturation factors. In mammals FASTKD2, mTERF3 and MALSU1 have been described as members of this group. The precise role of FASTKD2 and mTERF3 is not understood yet [21]. MALSU1 interacts with uL14m and promotes its incorporation into the mitoribosome. This interaction is conserved and also observed in the bacterial homolog, the ribosome silencing factor RsfS. Binding of RsfS to uL14 prevents the formation of an essential intersubunit bridge, which in turn prevents association of the two subunits. A recent study by Brown *et al.* describes a similar activity for the human homolog MALSU1 in a complex with mt-ACP and LOR8F8 (MIEF1 upstream open reading frame protein). Release of the complex later in the translation cycle enables mitoribosome assembly (Figure 4) [11]. Atp25 presents the homolog in yeast. Observations of the conserved parts point towards it having a similar activity in late assembly stages of the mtLSU as an anti-association factor by binding uL14m. Moreover, Atp25 is required for successful incorporation of bL9m [31].

MPV17L2 is another interaction partner of MALSU1, which was proven to be essential for mitochondrial protein biosynthesis [32].

RNA helicases: In bacteria, RNA helicases of the DEAD box helicase protein family play an important role during ribosome assembly ensuring correct rRNA folding. Their activity as ATPases is dependent on their interaction with RNA. The bacterial factors of this group RhlE, SrmB, CsdA and DbpA act at different stages of LSU formation and interact with each other by regulating their activity levels [12], [25]. No direct homologs of these proteins were found in human or yeast mitochondria [21]. However, the mammalian helicase DDX28 and the fungal Mrh4 and Mss116 show similar ribosome interactions to some of the bacterial DEAD box proteins and therefore might act in a similar way [12], [33]. In any case, those proteins are essential for mtLSU assembly [21], [34].

GTPases: The last big group of ribosome assembly factors is GTPases. Most of them are well conserved throughout the three organisms compared here. The interaction of those proteins with the ribosomes is GTP dependent. Generally, GTPases bind in a GTP-bound state, ribosomal particles stimulate their GTPase activity leading to hydrolysis of the nucleotide and subsequently to the release of the assembly factor, which enables subunit assembly and monosome formation (Figure 4) [21]. Human GTPBP7 and its homolog in yeast Mtg1 show several similarities that are characteristic for GTPases involved in mitoribosome assembly and act at a late assembly stage [35]. The bacterial homolog RbgA is not universally expressed. For example *E. coli* lacks this factor [21], [36], [37].

Mtg2 belongs to the Obg protein family. The *E. coli* homolog ObgE interacts with both ribosomal subunits when they are separated while preferring the LSU and especially the r-protein uL13. ObgE dissociates from the complete 70S ribosome after GTP hydrolysis (Figure 4) [38]. In mammals, two homologs of ObgE are expressed: ObgH1 (GTPBP5) and ObgH2 (GTPBP10). Both proteins interact with the mtLSU in an GTP-dependent manner and were proven to be essential for mitochondrial protein biosynthesis [35]. Similar to Mtg1, the GTPase activity of GTPBP10 is stimulated by the mtLSU [39]. In contrast, only an intrinsic GTPase activity was described for GTPBP5 [35]. Recently another human GTPase (GTPBP8) was proposed to act during mtLSU assembly similar to its essential homolog in *Bacillus subtilis* (*B. subtilis*), YihA [38], [40].

The bacterial specific GTPase Der differs from other involved GTPases, due to its two homologous GTPase domains (GD1 and GD2) which are both involved in ribosome assembly. GTP-binding to the GD2 domain is the key requirement for any ribosome interaction, whereas GTP-binding to the GD1 domain stabilizes the interaction with the LSU. Through GTP hydrolysis of the GD1 domain, the factor regulates its interaction with the two subunits as well as the assembled 70S ribosome. GTP hydrolysis is required for monosome formation, since the GD1 domain in its GTP-bound state masks the 30S binding site at the LSU. GTP hydrolysis at the GD2 domain releases the factor from the monosome (Figure 4)

[41]. YihI, acts as a GTPase activating protein for Der, recognizing bound GTP at both domains [25], [38].

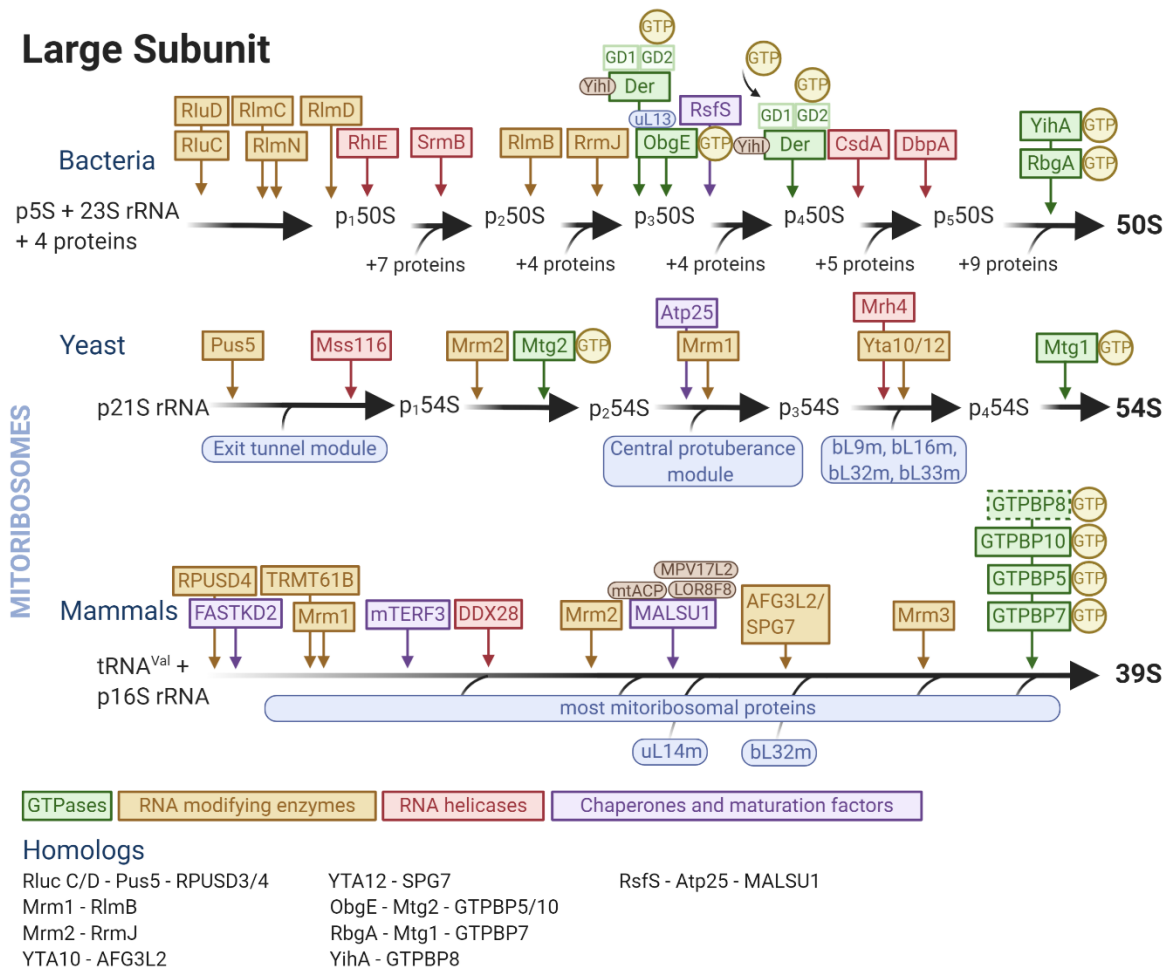


Figure 2. Ribosome assembly line – Large subunit (LSU). Assembly pathways for the LSU of mammalian and yeast mitoribosomes and bacterial ribosomes. The bacterial pathway is shown as a reference. The figure shows GTPases, RNA modifying enzymes, RNA helicases, chaperones and maturation factors involved (distinguished by colors). Interaction positions of the assembly factors are estimated. Homologs within the three organisms are listed at the bottom. Participation of GTPBP8 is only proposed at the moment, indicated by a dashed frame. (modified after De Silva *et al.* 2015 [21], Zeng *et al.* 2018 [12] and Shajani *et al.* 2011 [25] and created with BioRender.com).

Compared to LSU assembly in bacteria the process in mammalian mitochondria is still not completely understood, leaving the possibility of additional proteins being involved in it. 16S mt-rRNA could potentially be modified at more locations. Moreover, some participating factors in the bacterial system miss identified homologs in mammalian mitochondria.

Small subunit assembly (Figure 3)

Assembly of the SSU requires as well several chemical reactions to happen as well as the presence of multiple participating factors.

Nucleotide modifications: Similar to the 16S rRNA of the mtLSU, the 12S rRNA of the mtSSU is known to be modified at five locations. Responsible for these modifications are TFB1M, TRMT2B, NSUN4 and METTL15 [42]–[44].

TFB1M demethylates two adenines (A937 and A938) located within a stem loop structure of the 12S rRNA, close to its 3'-end [45]. The bacterial homolog is KsgA. These modifications are seen in almost all forms of ribosomes, suggesting the presence of a homologous protein in yeast mitochondria as well. However, activity of the identified fungal homolog (Dim1) as well as its presence in mitochondria have not been confirmed yet [25].

Another conserved modification between bacteria and mammalian mitochondria is the m⁴C methylation at position C839 of the mammalian 12S rRNA and C1402 of the bacterial 16S rRNA, generated by METTL15 and RsmH, respectively. In bacteria this modification interacts with the P-site codon and thereby plays a role in decoding, which might as well be the case in mitochondria [43], [46].

The methylation of 12S rRNA at m⁵U429 is catalyzed by TRMT2B, which is also responsible for modifications of mt-tRNAs [44]. NSUN4 and the bacterial homolog YebU are responsible for the last modification [21]. Another modifying enzyme expressed in bacteria and mammals is YbeY, which interacts with Era/ERAL1 through the conserved r-protein uS11. In bacteria, the protein is also responsible for the maturation of both ends of the 16S rRNA and is involved in LSU assembly during end maturation of the rRNAs expressed in the subunit (23S rRNA and 5S rRNA) [47]. RsmC, of which no homolog is found in mitochondria, performs also a methylation of the 16S rRNA [48]. Another RNA modifying protein with known function is Rsm22 in yeast mitochondria, catalyzing methylation of the 3'-end of the 15S rRNA. METTL17 in mammalian mitoribosomes might catalyze a similar process [49].

Chaperones and maturation factors: Multiple chaperones and maturation factors (RimJ, RimM, RbfA, RimP, DnaK-DnaJ-GrpE) are required for correct assembly of the SSU in bacteria. For most of them, no direct homologs have been described in mitochondria yet [25]. However, there is a mammalian homolog of RbfA, which interacts with the 12S rRNA in close proximity to ERAL1 and prevents translation initiation by overlapping with mt-tRNA binding sites (A- and P-sites) [50].

GRSF1 is found in mitochondrial RNA (mtRNA) granules, co-sediments with the mtSSU, and was proven to be essential for its assembly. However, its precise role in the pathway is still unknown [21].

RNA helicases: A single RNA helicase associated with the mtSSU, identified by co-immunoprecipitation with MRPS18B, has been described so far: the DEAD box protein DHX30. Since the protein co-sedimented with all three subpopulations of the mitoribosome, it might remain bound throughout all assembly stages, but further investigations are needed to clarify its activity [21], [33].

GTPases: The interaction of GTPases in SSU assembly is GTP-dependent, similar to interactions with the LSU. GTP hydrolysis mainly acts as the factor release mechanism. C4orf14 interacts with bL12m [51], whereas the fungal homolog Mtg3 was described to interact with uL4m. The bacterial homolog of Mtg3 represents YqeH [21]. However, this protein is not found in *E. coli*, but the GTPase RsgA, acts at a similar step in the assembly pathway of the SSU and also belongs to the YiqF/YawG family [52]. RsgA dissociates the two ribosomal subunits, but bound to GTP the protein has low affinity for the SSU and GTP hydrolysis releases the factor, enabling assembly of the 70S ribosome [53]. RbfA binds the SSU together with RsgA, which releases it in a GTP dependent manner in a later assembly step (Figure 4) [54].

Finally, ERAL1 the mammalian homolog of the Era-protein in *E. coli* is involved in mtSSU assembly. Era is an important regulator in bacterial ribosome processing and maturation, acting through cooperating with the SSU, more precisely the 3'-terminal end of the 16S rRNA [55]. It represents a checkpoint, by bringing the SSU to a conformational state suitable for assembly with the LSU [38]. In humans, ERAL1 also interacts with the 3'-end of the 12S mt-rRNA at the stem-loop region modified by TFB1M [47]. In addition, to its role in ribosome assembly, ERAL1 acts as a mtRNA chaperone. [21], [56].

Small Subunit

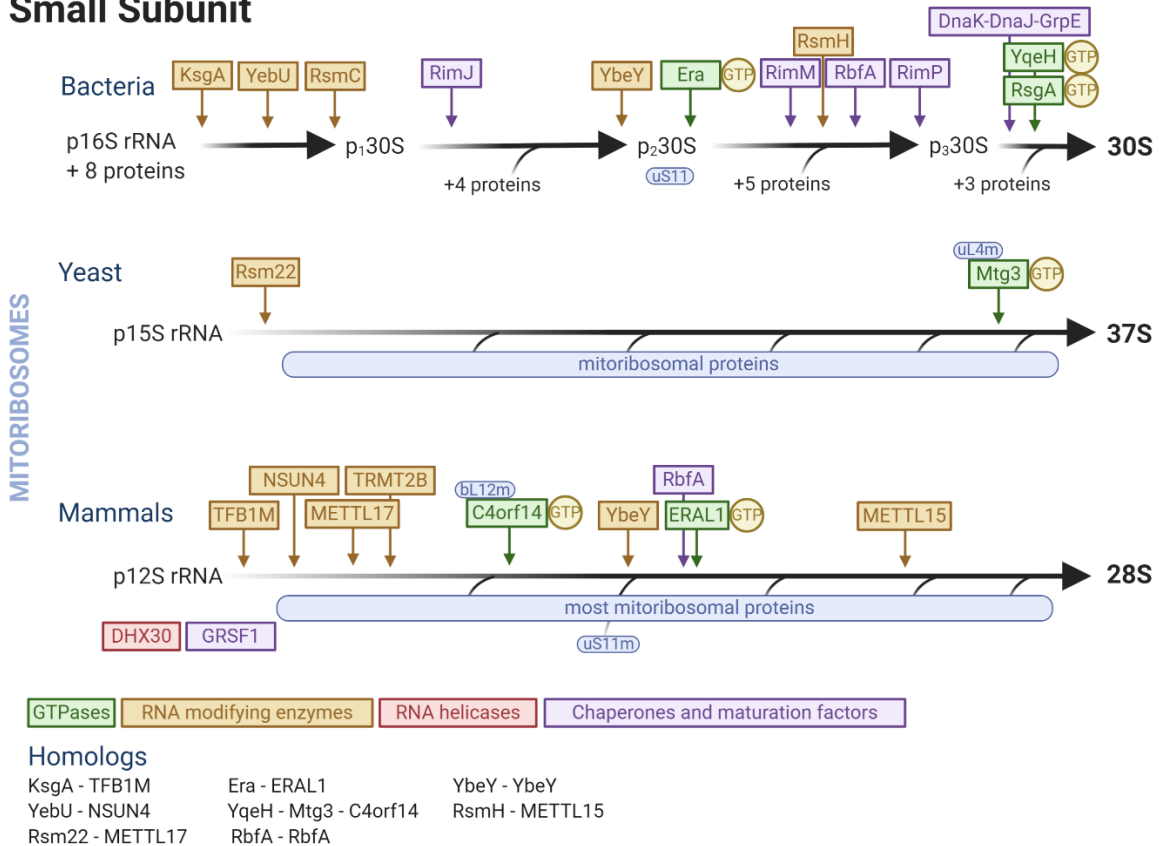


Figure 3. Ribosome assembly line – Small subunit (SSU). Assembly pathways for the SSU of mammalian and yeast mitoribosomes and bacterial ribosomes. The bacterial pathway is shown as a reference. The figure shows GTPases, RNA modifying enzymes, RNA helicases, chaperones and maturation factors involved (distinguished by colors). Interaction positions of the assembly factors are estimated. Homologs within the three organisms are listed at the bottom. (modified after De Silva *et al.* 2015 [21] and Shajani *et al.* 2011 [25] and created with BioRender.com).

As for the mtLSU, there is potential for additional proteins to be involved in the process. Especially chaperones and maturation factors involved in SSU assembly of bacteria represent an interesting group since most of them lack described homologs in mitochondria.

1.1.2 Mitochondrial protein biosynthesis

Similar to the translation cycle in cytosolic ribosomes, mitochondrial protein synthesis can be separated into three universally conserved steps: initiation, elongation and termination followed by recycling of the involved molecules. Factors needed in each of these steps are encoded in the nucleus and corresponding to mitochondria's endosymbiotic origin, many of those factors have homologs in bacteria. However, mitochondria underwent several evolutionary modifications, which resulted in species specific mitochondrial genomes and mitoribosomes. Therefore, variations observed in the translation process were anticipated [1].

Initiation

The first step of initiation marks the key checkpoint and thereby the rate-limiting step within the whole translation cycle. Aforementioned differences in ribosome structures and the whole process of protein biosynthesis play an important role in this first step, making it a rather species-specific process, which is depicted and summed up in Figure 4 to current confirmed knowledge and proposed models.

In-vitro studies and similar ribosomal interactions of the mitochondrial initiation factor 3 (mtIF3) to the bacterial initiation factor (IF) 3 indicate a similar mode of action for the two proteins as well as the related factor in yeast (Aim23). However, due to rather low amino acid sequence similarity, they would not be identified as homologs [57]. Recent studies focusing on the essentiality of mtIF3 propose a different function from the essential IF3 in bacteria. In these studies, the factor was proven to be dispensable for mitochondrial translation in different organisms including yeast and mammalian mitochondria. Nevertheless, the lack of mtIF3/Aim23 affected cell survival and mitochondrial function, due to imbalanced mitochondrial translation. Therefore, mtIF3 might have evolved from its bacterial ancestor and would fulfill a gene specific regulator function in mitochondria [58]–[60]. Further research in this field is needed to clarify the function of mtIF3 and other proteins that might have taken over the function of the bacterial IF3 in mitochondria, which is why the currently valid model, which describes a similar functionality as in bacteria, is described here.

Before interaction with the mt-mRNA the mtSSU is bound to mtIF3, which prevents premature assembly of the mitoribosome. This function is shared with the bacterial IF3 and Aim23 in yeast mitochondria. The first translation factor to actively bind during initiation is IF2 (mtIF2, lfm1). A GTPase that binds the SSU together with GTP. In bacteria, IF2 binding is followed by IF1 binding. Mitochondria lack this factor, but an insertion of 37 conserved amino acids in mtIF2 enables the GTPase to replace IF1 [61], [62]. The length of this insertion region varies within eukaryotic species and the full-length insertion is only found in vertebrates, whereas IF1 is lacking in all mitochondria. This indicates that IF1 might not be essential for mitochondrial translation initiation at all [63]. In contrast to mitochondrial initiation, the assembly pathway in bacteria has no strict order, meaning factors can bind independently. The kinetically preferred order is shown in Figure 4 and described below [62].

The next component to enter the complex is the mRNA, assisted by IF3 (mtIF3, Aim23). Three start codons are described in mammalian mt-mRNA: AUG, AUA and AUU [64]. These initiation base triplets are located at the far 5'-end of mt-mRNA, since mt-mRNA lacks a 5'-cap and 5'-untranslated region (UTR). In bacteria, the Shine-Dalgarno sequence, found in the 5'-UTR of the bacterial mRNA upstream to the start codon (usually AUG), interacts with the corresponding 3'-end rRNA in the SSU [62]. In yeast mitochondria, translation activators compensate for the lack of Shine-Dalgarno sequence by interacting with the 5'-UTR of mt-

mRNA and promoting translation [63], [65]. So far only one translation activator has been described in human mitochondria (TACO1) [30]. In addition to those translation activators, Rdm9 might be involved in mt-mRNA recruitment [63], [66].

Compared to the bacterial SSU and the yeast mt-SSU, which has mainly conserved bacterial structures [65], the mRNA entry channel of the human mtSSU has remodeled significantly. uS4 and uS3, which also present helicase activity in bacteria are missing completely. uS5m may replace uS4 at its location. Moreover, the mitochondrial specific proteins mS39 and mS27 are located at the entry channel, also acting in the recruitment of mt-mRNA [7], [67].

Mitochondria as well as bacteria use N-formylmethionine (fMet) for translation initiation. Bacteria and yeast have a dedicated tRNA-Met for this purpose, whereas mammals formylate a portion of the Met-mt-tRNA-Met used during elongation. In the mitochondrial matrix a formyl group from 10-formyltetrahydrofolate (10-formyl-THF) is transferred to the amino group of the tRNA by the mitochondrial enzyme methionyl-tRNA formyltransferase (mtFMT). The formylation enhances the affinity of mtIF2 for the initiator-mt-tRNA in mitochondria [68]. In yeast mitochondria, FMT1 is not essential. In fact, translation can even be initiated with non-formylated mt-tRNA, through a complex formed by lfm1 and Aep3, which could compensate for the missing IF1 [69]. The mammalian Met-mt-tRNA-Met is modified by NSUN3 and ABH1, before its formylation at the wobble position of the anticodon sequence (m⁵C). This modification enables the recognition of the non-universally conserved start codons AUU and AUA [70]. Entry of the fMet-tRNA-Met is facilitated by IF2 and IF3 and allows its placement at the SSU P-site and binding to the start codon. In bacteria, IF1 further directs the tRNA during this process [62].

In yeast mitochondria, the large MRP bS1m plays an important role through interaction with the 5'UTR of yeast mt-mRNA, a function that is conserved from the bacterial protein [65]. Moreover, mS46 (Rsm28) regulates translation of several mRNAs in yeast mitochondria [63], [67].

After successful binding between the start codon and fMet-tRNA-Met, the mtLSU is recruited which triggers GTP hydrolysis by IF2 (mtIF2, lfm1) and leads to the release of the initiation factors. GTP hydrolysis makes the step irreversible and locks the initiation complex [1], [30], [62].

In addition to the initiation factors, complete assembly of the ribosome triggers dissociation of aforementioned ribosome assembly factors, mainly through GTP hydrolysis [12], [21], [25]. In mammalian mitoribosomes, the mtLSU is bound by mTERF4 and NSUN4 which regulate ribosome assembly by facilitating interaction of the mtLSU with the mtSSU [21], [42].

A second GTPase hydrolysis event might take place before complete assembly, involving mS29 which shows intrinsic GTPase activity [71]. The corresponding MRP in yeast mitoribosomes was described to rather bind ATP than GTP, indicating a species-dependent

activity of the protein [31]. Further research is needed to completely understand the activity of mS29 and its role in mitochondrial translation.

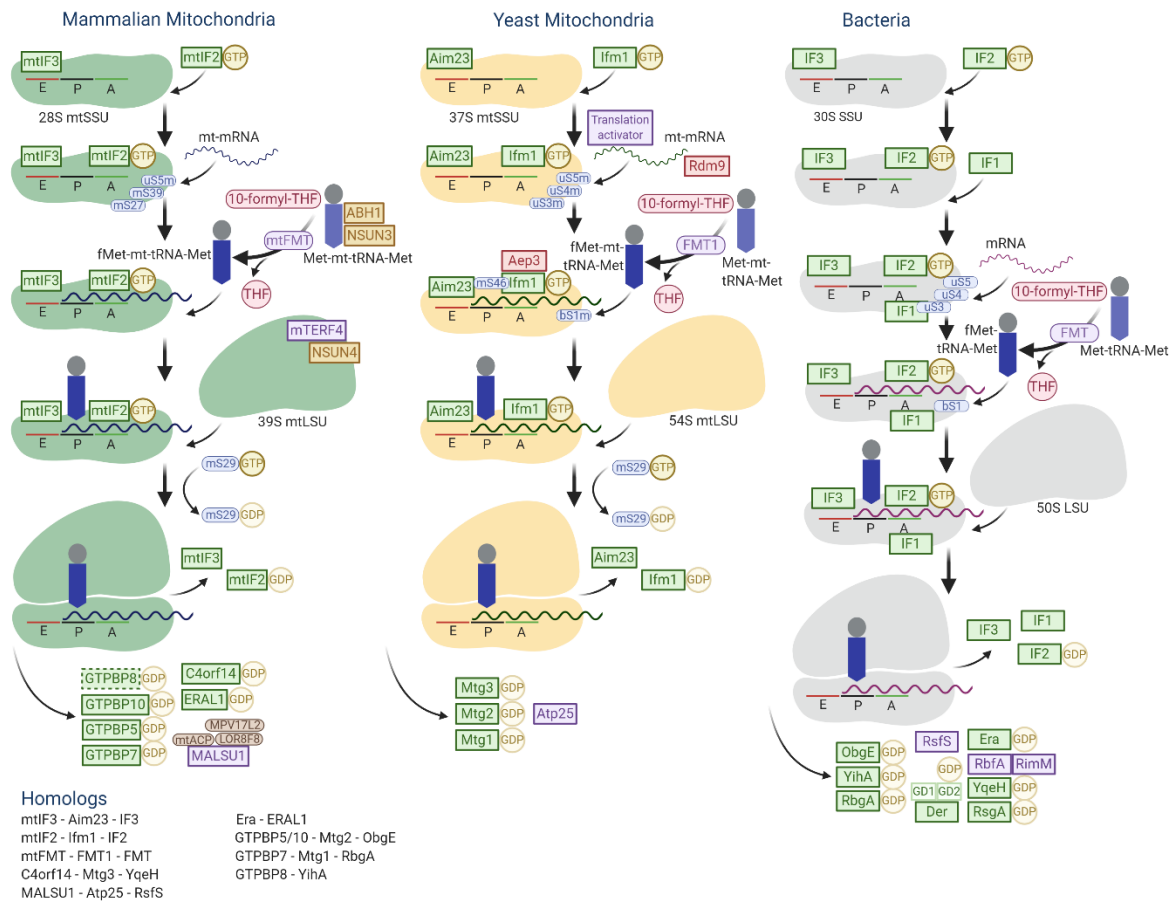


Figure 4. Translation initiation. Initiation represent the first step in the translation cycle. Mitochondria have evolved over time and the process differ from the one happening in bacteria. However, some factors/steps are conserved. Depicted is the process within mammalian and yeast mitochondria compared to bacteria. The SSU, bound with mtIF3/Aim23/IF3, forms an initiation complex with (mt)-mRNA and mtIF2:GTP/Ifm1:GTP/IF2:GTP. In bacteria, IF1 also binds the SSU. Mitochondria lack a homolog for IF1. mtIF2/Ifm1/IF2 recruits fMet-(mt)-tRNA-Met to the start codon in the P-site of the SSU. Once the tRNA is bound to the SSU, the LSU locates towards the SSU to form the final ribosomal monosome. The monosome formation triggers GTP hydrolysis by mtIF2/Ifm1/IF2 and GTPases involved in subunit assembly (shown at the bottom) leading to dissociation of the factors. Factor dissociation enables subunit assembly and monosome formation. In mitochondria an additional GTP hydrolysis might take place during monosome formation, performed by the mitoribosomal protein mS29. Homologs within the three organisms are listed at the bottom. (modified after Ott *et al.* 2016 [1] and Laursen *et al.* 2005 [72] and created with BioRender.com).

Detailed review of translation initiation in mammalian and yeast mitochondria as well as bacteria, determined the step as rather species-specific. Intensive research focusing on the process constantly reveals new features, as it was the case for mtIF3. There might even be additional proteins involved that have not been identified yet.

Elongation

After the initiation complex, including the assembled ribosome has formed, elongation starts. Elongation is the most conserved step in protein biosynthesis. Figure 5 highlights similarities of the step in all three lineages [73], [74].

Elongation follows a circular route, which can be subdivided into three main steps, decoding, peptide bond formation and translocation (Figure 5).

During decoding EF-Tu (mtEF-Tu, Tuf1), GTP and an aa-tRNA form the so-called ternary complex, which interacts with the A-site of the mitoribosome. In bacteria, the main interaction partner of the ternary complex is bL12 which also activates the GTPase activity of EF-Tu [62]. Correct matching of codon and anticodon leads to hydrolysis of GTP and subsequently to the release of GDP-bound EF-Tu (mtEF-Tu, Tuf1) [30], [62].

In mammalian mitoribosomes, the already before mentioned unique P-finger, formed by mL48 and mL40 at the CP of the mtLSU, contacts tRNAs at the A- and P-site, replacing the bL25 and uL5 at the corresponding positions. A long helix of mL64 additionally strikes towards the P-finger and therefore might as well be involved in its activity [7], [20].

Yeast have mainly conserved tRNA-ribosome interactions from bacteria [75]. mL40 and uL5m are part of the CP in the yeast mtLSU [12] and a loop formed by uS12m forms the decoding center of the mtSSU [65].

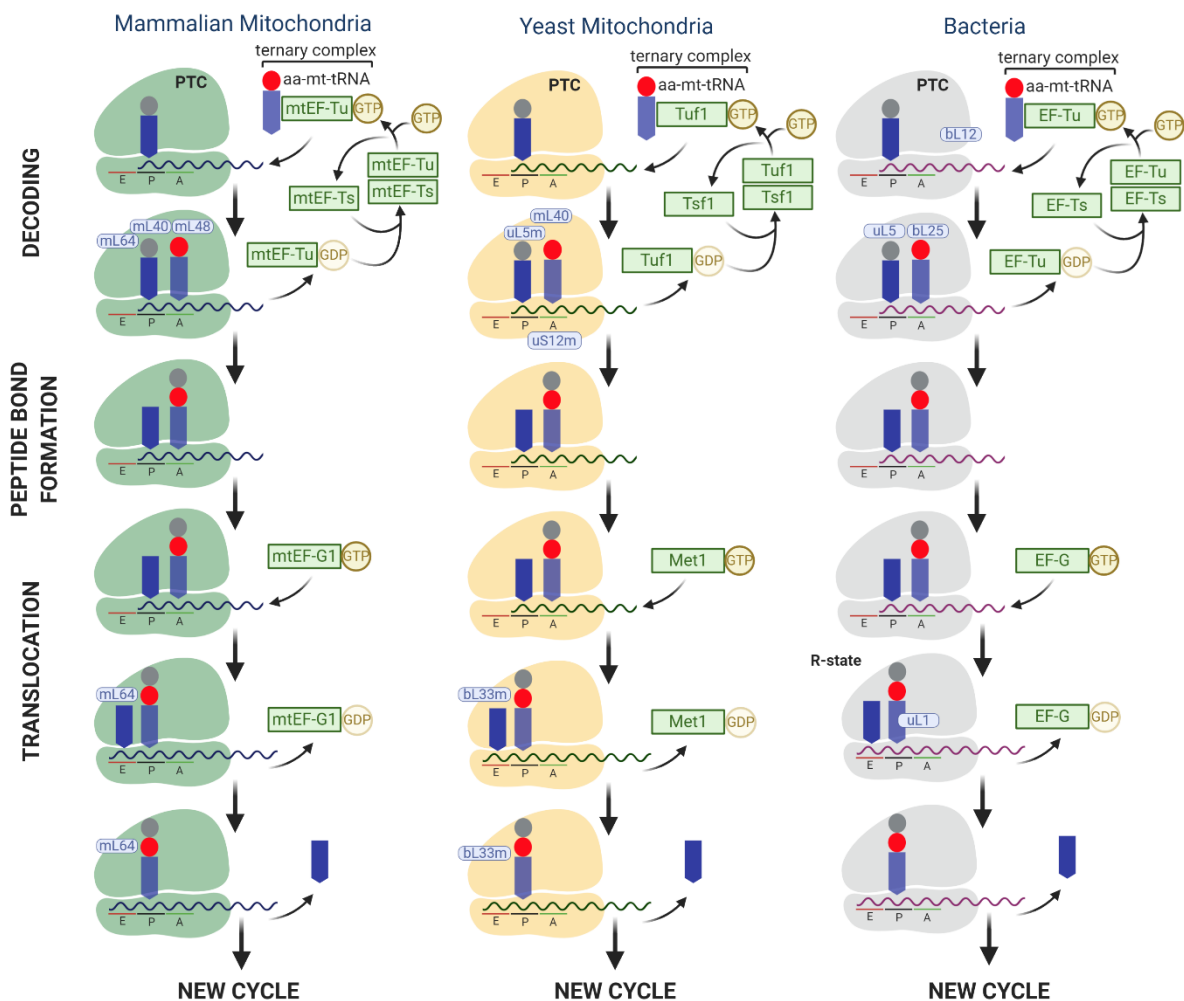
EF-Ts acts as a nucleotide exchange factor by replacing the GDP bound to EF-Tu. Due to its higher affinity for GTP, EF-Tu releases EF-Ts in the presence of GTP. Released EF-Ts and regenerated EF-Tu both re-enter the elongation cycle. In yeast, EF-Ts is not universally conserved. Mitochondria in *S. cerevisiae* lack the protein, whereas *Schizosaccharomyces pombe* (*S. pombe*) expresses Tsf1, which acts similar to the mammalian and bacterial protein [76]. A possible explanation could be the low affinity for guanine nucleotides of mtEF-Tu in *S. cerevisiae* and therefore its ability to self-recycle, as seen for other translation factors like EF-G and IF2 [77], [78].

In the PTC of the LSU peptide bond formation between the new aa-tRNA and the already present polypeptide chain is catalyzed. This step leaves a deacylated tRNA in the P-site and a dipeptidyl-tRNA in the A-site.

The third elongation factor EF-G (mtEF-G1, Met1) initiates the last step of the elongation cycle, translocation. The factor initiates a conformational change of the mitoribosome, represented by a movement of three nucleotides along the mRNA towards the 3'-end [38]. After successful translocation, dipeptidyl-tRNA is located at the P-site and the deacylated tRNA at the E-site. In mammalian mitoribosomes, mL64 interacts with the mt-tRNA located at the E-site [7].

In yeast mitochondria, a similar interaction is performed by bL33m, whereas in bacteria, the conformational change switches the ribosome from a non-rotated to a rotated state (R-state) and leads to closing of the uL1 stalk towards the P-site tRNA [62], [75].

The deacylated tRNA exits the mitoribosome through the E-site and can be recharged. EF-G (mtEF-G1, Met1) promotes the process on cost of GTP hydrolysis and dissociates from the ribosome once translocation is finished, restoring the start conditions of the ribosome. A new aa-tRNA can enter the now vacant A-site of the ribosome, starting the next elongation cycle. Summarizing the energy consumption of elongation, two GTP molecules are hydrolyzed for each amino acid added to the polypeptide chain [1], [30], [62].



Homologs

mtEF-Tu - Tuf1 - EF-Tu
 mtEF-Ts - Tsf1 - EF-Ts
 mtEF-G1 - Met1 - EF-G

Figure 5. Translation elongation. The second step of translation, elongation is the most conserved. Depicted is the elongation cycle divided in three steps of decoding, peptide bond formation and translocation in bacteria and mitochondria. mtEF-Tu/Tuf1/EF-Tu, GTP and an aa-tRNA form the ternary complex, which translates the mRNA sequence. Correct matching of codon and anticodon lead to hydrolysis of GTP and the release of GDP-bound mtEF-Tu/Tuf1/EF-Tu. mtEF-Ts/Tsf1/EF-Ts

regenerates mtEF-Tu/Tuf1/EF-Tu to the GTP-bound state for the next cycle. In the PTC of the mtLSU peptide bond formation is catalyzed, leaving a deacylated tRNA in the P-site and a dipeptidyl-tRNA in the A-site. In the last step a conformational change of the ribosome takes place, promoted by GTP hydrolysis of mtEF-G1/Met1/EF-G. The dipeptidyl-tRNA is now located at the P-site and the deacylated tRNA leaves the ribosome through the E-site. This translocation is related to a conformational change of the ribosome, leading to a rotated state (R-state) in the bacterial ribosome. With the binding of a new ternary complex the cycle restarts. Homologs within the three organisms are listed at the bottom. (modified after Ott *et al.* 2016 [1] and created with BioRender.com).

Elongation is a highly conserved step, appearing to be fully described in all three systems compared here.

Termination

Elongation continues until a stop codon enters the A-site of the ribosome. In contrast to the previous step, termination is less conserved, showing high levels of species specification even within the mammalian system. Figure 6 highlights these differences in mitochondria and bacteria.

Three stop codons are known in mammalian cytosolic translation: UGA, UAA and UAG. The human mitochondrial protein biosynthesis in contrast shows a reduced amount of stop codons, since UGA codes for tryptophan [79]. In human, the sequence-specific mitochondrial release factor 1a (mtRF1a) recognizes termination triplets in the A-site. This interaction with the mt-mRNA initiates a structural change of the RF which in turn facilitates separation of the final amino acid from the mt-tRNA in the PTC of the mtLSU. GTP provides the required energy for this step (Figure 6) [80]. The factor bound to GDP as well as the nascent polypeptide dissociate from the mitoribosome, leaving behind the deacylated tRNA in the P-site of the mitoribosome [30].

However, two of the 13 open reading frames (ORF) in mitochondria do not use UAG or UAA as a stop codon. Instead, the coding sequence ends with AGA and AGG [64]. Those two triplets lack a corresponding mt-tRNA. To still enable translation termination in a canonical matter involving mtRF1a, a -1 frameshift putting UGA into the A-site has been proposed and described in different species [81]. However, this mechanism is not seen in human mitochondrial ORFs terminating with AGA/AGG. The existence of two unassigned codons indicates the need of additional termination features [24], [82].

The peptidyl-tRNA hydrolase immature colon carcinoma transcript 1 (ICT1) represents a potential additional termination factor, acting in a similar way to the bacterial alternative rescue factor (Arf) B (Figure 8) used to rescue stalled ribosomes [83]. In this mechanism, the peptidyl-tRNA is released from the mRNA downstream of the A-site due to an interaction of the positively charged C-terminal helix of the rescue factor with the mRNA. However, for this process to take place, ICT1 would have to be freely available inside mitochondria. This is the case in yeast but not in mammalian mitochondria [84].

In addition to mtRF1a and ICT1, two other RFs are found in mitochondria: mtRF1 and C12orf65. Their functionality is not completely described yet but they might play a role in recycling/rescue of stalled mitochondrial ribosomes [1]. Due to its structural composition, C12orf65 can be placed in the same group as ICT1 and ArfB. Conserved sequences within the different proteins even identify them as homologs. C12orf65, in contrast to ICT1, is not incorporated into the mitoribosome. Mutations and the complete lack of the protein are associated with mitochondrial pathologies due to defected mitochondrial translation [1]. In conclusion, so far mtRF1a is the only identified mtRF to be involved in translation termination *in-vivo* [85]. The fungal homolog of mtRF1a is Mrf1, which is expected to act in a similar way to the human protein [1].

In contrast to the described process in mitochondria, bacteria use two individual release factors (RF1 and RF2), recognizing the stop codons UAG/UAA and UGA/UAA, respectively. The factors bind at the A-site and catalyze peptidyl-tRNA hydrolysis in the PTC. For the release of RF1/RF2 from the ribosome an additional RF is needed, RF3. [62], [86].

A homolog for RF2 as well as RF3 is missing in mitochondria [87]. To fully understand the process of termination further research is needed. However, currently two models are described mainly differing in GDP/GTP affinity of RF3. The total energy consumption is equal in both models [62]. Only one model is shown (Figure 6) which was confirmed and described in recent studies [88], [89].

In this model, the affinity of RF3 for GTP and GDP is approximately the same. Due to the cellular concentrations of the two molecules, the factor is more likely to bind in the GTP-bound state (RF3:GTP). RF3:GTP can bind simultaneously with RF1 or after peptidyl-tRNA hydrolysis. In any case, the binding of the factor shifts the ribosome complex to the R-state and peptide release stabilizes the complex in this state. A confirmation for interaction of RF3 with the ribosome in the GTP-state is the fact that RF3:GDP failed to induce the R-state. In this state, the interaction between RF1/RF2 and the decoding center, mainly formed through uL11, can no longer be maintained, leading to the release of the factor.

The presence of RF3:GTP is essential for the dissociation of RF1, whereas RF2 is more dynamic and therefore less dependent on ribosome conformation and the presence of RF3. RF3 itself is independent of peptide release and ribosome dynamics but dependent on the presence of RF1/RF2. If RF1 is present, the factor can easily dissociate from the ribosome even in the non-rotated state. This is mainly related to the position of RF3 relative to uL11, which is influenced by RF1/RF2. In fact, the order for the factor release is serendipitous. If RF1 exits first, RF3 uses GTP hydrolysis to release from the ribosome.

GTP hydrolysis by RF3 is therefore influenced by multiple factors, including peptide release, subunit rotation and conformation of the release factors. However, it seems that RF3 mainly uses GTP hydrolysis as a rescue mechanism for its release from termination complexes that do not contain RF1. Interactions between RF2 and RF3 have not been studied to this extent [88], [89]

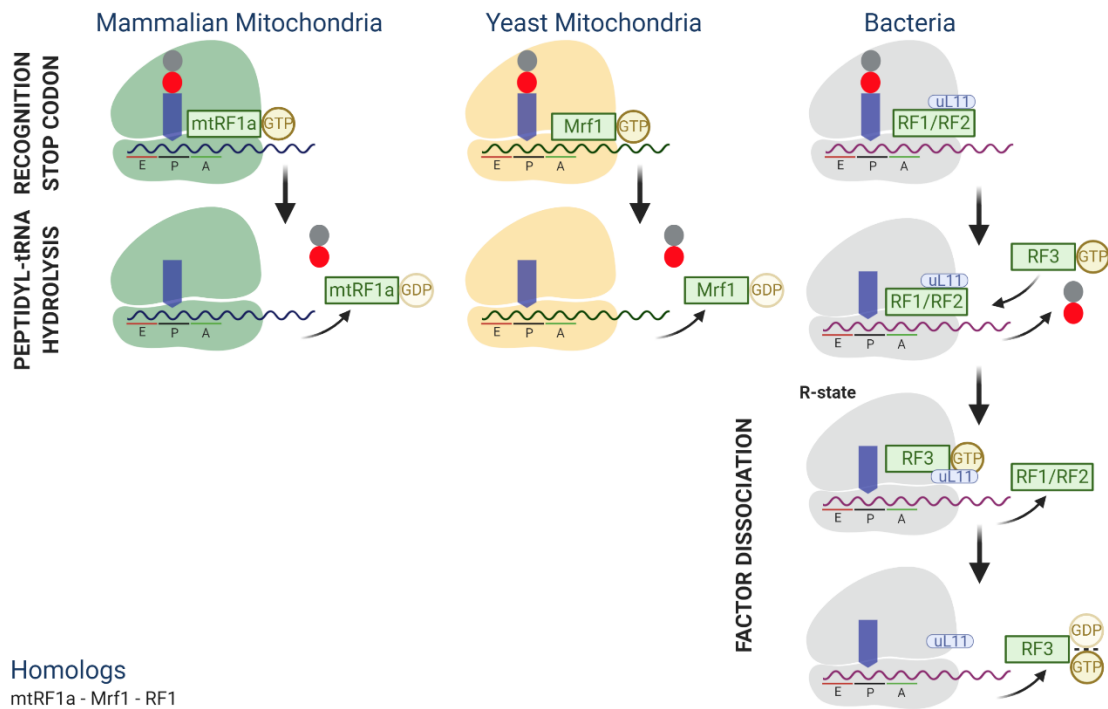


Figure 6. Translation termination. Translation ends when a stop codon enters the A-site of the ribosome. Differences in the process between bacteria and mitochondria are shown. In human mitochondria, mtRF1a recognizes the stop codon (UAA or UAG) and initiates peptidyl-tRNA hydrolysis in a GTP-dependent manner. Mrf1, the homolog in yeast acts in a similar way. In bacteria, stop codons are recognized by RF1 (UAG/UAA) or RF2 (UGA/UAA). Those factors dissociate after polypeptide release, promoted by a third release factor RF3. Interactions between the RFs change the conformation of the ribosome, leading to a rotated state (R-state) as well as the conformation of the factors themselves. RF3 dissociates from the ribosome either bound to GDP or GTP. GTP hydrolysis by RF3 depends on multiple factors, including peptide release, subunit rotation and conformation stages of the involved RFs. RFs in bacteria mainly interact with the ribosome through ribosomal protein uL11. Homologs within the three organisms are listed at the bottom. (modified after Tsuboi et al. 2009 [90] and created with BioRender.com).

The step of translation termination in mammalian mitochondria shows some gaps that require more research in order to fully understand the process. Also, in bacteria described models are disagreeing to certain extents

Recycling

After recognition of the stop codon and peptidyl-tRNA hydrolysis, the translation complex has to separate and the involved components are recycled for the next translation cycle. Mitochondria have a specialized homolog of EF-G, mtEF-G2 (in yeast Met2) for this step [90]. mtEF-G2 binds together with GTP and the mitochondrial recycling factor 1 (mtRRF1) (yeast homolog = Rrf1) in a complex that induces ribosome splitting (Figure 7) [1], [30]. In contrast, bacteria only have one EF-G factor which acts during elongation and recycling [90]. Together with the bacterial RRF, the factor binds to the A-site of the ribosome. EF-G

pushes RRF against the key intersubunit bridge and by this initiates ribosome splitting [62]. GTP hydrolysis by EF-G is required for this action of subunit dissociation and for following release of EF-G and RRF. However, in mitochondria GTP is a requirement for mtEF-G2 binding to the mitoribosome but splitting is initiated without GTP hydrolysis. GTP hydrolysis takes place after subunit dissociation, necessary for the release mtEF-G2 and mtRRF1 from the mtLSU [90].

In both, mammalian and yeast mitochondria, IF3 migrates towards the SSU and by its binding assures dissociation of ribosomal subunits before the next translation cycle. In bacteria, binding of IF3 triggers the release of mRNA and deacylated tRNA from the SSU and its activity as anti-association factor is further enhanced by interaction with IF1 (Figure 4) [1], [62].

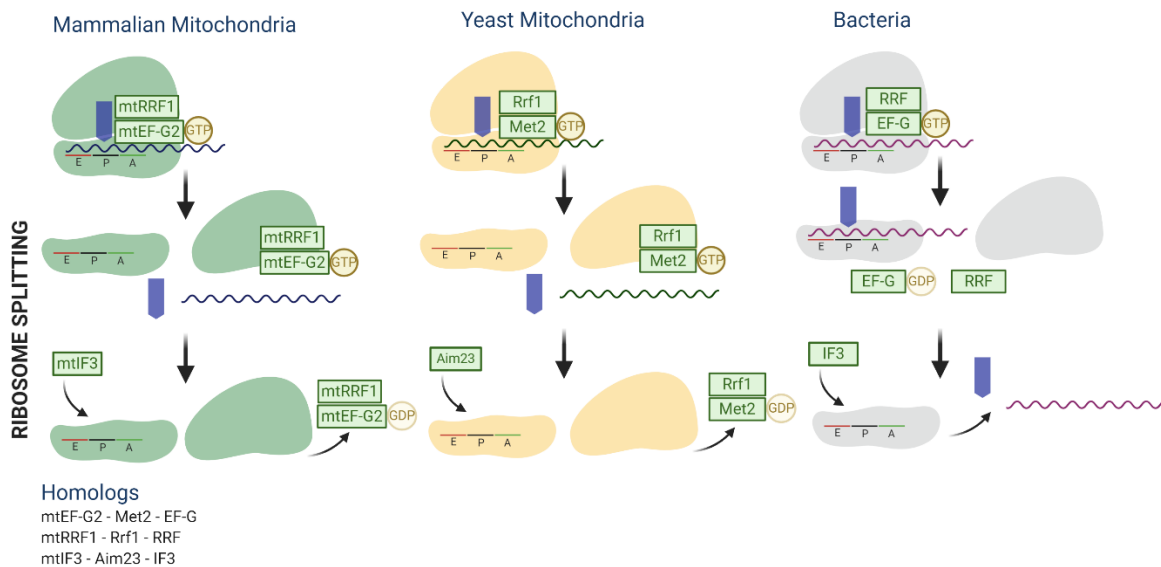


Figure 7. Translation complex recycling. mtEF-G2:GTP/Met2:GTP together with mtRRF1/Rrf1 in mitochondria and EF-G:GTP with RRF in bacteria initiate recycling by promoting ribosome splitting. Splitting requires GTP hydrolysis in bacteria, whereas in mitochondria GTP hydrolysis by mtEF-G2/Met2 is only used for factor release from the mtLSU after subunit dissociation. mtIF3/Aim23 and IF3 respectively assure subunit dissociation until the next translation cycle. IF3 further triggers release of mRNA and deacylated tRNA from the SSU. Homologs within the three organisms are listed at the bottom. (modified after Tsuboi et al. 2009 [90] and created with BioRender.com).

Mitoribosome splitting is one of the least understood steps in mitochondrial translation. Dissociation of the two subunits in bacteria is coupled to hydrolysis of the GTP bound to EF-G whereas in mitochondria, GTP hydrolysis is thought to occur after dissociation [90]. In bacteria, this coupling of ribosome dissociation to an energy consuming step serves to prevent spontaneous dissociation of the ribosomal subunits. It is unclear what factor serve this purpose in mitochondria.

Rescue of stalled ribosomes

During the process of translation ribosomes can get stalled on the transcript within all mentioned organisms. Circumstances that can lead to such situations include the presence of stable secondary or tertiary pseudoknot structures on the mRNA, starvation of amino acids as well as mutated or insufficient aa-tRNAs. Moreover, the loss of stop codons and truncations of mRNA can stall translation.

Bacteria have evolved a set of mechanisms to rescue stalled ribosomes, since loss of functional ribosomes can be lethal [85]. mRNA structures like pseudoknots or stem-loops, can often be overcome by combined interaction of the RNA helicases uS3, uS4 and uS5 [62]. Those proteins are missing in mammalian mitoribosomes and a helicase activity of them in yeast mitoribosomes has not been confirmed yet.

The main rescue mechanisms in bacteria is *trans*-translation, which involves a RNA species combining features of mRNA as well as tRNA, therefore called tmRNA. This tmRNA binds the empty A-site of the ribosome together with SmpB, enabling elongation until the stop codon in its mRNA domain is reached. The original mRNA, as well as the nascent polypeptide, are tagged for degradation by RNases and proteases respectively (Figure 8) [91].

In case ribosomes cannot be rescued by *trans*-translation in bacteria, ArfA and ArfB represent back-ups. Their expression is regulated by *trans*-translation levels. The mechanism of ArfB was already mentioned before. The factor triggers polypeptide release by interaction with the PTC. Additional interaction downstream at the SSU occupies the mRNA channel and by this straddles ribosomal subunits. In contrast, ArfA recruits RF2 to the ribosome. Both factors do not target the polypeptide or the mRNA for degradation (Figure 8) [83].

Moreover, bacteria have specialized EFs which can prevent ribosome stalling such as EF-P. This factor comes into action when ribosomes stall due to low rates of peptide bond formation. The L-shaped EF-P binds between the P- and E-site of the ribosome positioning them towards the PTC and thereby bringing them back to their productive orientation [62], [92].

Concerning ribosomes stalled in mitochondria, no events of *trans*-translation or alternative rescue mechanisms have been confirmed so far. Possible mechanisms are listed in Figure 8. The aforementioned mitochondrial RF factors mtRF1arf, C12orf65 and ICT1, in its free form, represent potential candidates acting similar to bacterial Arfs. Nevertheless, their function is still subject of intense research. The proposed -1 frameshift for recognition of unusual stop codons might also work for stalled mitoribosomes by repositioning them and thereby initiating termination following the canonical way. Bacteria rescue ribosomes in this way if they stall due to a lack of charged tRNAs [93].

Moreover, the bacterial protein LepA was long believed to rescue ribosomes by initiating a one-codon backwards movement [38]. However, recent studies actually propose a different role of LepA in translation, during ribosome assembly and initiation through interaction with the Shine-Dalgarno sequence [94]. The mitochondrial homolog Guf1 is described as essential for mitochondrial protein biosynthesis [95]. Taken into account the fact that mt-mRNA lack the Shine-Dalgarno sequence, the factor might act in a different step of translation or during rescue of stalled ribosomes [85].

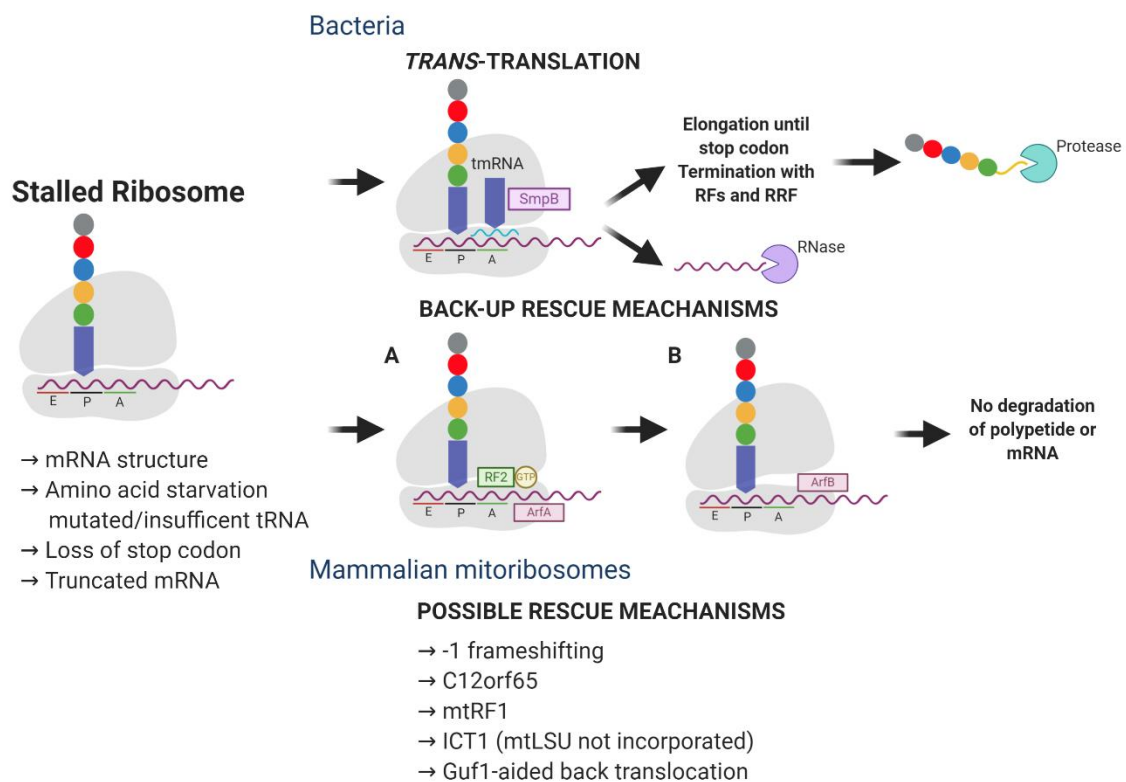


Figure 8. Rescue mechanisms for stalled ribosomes. Different circumstances during translation can stall the ribosome on the transcript. Bacteria have evolved a set of mechanisms to rescue stalled ribosomes which are shown in the top part of the figure. In *trans*-translation, tmRNA binds the empty A-site of the ribosome together with SmpB. Through this the inefficient mRNA is released and degraded by RNase. Elongation continues until the stop codon in the mRNA domain of tmRNA is reached. The nascent polypeptide is tagged for degradation by proteases. Alternative to *trans*-translation, the bacterial factors ArfA and ArfB can rescue ribosomes. ArfA binding recruits the RF2 to the ribosome and initiates translation/recycling in a canonical way. ArfB interacts with both subunits leading to peptidyl-tRNA hydrolysis and straddling of the subunits. Both factors do not target the polypeptide or the mRNA for degradation. Rescue mechanisms in mitochondrial translation are still the subject of intensive research and have not been confirmed yet. (modified after Ayyub et al. 2020 [85] and created with BioRender.com).

After reviewing the process of mitochondrial protein biosynthesis, steps most likely to require participation of additional proteins, potentially MGPX, could be determined as: Mitoribosome assembly, initiation and mitoribosome splitting. Additionally, there might be so far undescribed rescue mechanisms for stalled mitoribosomes present in mitochondria.

1.2 GTPases

As molecular switches, GTPases switch between a GDP-bound inactive and a GTP-bound active state. This switch is connected with a conformational change and the interaction with effector molecules. The GTP-bound state hereby represents the higher affinity state. Through this mechanism GTPases participate in the regulation of several cellular processes, including translocation of proteins, differentiation, protein translation and cell signaling [96].

Focusing more closely on their functionality, GTPases follow a circular process. They bind and hydrolyze GTP, leaving the protein bound to GDP. This GDP can be released to restart the whole process. To a certain extent the GTPases regulate this process themselves by using intrinsic GTP activity, however other proteins can also influence their activity. In eukaryotes, GTPase-activating proteins (GAPs), guanine nucleotide exchange factors (GEFs) and guanine nucleotide dissociation inhibitors (GDIs) are common regulators for GTPases [97], [98]. In prokaryotes, GAPs and GEFs are less common, but an enhancement of GTPase activity can be seen following interactions with ribosomal proteins and rRNA, as described previously [38].

GTPases characteristically contain a G-domain, responsible for GTPase activity and including 4-5 G-motifs (G1-G5), as well as a N- (NTD) and a C-terminal domain (CTD). G1 is also called the P-loop or Walker A motif and is shared with other nucleotide binding proteins like adenosine triphosphate (ATP) binding proteins, ATPases.

The effector region G2 is characteristic for GTPase families, since sequences within this domain differ between protein families. The domain is responsible for interaction with the effector molecules and coordination of Mg^{2+} binding to the β - and γ -phosphate. The structure of G2 differs significantly between GTP- and GDP-bound states.

Such a conformational change is also observed in the G3 motif which is why those two regions are also referred to as switch I and switch II region, respectively. G3, also called Walker B is involved in Mg^{2+} coordination with its typical DX_2G motif.

G4 determines nucleotide specificity, since it only forms hydrogen bonds with guanine rings. G5 also interacts with guanine through water-mediated hydrogen bonds but the region is not strictly conserved. G motifs within the G-domain are considered highly conserved among different species. However, their functionality and level of conservation can vary [38], [99].

Built on similarities in sequence and structure two classes of GTPases can be distinguished. The translation factors (TRAFAC) class, combining proteins involved in cell motility, signal transduction, intracellular transport and translation.

The second class is the signal recognition particle, MinD and BioD (SIMIBI) class, including GTPases involved in signal recognition, MinD-like ATPases and a fraction of phosphate transferase or kinase activity showing proteins.

These two big classes can be subdivided into families and subfamilies with similar structure, sequence and domain architecture [100]. Some GTPases within these families are highly conserved between organisms, examples of such proteins have already been mentioned afore, which are involved in protein biosynthesis.

The importance of these molecular switches in mitochondrial function was highlighted in the chapter on mitochondrial protein translation. Although the essential function of MGPX within this process remains to be determined.

Comparison of conserved domains within the amino acid sequence of MGPX identified the bacterial homolog BGPX, showing 30% sequence identity [101]. In contrast to MGPX, BGPX is known to be dispensable for protein synthesis in *B. subtilis* [102] and *E. coli* [103]. No homolog for MGPX has been identified in fungi.

1.2.1 BGPX

Already described structural and functional properties of BGPX might be helpful in identifying biochemical activities of its human homolog MGPX. BGPX is a member of the Obg-HflX superfamily within the TRAFAC class of GTPases. The NTD can be divided into two separate domains. ND1 consists of a four-stranded parallel β -sheet flanked by four α -helices and a helical domain (HD) formed by two long α -helices. HD links ND1 to the G-domain (ND2). BGPX therefore consists of four domains: ND1-HD-ND2-CTD (N to C terminus) (Figure 9, A+B) [104]. The human mitochondrial homolog shows an extension in the N-terminal sequence which acts as a mitochondrial matrix-targeting sequence (Figure 9, C) [38].

The ND2 shows typical folding for Ras-like GTPases including aforementioned P-loop and switch I and II motifs. Worth mentioning is the substitution of the catalytic glutamine within the DxxGQ motif by phenylalanine. This substitution is universally observed throughout the BGPX's protein family. Usually mutations in this motif influence GTPase activity. However, this is not the case for BGPX or any other protein belonging to this family [105].

The ND1 of BGPX was shown to have nucleotide triphosphate (NTP) hydrolysis activity, with higher affinity for ATP but also weak GTPase activity. Hydrolysis by the domain requires the presence of Mg^{2+} ions but misses a P-Loop/Walker-A motif, both common features of NTPases. In homologs of BGPX the ND1 is conserved, pointing towards an ATPase activity of the domain also in homologs. Nevertheless, in some homologs the domain is inactive [104].

Interestingly, the ND2 also showed ATPase activity which was even higher than the GTPase activity. Neighboring domains regulate these NTPase activities, showing inhibiting effects (Figure 9, A). Release of this inhibition might be connected with nucleotide binding [104]. GTP hydrolysis of BGPX is also increased by interaction with the 50S ribosomal subunit which is the case for most GTPases involved in ribosome assembly and translation. BGPX was shown to also interact with the 30S subunit as well as with the complete 70S ribosome. The second nucleotide binding domain ND1 and the ability to hydrolyze two NTPs could be an explanation for different ribosome bound states as it is the case for the GTPase Der, containing two homologous G-domains [41]. These interactions could indicate a role of the protein in similar processes [104].

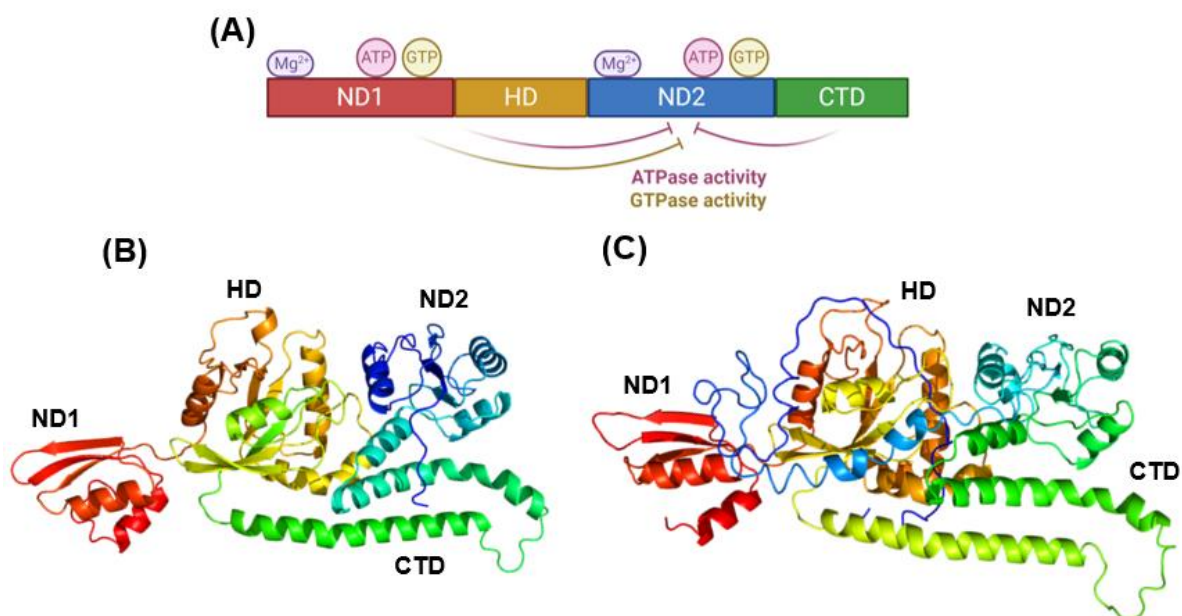


Figure 9. Structural models of BGPX and MGPX. (A) Schematic structure of BGPX. BGPX consists of four domains: A N-terminal domain (ND1) that can bind and hydrolysis ATP and GTP depending on the presence of Mg²⁺. A helical domain (HD) connects the ND1 with the G-domain (ND2). The ND2 is also able to hydrolyze ATP, even more efficiently than GTP, indicating that BGPX might rather be an ATPase than a GTPase. The last domain is the C-terminal domain (CTD). Nucleotide hydrolysis activity of the ND2 is negatively regulated for ATP by coupled ND1 and HD as well as the CTD. ND1-HD also inhibits the GTPase activity of ND2. Release of this inhibition mechanism might be connected to nucleotide binding. (modified after Jain *et al.* 2013 [104] and created with BioRender.com). Using the corresponding amino acid sequences structural models of BGPX (B) and MGPX (C) were generated using the Phyre2 web portal for protein modeling, prediction and analysis (Kelley *et al.* 2015 [106]). Images are colored by rainbow N to C terminus. Domain annotations are estimated.

Studies on the role of BGPX in protein biosynthesis propose a role as a rescue factor for stalled ribosomes. In this process, the protein would bind the empty A-site of the ribosome by mimicking the acceptor arm of tRNAs through its NTD. This binding takes place after the

polypeptide was released by bacterial RFs like ArfA and ArfB. BGPX induces the release of the tRNAs still bound to the ribosome and mRNA in the P- and E-site and lead to general ribosome splitting. Ribosome splitting is initiated by disruption of the central bridges between the two subunits and a corresponding conformational change, a mechanism similar to class I release factors. Moreover, BGPX showed structural similarity to RF3. Nevertheless, ribosome-interaction sites of BGPX differ from general GTPase binding sites at the 50S subunit, indicating a non-canonical GTPase activity for BGPX compared to other translation factors. GTP hydrolysis is used by BGPX as a release mechanism from the LSU [107]. Following the initiated separation, BGPX binds to the A-site of the SSU and could thereby prevent premature reassembly of the ribosome and binding of other translation factors, similar to IF3 [108]. BGPX thereby would offer an alternative and more flexible path for translation termination in bacteria which might especially be important during heat shock [107].

Heat shock can significantly affect ribosomes and alter rRNA structures within the subunits. A model of how bacteria overcome these rRNA structures proposed another biochemical activity for BGPX by acting as a rRNA helicase. In this model, the protein binds the LSU with ATP bound in the ND1 and GTP bound in the ND2. The HD targets the PTC of the LSU, through an interaction with the domain V of the 23S rRNA. ATP hydrolysis by the ND1 induces a conformational change which leads to the release of the HD, allowing the PTC to unwind and refold in the correct conformation. BGPX dissociates from the LSU in a GTP-dependent manner, leaving behind an active and functional 50S subunit [109].

As a homolog of BGPX, MGPX might act in a similar way. However, no ATPase activity, helicase activity nor specific interaction with the mitoribosome or other mitochondrial proteins have been described yet. In contrast to BGPX, MGPX evolved an essential role in mitochondrial protein biosynthesis which could indicate participation in the canonical pathway rather than in stress situations, as it is proposed for BGPX.

1.3 Aim

The relevance of the project stems from the fact that MGPX in human mitochondria has evidently evolved an unknown but essential role in mitochondrial protein synthesis, a process essential for human life. The goal of the project is to understand the specific biochemical activities of MGPX and to determine its role in mitochondria, which could improve the general understanding of mitochondrial protein biosynthesis. Since mitochondria dysfunction is related to multiple human diseases, better understanding of their function might also impact treatment options for patients suffering from those pathologies.

2 Materials and Methods

All chemicals and reagents were obtained from Sigma-Aldrich, unless otherwise stated.

2.1 Cell culture

All experiments involving cell culture were performed in a laminar flow hood and under sterile working conditions to avoid contaminations with microorganisms.

143B cells, a cell line derived from human osteosarcoma, were used as standard cells which were used for knock-out (KO) and transduced stable cell lines.

For virus production as well as transfection experiments human embryonic kidney cells (HEK) 293T cells were used. A cell line known for its efficient transfectability.

Both cell lines, 143B and HEK293T cells, are adherent cells and grow under standard cell culture conditions (37°C, 5% CO₂). Dulbecco's Modified Eagle's Medium (DMEM), high glucose, GlutaMAX™ Supplement, pyruvate (gibco, #10569-010) was used as culture medium. Before usage 10% fetal bovine serum (FBS) and 1% Penicillin/Streptomycin were added and the medium was sterile filtered (0.22 µm filter), referred to as DMEM complete.

In addition to those two cell lines, a cell line tolerant to mtDNA depletion derived from 143B cells and established by ethidium bromide (EtBr) treatment, in the David M. Sabatini Laboratory, was used. Such cell lines are referred to as rho0 cells (here 143B rho0 cells). Rho0 cells are able to proliferate without OXPHOS. However, they dependent on the availability of uridine and pyruvate for their survival in culture [110]. Uridine (200 µg/mL) was therefore added fresh to the culture medium of those cells.

Cells were passaged using 0.05% Trypsin-EDTA (gibco, #25300-054), once confluency was reached.

2.2 Cloning plasmids

To generate a KO and stable cell lines as well as to perform transfection experiments, required DNA plasmids were cloned, using four different backbone plasmids: LC2OPTI (slightly modified version of Addgene, #49535), pGS45 (established in the David M. Sabatini Laboratory, not commercially available), pMXs_MCart1 (Addgene, #133253) and pRK5 (Addgene, FLAG-tag = #46334, HA-tag = #46335). Plasmids were Ampicillin and Blasticidin resistant (LC2OPTI resistant for Puromycin), partially regulated by doxycycline (DOX) (pGS45 plasmids) and included different epitope tags (3x FLAG-tag, HA-tag). As a control protein for future experiments, a plasmid for citrate synthase (CS) was cloned as well. All cloned plasmids including their characteristics are listed in Table 2.

Table 2. List of cloned plasmids.

Plasmid	Protein-Tag	Backbone plasmid
MGPX	3x FLAG-tag	pGS45
MGPX	3x FLAG-tag	pRK5
MGPX	HA-tag	pRK5
MGPX-mutants	3x FLAG-tag	pGS45
BGPX	3x FLAG-tag	pGS45
ICT1	3x FLAG-tag	pMXs
ICT1	3x FLAG-tag	pRK5
DDX28	3x FLAG-tag	pRK5
MRPS27	3x FLAG-tag	pRK5
TRMT61B	3x FLAG-tag	pRK5
TRMT61B	HA-tag	pRK5
CS	3x FLAG-tag	pMXs
CS	3x FLAG-tag	pRK5

2.2.1 Fragment generation PCR

In the first step of this process, the insert fragment for the plasmids was generated by PCR. After *in-silico* construction of the plasmid, using the website Benchling, primers for the target gene modification, including the necessary overhangs for Gibson assembly, were designed and ordered (Integrated DNA Technologies). Those primers were used in a PCR reaction with the KAPA HiFi HotStart PCR Kit (Roche Diagnostics, #KK2501). As templates served already established in-house plasmids (MGPX, MGPX mutants), gene blocks (BGPX) (obtained from Twist Bioscience) or human cDNA (ICT1, DDX28, MRPS27, TRMT61B, CS). The PCR reaction mix and protocol are listed in Table 3 and Table 4, respectively. Annealing temperatures and extension times varied according to primer melting temperatures and amplicon sizes. For products with high GC-content the GC Buffer delivered with the PCR Kit was used. Primers and templates used for the different plasmids are listed in Table 5. An additional table with all primers used for cloning of MGPX mutants is included in the appendix (Supplemental table 1). Listed primers were used for initial amplification of the target sequence. In some cases, a second PCR was performed to generate necessary overhangs for Gibson assembly, matching used backbones.

Table 3. Reaction mix plasmid fragment generation PCR.

Compound	Volume
Nuclease-free H ₂ O	up to 50 µL
Buffer (5x)	10 µL
dNTP mix (10 mM)	1.5 µL
Kappa HiFi polymerase	0.25 µL
Forward primer (FwdP) (10 µM)	1.5 µL
Reverse primer (RevP) (10 µM)	1.5 µL
Template DNA	0.1-10 ng
Total reaction volume	50 µL

Table 4. Protocol plasmid fragment generation PCR

Step	Temperature	Time	Cycles
Initial Denaturation	95°C	3 min	
Initial Annealing	98°C	20 s	
Annealing	55-72°C	20 s	32x
Extension	72°C	30-180 s (15-60 s/kb)	
Final Extension	72°C	1 min/kb	
Hold	4°C		

Table 5. Primers for fragment generation PCR.

Plasmid	Primers
MGPX	FwdP: CACTTCCTACCCTCGTAAAGTCGACACCGgccaccATGTGGGCCCTGCGGGCCGCCGTAC RevP: GGCAAATTCGGGAAGCTCTTTCCAGGAgggagcggcggaggaagc
BGPX	FwdP: CTTCCTACCCTCGTAAAGTCGACACCGgccaccATGTGGGCTCTGCGCGCCGCCGTGCGA RevP: caaatttgtaatccagaggtgattgatCTCATTATCGTCGTCATCTTTGTAATCAA
TRMT61B	FwdP: tgaattcgtcgacgccaccATGCTAATGGCATGGTGCCGCGGTCC RevP: GTTAAGTTGTGGTTTGACCTTCCTCAACTTGACAAGAAAAGCTG
ICT1	FwdP: aattcgtcgacgccaccatgGCGGCCACCAGGTGCCCTGCGCTG RevP: acctccacctcctcgggccgcGTCCATGTCGACCCTCCTGCTTG
DDX28	FwdP: aattcgtcgacgccaccATGGCTCTAACGCGGCCGGTGCGGCTCT RevP: acctccacctcctcgggccgcGGTTGCTTGGGGCAAAGGCTCTT
MRPS27	FwdP: attcgtcgacgccaccatgGCTGCCTCCATAGTGC GGCGCGGGAT RevP: ctccacctcctcgggccgcGGCAGATGCCTTTGCTGCTTTCTGAG
CS	FwdP: attcgtcgacgccaccATGGCTTTACTTACTGCGGCCGCCGGCT RevP: tctcggcggccgcCCCTGACTTAGAGTCCACAACTTCATCAGACC

After the PCR run was completed, 10x LI-COR orange loading dye was added to the product and the whole volume was loaded into a 1% Agarose DNA gel (in Tris-Acetate-EDTA (TAE) buffer) containing EtBr (0.05 µg/ml). Gel electrophoresis ran for approx. 1 h and 30 min at 120 V at room temperature (RT). Product sizes were confirmed at the Azure™ c200 gel imaging workstation (Azure Biosystems), before the correct bands were cut out using a razor blade. The QIAquick Gel Extraction Kit (QIAGEN, #28706) was used to extract DNA from the gel. Therefore, the bands were first transferred to a 2 ml microcentrifuge tube and incubated in QC buffer (3 volumes of buffer to 1 volume of gel) for 10 min, at 50°C with agitation. Once the gel had completely dissolved isopropanol (1 gel volume) was added and carefully mixed with the sample, before the whole volume was transferred to a QIAquick spin column and placed on a vacuum manifold. 2 washing steps were performed, first with QC buffer followed by PE buffer. To remove any residual wash buffer from the columns, a centrifugation step at full speed (RT, 2 min) was performed. For DNA elution, the columns were transferred to a new 1.5 mL collection tube and incubated for 5 min with elution buffer before the samples were spun down at 12,000 x g for 1 min at RT. The eluted DNA was measured at the NanoDrop™ One/OneC Microvolume UV-Vis Spectrophotometer (ThermoFisher Scientific), absorbance A260.

2.2.2 Backbone generation

Backbones used for Gibson assembly were Ampicillin and Blasticidin resistant, partially regulated by DOX and included the required epitope tags. Plasmids used as backbones were linearized in an enzymatic digest with matching restriction enzymes. The reaction mix (Table 6) was incubated at 37°C overnight. The product was validated after gel electrophoresis by imaging and the correct band was cut out to extract DNA (QIAquick gel extraction kit).

Table 6. Reaction mix for backbone linearization.

Compound	Volume
Template plasmid	3 µg
Restriction enzyme	2 µL
NEB®-Buffer CutSmart (NEB® #B7204S)	5 µL
Nuclease-free H ₂ O	Up to 50 µL
	50 µL

2.2.3 Gibson assembly

In the Gibson assembly, the generated insert fragment was ligated with the corresponding backbone to form the target plasmid, following the original idea and procedure from Gibson *et al.* [111]. A molecular ratio of 1:2 for the input of backbone and fragment was approached

by adding approx. 0.05 pM DNA/fragment to the reaction. Depending on the fragment size the molecular ratio was adjusted. After addition of Gibson Assembly® 2x Master Mix (NEB®, #E2611), the reaction was incubated at 50°C for 20 min. The assembled constructs were afterwards used for bacterial transformation.

2.2.4 Bacterial transformation

For the bacterial transformation NEB® Stable Competent *E. coli* (High Efficiency) (NEB®, C3040) were slowly thawed on ice before about 5% volume from the Gibson assembly reactions were added to the cells. Cells were incubated for 30 min on ice. In the meantime, agar plates (Teknova, #L1010) with 100 µg/mL Carbenicillin were labeled, glass beads were added and they were prewarmed at 37°C. After incubation on ice, a heat shock at 42°C for 40 s in a water bath was performed. Cells were allowed to recover for 1 min on ice before NEB® 10-beta/Stable Outgrowth medium (NEB®, B9035S) was added and cells were incubated for 1 h at 30°C with gentle agitation. After this recovery, bacteria were plated on the prepared agar plates and spread evenly using added glass beads. Before placing the plates in the warm room at 30°C to incubate overnight, the glass beads were removed. All steps were performed under the Bunsen burner flame and sterile materials were used to avoid any kind of contamination.

On the next day, the plates were checked for visible colonies, which were validated by colony PCR, using primers flanking the Gibson reaction assembly areas. Therefore, single colonies were picked with a 10 µL sterile pipet tip and transferred to a PCR tube containing 10 µL nuclease-free H₂O. The colonies were then cooked at 90°C for 5 min and afterwards spun down. 1 µL of the supernatant was used as template in the colony PCR and added to the prepared GoTaq Master mix (Table 7). The PCR protocol for the colony PCR is listed in Table 8, annealing temperature and extension time were adjusted to the used primers and the product size. Correct colonies were confirmed by validating PCR product sizes (gel electrophoresis and imaging as described above).

Table 7. GoTaq Master Mix for colony PCR

Compound	Volume
GoTaq Green 2x Master Mix (Promega Corporation, #M7123)	10 µL
Nuclease-free H ₂ O	7 µL
FwdP (10 µM)	1 µL
RevP (10 µM)	1 µL
Master Mix/sample	19 µL
Template (cooked colonies)	1 µL
	20 µL

Table 8. Protocol colony PCR

Step	Temperature	Time	Cycles
Initial Denaturation	95°C	2 min	
Initial Annealing	95°C	30 s	
Annealing	55-72°C	20 s	40x
Extension	72°C	30-140 s (1 min/kb)	
Final Extension	72°C	1 min	
Hold	4°C		

Validated colonies were inoculated into 50 mL bacterial culture tubes containing, Lysogeny broth (LB) media (gibco, #10855-021) with Ampicillin (100 µg/mL) and incubated overnight at 30°C on a shaker.

DNA was isolated from the culture using the QIAprep Spin Miniprep Kit (QIAGEN, #27106). The cultures were spun down for 15 min at 4°C and 3,000 g. The supernatant was discarded and the pellets were resuspended in buffer P1. Buffer P2 was added to the dissolved pellet and incubated for 3 min before buffer N3 was added to neutralize the lysis. After inverting the tubes multiple times, samples were centrifuged for 15 min at RT and 17,000 g. The complete supernatant was transferred to a QIAprep spin column on a vacuum manifold. Next, columns were first washed with buffer PB, followed by 2 washing steps with buffer PE. To remove the residual wash buffer, columns were spun down for 2 min (RT/17,000 g). After transferring the QIAprep spin columns to a fresh 1.5 mL collection tube, elution buffer was added. Once the incubation (5 min) was finished, DNA was eluted by centrifugation at 10,000 x g, RT for 1 min. DNA concentration was determined at the NanoDrop™ One/OneC Microvolume UV-Vis Spectrophotometer, absorbance A260. To validate generated plasmids, diagnostic enzymatic digests were performed and plasmids were submitted for sequencing to QuintaraBio.

2.2.5 Virus production

Aforementioned HEK293T cells were used for lentivirus (pGS45, LC2OPTI) and retrovirus (pMXs) production. Virus was produced from each plasmid, used for establishment of stable cell lines (MGPX 3x FLAG-tag, MGPX KO cell line, MGPX mutants, BGPX, ICT1, CS).

All plasmids used are listed in Table 9. The day before transfection cells were seeded in 6-well cell culture plates in a density of 750,000 cells/well and cultivated with serum-free medium (Opti-MEM®, gibco, #31985-070) + 5% FCS under standard conditions. For the transfection mix, the separate components of the virus were mixed together in serum-free medium. Next the plasmid DNA (construct) and the transfection agent TransIT®-LT1 (Mirus, MIR 2304) were added (Table 9). The mix was vortexed, spun down and incubated for 15 min at RT before adding to HEK293T cells.

16 h after transfection, the media was changed (serum-free medium + 30% FCS) and after additional 16 h the first virus harvest was performed. This step included a media change (serum-free medium + 30% FCS). The collected virus was stored on ice at 4°C until the second and final harvest, performed 16 h after the first harvest. The harvested virus was either directly used for viral spinfection or transferred to cryotubes and stored at -80°C. Virus harvest was performed in a BSL-2 laminar flow hood according to relevant safety guidelines. Virus waste was collected separately and disposed following corresponding regulations.

Table 9. Transfection mix for virus production

Plasmid/Virus Proportions	Ratio	DNA µg/well	Volume µL/well
<i>Lentivirus (pGS45, LC2OPTI)</i>			
psPAX2 (Addgene, #12260)	2.1	0.368	
Envelope (pCMV-VSV-G) (Addgene, #8454)	1.5	0.263	
Construct (Cloned Plasmid)	2.1	0.368	
LT1	-	-	4
Total		1	
<i>Retrovirus (pMXs)</i>			
gag-pol (Addgene, #14887)	5	0.5	
Envelope (pCMV-VSV-G)	1	0.1	
Construct (Cloned Plasmid)	6	0.6	
LT1	-	-	3.6
Total		1.2	

2.2.6 Viral Spinfection

Safety and disposal regulations mentioned before for virus production were again followed during the process of viral spinfection. The spinfection was performed for establishment of stable cell lines (MGPX 3x FLAG-tag, MGPX KO cell line).

First, required cells were seeded in 6-well cell culture plates in a density of 100,000 cells per well with 3 mL DMEM complete, including 10 µg/mL Polybrene (143B wild-type (WT) for MGPX KO cell line, ICT1 and CS, MGPX KO cells for MGPX 3x FLAG-tag, MGPX mutants and BGPX). Before adding the virus to the cells, the virus was filtered using a sterile syringe filter (0.45 µm). A 2-fold dilution series was done on 4 wells, (1 mL – 0.125 mL). The remaining two wells were used for a non-virus control and a fluorescence control to validate successful transduction. Before putting the plates in the incubator, they were centrifuged for 45 min at 37°C and 2,200 rpm in a swing bucket centrifuge. 16 h after the spinfection, a media exchange was performed to remove the virus from the cells. Once the fluorescence control showed protein expression, Blasticidin (10 µg/mL) was added to select cells, which

was confirmed by cell death in non-virus control cells. Successfully transduced cells were expanded for further cultivation and usage in experiments.

For the MGPX KO cell line Puromycin (1 $\mu\text{g}/\text{mL}$) was used for drug selection and after successful selection single clones were isolated to evaluate their phenotype and determine a suitable KO clone for further use. 1 clone/cell was therefore transferred into a well of a 96-well cell culture plate by fluorescence activated cell sorting (FACS). The plates were precultured with 143B WT cells. The culture medium was a mixture of 60% fresh DMEM, 30% FBS and 10% preconditioned DMEM (used medium from 143B WT cultures) + 1% Penicillin/Streptomycin and uridine (200 $\mu\text{g}/\text{mL}$). The plates were cultivated under standard conditions until the medium was used up. The medium was then changed to DMEM complete + uridine (200 $\mu\text{g}/\text{mL}$) and Puromycin (1 $\mu\text{g}/\text{mL}$) to select KO cells within the wells. Those cells were further expanded and tested for their phenotype by cultivation in DMEM galactose (DMEM - D-Glucose, - Sodium Pyruvate, + L-Glutamine (gibco, #11966-025) + 4.5 mg/mL galactose). In case of successful MGPX KO, no cell growth was observed in DMEM galactose. MGPX KO cells were further cultivated with uridine (200 $\mu\text{g}/\text{mL}$) to ensure cell growth.

2.3 Transfection

For experiments focusing on transient protein expression, HEK293T cells were transfected with generated plasmids (pRK5 backbone). Therefore, 2 million cells were seeded in a 10 cm cell culture plate and transfected the following day. A total of 5 μg of plasmid was used per plate, which consisted of 100 ng plasmid of interest and 4.9 μg of backbone plasmid. For co-transfections plasmids of interest were combined in a ratio of 1:1 (50 ng per plasmid). DNA was mixed with 350 μL serum-free DMEM and 15 μL Polyethylenimine (PEI) (Sigma-Aldrich, #408727) and incubated for 15 min at RT before dropwise addition of the transfection mix to cells. Cells were cultivated for two days at standard conditions.

2.4 Western blot

To prepare samples for sodium dodecyl sulfate polyacrylamide gel electrophoresis (SDS-PAGE) and Western blot, clarified cell lysates were mixed with Laemmli 5x SDS buffer. If not mentioned otherwise, 1% Triton X-100 buffer (Table 11) was used for cell lysis. During the SDS-PAGE proteins were separated according to their molecular weight. Pre-made 12% Tris-Glycine gels (InvitrogenTM, #XP00122BOX) and the protein ladder NEB® Color Prestained Protein Standard, Broad Range (11–245 kDa) (NEB# P7712) were used. After 1.5-2 h at 110 V in 1x SDS running buffer all proteins were separated. For the wet protein transfer, the following stack was prepared: anode, sponge, filter paper, gel, membrane, filter

paper, sponge, cathode. Before the blotting, the polyvinylidene fluoride (PVDF) membrane was activated with 100% methanol for 5 min. The transfer was done in a transfer tank filled with 1x transfer buffer under 45 V over 2 h at RT.

For the following incubation and washing steps, a shaker was used. Membrane blocking was performed using 5% non-fat milk in Tris Buffered Saline with Tween (TBST) (120 mM NaCl, 2.5 g/L Tris-HCl, 4 mM Tris BASE, 0.1% (w/v) Tween20) for 1 h at RT. After 3 washing steps with TBST for 10 min each the membrane was cut according to the molecular weight of target proteins. The separated pieces of the membrane were incubated with the corresponding primary antibody (diluted 1:1,000 in 5% bovine serum albumin (BSA) in TBST) overnight at 4°C (Table 10).

The following day, the membrane was washed 3 times with TBST for 5 min each to wash of the primary antibody before the corresponding HRP-linked secondary antibody (Cell Signaling Technologies, Anti-rabbit - #7074, Anti-mouse - #7076) (diluted 1:3,000 in 5% non-fat milk in TBST) was added and incubated for 1-2 h at RT. After 3 final washing steps with TBST (10 min each), the membrane was placed in a film cassette and enhanced chemiluminescence (ECL) solution (Pierce™, #32106) was added for 1 min. The exposure time for films varied depending on signal strength (average ~5 min). Afterwards, the films were developed on the X-OMAT film processor. A Canon 8800F scanner was used to digitalize the film. Grey scales were analyzed via Adobe photoshop (version CC 2019 (20.0.6)).

Table 10. Used antibodies for Western blot.

Protein	Species	Molecular weight	Reference
FLAG-tag	mouse	-	Sigma-Aldrich, #F1804
HA-tag	rabbit	-	Cell Signaling Technology, #3724
mTOR	rabbit	289 kDa	Cell Signaling Technology, #2983
MGPX	rabbit	56 kDa	LSBio, #LS-C377148-50
MRPL11	rabbit	21 kDa	Cell Signaling Technology, #2066
MRPL44	rabbit	38 kDa	proteintech®, #16394-1-AP
MRPS27	rabbit	48 kDa	proteintech®, #17280-1-AP
MRPS18B	rabbit	29 kDa	proteintech®, #16139-1-AP
ICT1	rabbit	24 kDa	proteintech®, # 10403-1-AP

Table 11. Components 1% Triton X-100 buffer

Component	Concentration
HEPES pH 7.4	40 mM
NaPyro-Pi	10 mM
Na Beta-Glycerol-Pi	10 mM
MgCl ₂	2.5 mM
Triton X-100	1%
Protease inhibitor Mini Tablets EDTA-free (Pierce™, #A32955)	1x

2.5 Immunofluorescence staining

Before cell seeding, a Corning® BioCoat Fibronectin 96-well microplate (Corning, #354409) was coated with Poly-L-ornithine solution (Sigma-Aldrich, P4957) for 1 h at 37°C. The microplate was afterwards washed 3 times with PBS (pH 7.4, gibco, #10010023). The day before the immunofluorescence staining (IF), 5,000 cells/well were seeded into the coated plate.

The following day cells were fixated with 4% methanol-free paraformaldehyde for 15-20 min at RT. After 3 washing steps with PBS, a methanol permeabilization was performed. Therefore, the plate was incubated with ice-cold 100% methanol for 10 min at -20°C, followed by a rinse step with PBS for 5 min before blocking/permeabilizing for 1 h at RT in the blocking buffer (5% normal donkey serum, 0.3% Triton in PBS). Before incubation with the primary antibody the plate was washed 3 times with PBS. The primary antibodies were diluted 1:500 in the antibody dilution buffer (1% BSA, 0.3% Triton in PBS). Used antibodies with dilution rates are listed in Table 12. Cells were incubated with the primary antibody overnight at 4°C. The next day the primary antibody was removed and 3 washing steps, 5 min each with PBS were performed before the corresponding secondary antibody (AlexaFluor 488 or AlexaFluor 546, Invitrogen™) (diluted 1:500 in antibody dilution buffer) was added. The plate was incubated with the secondary antibody for 1-2 h at RT in the dark. For nuclei staining, Hoechst 33342 (dilution 1:2,000) was added. After 3 final washing steps with PBS (5 min each), pictures were taken with the Zeiss Observer.Z1 microscope using a 20x objective and edited with the software Zen.pro 2012 software.

Table 12. Used antibodies for IF staining.

Protein	Species	Reference
COX IV	rabbit	Cell Signaling Technology, #4850S
FLAG-tag	mouse	Sigma-Aldrich, #F1804

2.6 Seahorse assay

The Agilent Seahorse XFp Cell Mito Stress Test (referred to as Seahorse assay) was performed to analyze mitochondrial function. The plate-based assay enables direct measurement of the oxygen consumption rate (OCR) of live cells in real time. All used materials and reagents were obtained by Agilent Technologies, Inc.

The day prior the test, cells were seeded into a Seahorse XFp Cell Culture Miniplate 96-well plate (15,000 cells/well) and incubated overnight under standard conditions with DMEM complete. For each cell line, four replicates were seeded and measured.

24 h before the assay, the sensor cartridge containing the drug ports (XFe96 FluxPak) was hydrated with H₂O and prewarmed at 37°C.

The day of the assay, the medium in the 96-well plate was changed to Seahorse XF DMEM medium pH 7.4 (Table 13) with a final volume of 180 µL/well, after washing the cells one time with Seahorse XF DMEM medium pH 7.4. 1 h before the start of the assay, the cell culture plate was moved to a 37°C non-CO₂ incubator. The H₂O at the sensor cartridge was changed for Agilent Seahorse XF Calibrant solution and incubated for 1 h at 37°C. After this incubation the drug ports of the cartridge were loaded (Table 14) and the calibration of the Agilent Seahorse XFp Analyzer was started. Next the Seahorse XFp Cell Culture Miniplate 96-well plate was added to run the assay.

Evaluation of the assay results was done using the software Wave (version 2.6.1) from Agilent Technologies, Inc.

Table 13. Concentrations supplements for Seahorse XF DMEM medium pH 7.4.

Supplement	Concentration
Glucose	10 mM
Pyruvate	1 mM
Glutamine	2 mM

Table 14. Drug concentrations used for Seahorse assay.

	Compound	Stock conc. (mM)	Conc. in Port (µM)	Conc. per Well (µM)	Vol. per Port (µL)
Port A	Oligomycin	5	10	1	20
Port B	FCCP	2	5	0.5	22
Port C	Piericidin	5	25	2.5	25
	Antimycin	10	100	10	

2.7 Mitochondria Isolation

Mitochondria isolation was performed following the Cold Spring Harbor Protocol “Isolation of Mitochondria from Tissue Culture Cells” with some modifications [112].

Before isolation, cells were expanded and grown to 100% confluency. Once confluency was reached, cells were collected using 0.05% trypsin.

From this point, on all steps were performed unsterile and on ice. Materials and reagents/buffers used were prechilled and all centrifugation steps were performed at 4°C. First, the cell pellet was resuspended in ice-cold RSB hypo buffer (Table 15) and transferred to a 15 mL Dounce homogenizer. Cells were allowed to swell for 10 min before they were broken up using pestle B. Next, 2.5x MS homogenization buffer (Table 15) was added to achieve a final concentration of 1x MS homogenization buffer and mixed by inverting several times. The homogenate was transferred into a 50 mL centrifugation tube. To ensure a complete transfer, the homogenizer was rinsed with 1x MS homogenization buffer and the volume in the centrifugation tube was brought up to 30 mL with 1x MS homogenization buffer. The homogenate was centrifuged for 5 min at 1,300 x *g* to remove nuclei, unbroken cells and large membrane fragments. After centrifugation, the supernatant was poured into a fresh 50 mL centrifugation tube. This step was repeated until no pellet was visible anymore. To pellet mitochondria, the homogenate was centrifuged twice for 15 min at 12,000 x *g*, discarding the supernatant in both steps. Finally, mitochondria were resuspended in potassium lysis buffer (Table 16) and incubated for 15 min at 4°C with gentle agitation. Lysates were clarified by centrifugation for 10 min at 4°C and max speed (> 12,000 x *g*). The supernatant was collected into a fresh tube. Mitochondria isolates were stored at -80°C until further usage.

Table 15. Buffer compositions for mitochondria isolation

MS Homogenization Buffer (2.5x)	
Reagent	Final concentration
Mannitol	525 mM
Sucrose	175 mM
Tris-HCl (pH 7.5)	12.5 mM
EDTA (pH 7.5)	2.5 mM
RSB Hypo Buffer	
Reagent	Final concentration
NaCl	10 mM
MgCl ₂	1.5 mM
Tris-HCl (pH 7.5)	10 mM

Table 16. Components potassium lysis buffer

Component	Concentration
HEPES pH 7.8	40 mM
KCl	125 mM
MgCl ₂	10 mM
Digitonin (Merck, #300410-1GM)	4%
Protease inhibitor Mini Tablets EDTA-free (Pierce™, #A32955)	1x

2.8 Sucrose gradient analysis of mitochondrial ribosomes

In order to protect RNA from degradation during all preparation steps, DNase- and RNase-free materials were used and all areas and equipment were cleaned with RNase Zap (Invitrogen™, #AM9780). Sucrose gradients were made at the Gradient station ip (Biocomp Instruments). Following the protocol provided by the L. Stirling Churchman Laboratory, cells were scraped and lysed in Lauryl Maltoside lysis buffer (Table 17), either containing MgCl₂ (20 mM) or EDTA (5 mM). Cells were dounced 5-6 times in a glass homogenizer before lysate clarification (centrifugation for 5 min at 4°C and 10,000 x g). 450 µL of the clarified lysate were loaded on 10-50% continuous sucrose gradients which were centrifuged at 4°C and 40,000 rpm for 3.5 h. Sucrose solutions were prepared in Lauryl Maltoside lysis buffer with reduced concentrations of detergent (0.1%) and MgCl₂ (10 mM) and without NH₄Cl. Equal fractions, containing 1 mL each were collect from the top to the bottom at the Gradient station ip. During fraction collection, absorbance related to RNA content (254 nm) was measured by a UV monitor.

Equal aliquots of each fraction were analyzed for mitoribosomal protein expression by Western blot.

Table 17. Components Lauryl Maltoside lysis buffer

Component	Concentration
Tris pH 7.5	10 mM
MgCl ₂ / EDTA	20 mM / 5 mM
NH ₄ Cl	50 mM
DTT	0.5 mM
Lauryl Maltoside (GoldBio, #DDM5)	0.25%
Protease inhibitor Mini Tablets EDTA-free (Pierce™, #A32955)	1x

2.9 Immunoprecipitation

If not mentioned otherwise all pipetting, centrifugation and incubation steps during immunoprecipitation (IP) were performed on ice or at 4°C, to avoid protein degradation. Input samples were either mitochondria lysates or whole cell lysates.

Lysates were bound to Anti-FLAG® M2 Magnetic Beads (Sigma-Aldrich, #M8823) or ANTI-FLAG® M2 Affinity Gel (Sigma-Aldrich, #A2220), which were prior equilibrated in the used lysis buffer. For the binding, samples were incubated for 10 min (Magnetic beads) or 1.5-2 h (Affinity Gel) at 4°C with gentle agitation. This step was followed by 3 washing steps with wash buffer (lysis buffer with reduced concentration of detergent and varying salt concentrations). For the ANTI-FLAG® M2 Affinity Gel, 2 washing steps in unmodified lysis buffer were performed in advance to remove excessive unbound protein. If potassium was used during salt washes, the wash buffer was switched to a buffer containing NaCl in the final washing step, to avoid precipitation of proteins in the samples through interaction of potassium with the Laemmli 5x SDS buffer.

For samples analyzed by mass spectrometry, protein was eluted from beads by resuspending in 5-10x volume of the original bead volume elution buffer (Lysis buffer + FLAG peptide (1 mg/mL)) and incubated at 37°C for 30 min. The elution was transferred to a fresh tube and Laemmli 5x SDS buffer was added to 1x.

Samples were then loaded on a 4-12% gel (Invitrogen™, # NP0323PK2 BOX NuPAGE Bis-Tris) and separated according to their molecular weight by electrophoresis for 1 h at 200 V in 1x MES-SDS running buffer (Boston BioProducts, #BP-177). Once the run was completed the gel was placed in a 15 cm dish and washed with deionized H₂O for 2-4 min before Coomassie Instant Brilliant Blue (expedeon, #ISB1L) was added for staining overnight. The following day, the stain was washed out by rocking the gel in deionized H₂O for 2-3 h.

The bands of interest were cut out and stored in 50% methanol in H₂O until mass spectrometry analysis, performed by the “Proteomics Core Facility” of the Whitehead Institute for Biomedical Research. The core uses a “bottom-up” proteomics technology, where proteins are digested by proteases, chromatographically separated and analyzed by tandem mass spectrometry on a Thermo Orbitrap Elite or Thermo Exploris 480 mass spectrometer operated in conjunction with nanoflow HPLC systems. Protein identification and quantitative information are obtained from the acquired data through the use of database search engines and species-specific databases.

For samples analyzed by Western blot, samples were eluted in Laemmli 5x SDS buffer diluted 1:1 in lysis buffer by incubating at 37°C for 30 min. To remove the beads, elutions were centrifuged for 1 min at max speed (>20,000 x g). Samples were further on treated according to the workflow described above for Western blot.

2.10 Statistical evaluation and Data processing

If not mentioned otherwise, preparation and processing of obtained results and data was done in Microsoft Excel 2016. For statistical evaluation GraphPad Prism 8.3.1.549 was used. D'Agostino & Pearson test for normal distribution and unpaired t-test with Welch's correction were performed to detect significant differences in analyzed data sets ($p\text{-value} \leq 0.05$).

Figures for visual demonstration of data were made in GraphPad Prism 8.3.1.549 as well as with the website BioRender.

3 Results

3.1 Knock-out of MGPX effects mitoribosome assembly

Cells lacking MGPX are unable to respire due to a related defect in mitochondrial translation. So far it is unknown where in the process this defect appears.

As described above, GTPases are important factors in all steps of mitochondrial protein biosynthesis including mitoribosome assembly. Some of those steps are still not completely described, opening up the possibility of additional proteins being involved. Identifying binding of MGPX to a specific mitoribosomal subunit could point towards a specific step of mitochondrial translation involving MGPX.

Mitoribosome assembly was assessed using sucrose density gradients and ultracentrifugation. Within a defined gradient, mitoribosomal subunits are expected to sediment according to their sedimentation coefficient (28S, 39S, 55S). Fractions collected from the top of the gradient after centrifugation can be analyzed by immunoblotting by probing for MRPs of both subunits. Automated fraction collection, as performed in our case, enables simultaneous RNA measurement. In the experiments shown here, 10-50% continuous sucrose gradients were used and centrifuged for 3.5 h at 40,000 rpm and 4°C, loaded with cell lysates of 143B WT, MGPX KO and MGPX add-back (AB) cells (expressing FLAG-tagged MGPX).

An ideal sedimentation profile would show clear peaks for the mtSSU and mtLSU as well as a peak for the assembled monosome, indicated by the presence of MRPs of both subunits within the same fraction.

Removal of Mg^{2+} ions induces splitting of the monosome, since ribosome assembly is strongly dependent on the presence of Mg^{2+} ions. EDTA is a common chelator used for this purpose. Exchanging Mg^{2+} with EDTA in used buffers would therefore change the sedimentation profiles, by shifting MRPs to their corresponding individual subunits and lack of a peak representing assembled ribosomes.

143B WT cells showed a sedimentation profile as expected: the 28S mtSSU was detected in fraction 4, the 39S mtLSU mainly in fraction 5 and the assembled monosome in fraction 6 (Figure 11, A). MRPLs were also detected in fraction 4, suggesting that the real peak might reside in between the two fractions. Probed MRPSs (MRPS18B and MRPS27) were also detected in other fractions with reduced intensity (1-3).

MRPL11 and MRPL44 were not detected in fraction 6 of MGPX KO cells indicating a lack of assembled mitoribosomes, which might be related to a defect in mtLSU maturation. Signals detected for the mtSSU were as also reduced in fraction 6.

However in MGPX AB cells, a sedimentation profile similar to WT cells was restored. Probing for FLAG-MGPX showed that the protein tends to sediment in the upper fractions (1-3) in $+MgCl_2$ gradients, where in general free protein accumulates. Induced by DOX treatment MGPX is likely to be overexpressed. In that case enhanced levels of free protein are

expected, since the protein's abundance will exceed the one of its binding partners. Nevertheless, MGPX co-sedimented with both mitoribosomal subunits and the monosome, while CS did not, which suggests binding of MGPX to the mitoribosome (Figure 11, A).

Inducing ribosome splitting by sequestering Mg^{2+} from the environment through addition of EDTA caused an expected shift of MRPs to their individual subunits, which was observed in all tested cell lines (Figure 11, B). Success of EDTA treatment can be evaluated by measurement of RNA content, performed during fraction collection. A clear shift of subunit peaks was observed, whereas a peak for assembled ribosomes is absent. However, mt-rRNAs cannot be distinguished from cytosolic rRNAs by this measurement (Figure 10).

Interestingly, sedimentation profiles of MGPX differed strongly between the two treatments. In presence of EDTA, co-sedimentation of MGPX with both mitoribosomal subunits is enhanced, as indicated by shifted peaks to fraction 4 and 5. Sedimentation of CS is not affected by addition of EDTA, which rules out the possibility that this might be a general profile for mitochondrial proteins (Figure 11, B). This observation suggests intensified binding of MGPX to the individual subunits, potentially related to mitoribosome disassembly.

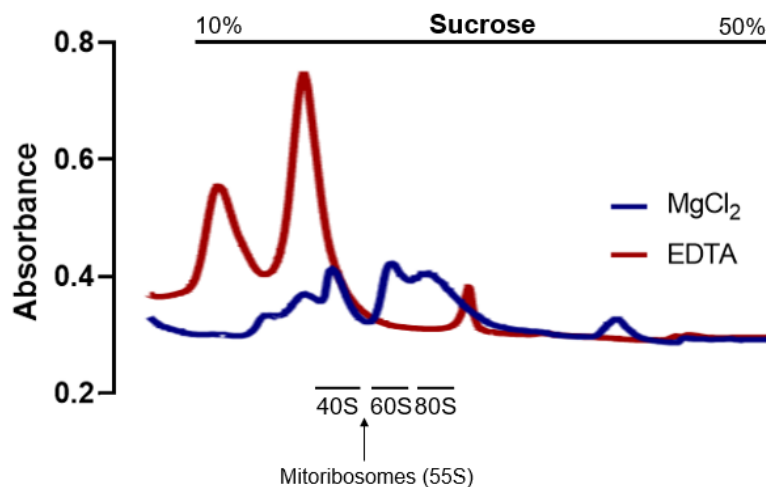
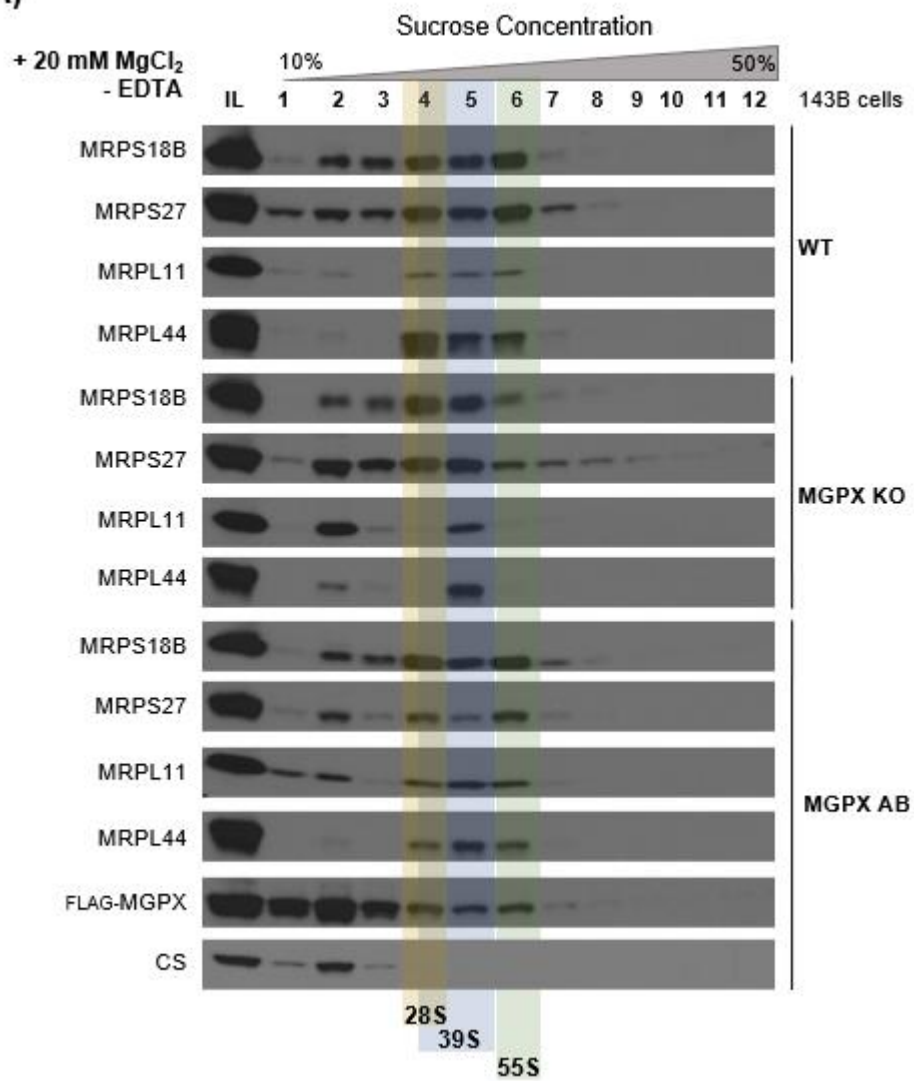


Figure 10. EDTA induces ribosome splitting. During fraction collection of sucrose density gradients, RNA content of fractions was measured by UV-detection of the absorbance at 254 nm. Measured RNA mainly correlates to cytosolic ribosomes and peaks for the individual subunits as well as the assembled monosome are annotated. The arrow points towards the approximate position of the 55S mitoribosomes within the trace, highlighting the difficulty to distinguish mt-RNA from cytosolic RNA. Shown are overlaid UV-traces of 143B WT cells + 20 mM $MgCl_2$ and + 5 mM EDTA.

(A)



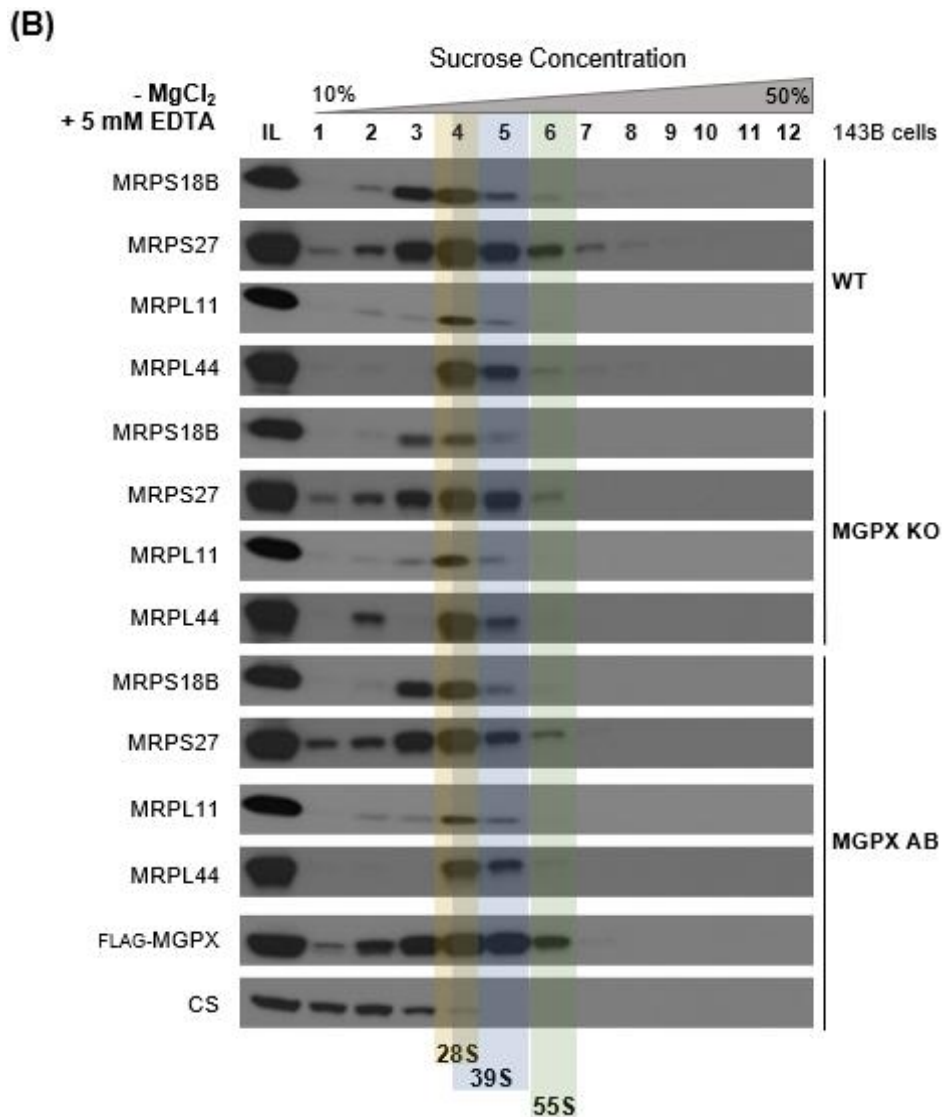


Figure 11. MGPX KO affects the sedimentation profile of mitoribosomes in 143B cells. Mitochondrial ribosomes from 143B WT cells, 143B MGPX KO cells and 143B MGPX AB cells (expressing FLAG-MGPX) were resolved on 10-50% sucrose gradients. Gradients were centrifuged for 3.5 h at 40,000 rpm and 4°C. After centrifugation 12 equal fractions were collected from the top and MRPs of both subunits (MRPS18B, MRPS27, MRPL11 and MRPL44), FLAG-MGPX and control protein citrate synthase (CS) were detected by immunoblotting. 143B WT and MGPX AB cells were cultivated in DMEM galactose prior to the experiment to enhance cellular respiration. Protein expression in MGPX AB cells was induced by addition of DOX (10 ng/mL). In both panels, fractions showing main sedimentation of the individual subunits as well as the monosome are highlighted. **(A)** Samples treated with MgCl₂ (20 mM) to preserve monosome stability. **(B)** Exchanging MgCl₂ with EDTA (5 mM) to induce ribosome splitting.

Observed sedimentation profiles showed that mitoribosome assembly in 143B cells is dependent on the presence of Mg²⁺ ions. Cells lacking MGPX did not show fully assembled mitoribosomes, indicating that MGPX elimination might lead to a defect in mtLSU maturation

ultimately affecting monosome formation. MGPX AB cells were able to restore a sedimentation profile similar to 143B WT cells.

In none of the tested cell lines monosomes were detected when EDTA was added and MRPs were shifted to their corresponding subunits. An interesting observation is that MGPX seems to bind separated mitoribosomal subunits stronger when monosome assembly is inhibited, which could be related to a function in mitoribosome assembly. Alternatively, the depletion of Mg by EDTA may alter the nucleotide binding state of MGPX, and thereby alter its affinity for the ribosomal subunits.

3.2 MGPX binds MRPs when mitoribosomes are disassembled

Since sedimentation profiles obtained by sucrose density gradients showed co-sedimentation of MGPX and MRPs of both subunits when mitoribosomes are disassembled, IPs with similar conditions were performed in order to verify these binding interactions. Therefore, 143B cells stably expressing FLAG-tagged ICT1, MGPX and CS were precipitated using two different buffer conditions (+ 20 mM MgCl₂ / + 5 mM EDTA). ICT1 (also known as MRPL58), a component of the mtLSU, was previously described to precipitate with the whole mitoribosome [113] and was therefore included as a positive control for ribosome dissociation. MRPs of both subunits are expected to co-precipitate with ICT1, representing the assembled monosome. In contrast, after addition of EDTA, no binding to MRPs should be detected. CS is expected to not interact with the mitoribosome at all. Hence, no MRPs should co-immunoprecipitate with the protein. Protein-protein interactions between the protein of interest (MGPX) and probed MRPs can be identified by simultaneous detection of both proteins in IPs.

As expected, ICT1 precipitated with all probed MRPs (MRPS18B, MRPS27, MRPL11, MRPL44) in the presence of Mg²⁺ ions, whereas binding to the mtSSU is reduced if mitoribosomal subunits are separated (EDTA treatment). However, the negative control CS, showed co-immunoprecipitation with probed MRPs in long exposures. The fact that certain proteins were only detected during long exposures indicates that these protein-protein interactions are not particularly strong and might be caused by general protein binding to the mitoribosome, especially in the EDTA treatment (Figure 12, A). Nevertheless, this observation has to be taken into account, when interpreting results for MGPX.

Similar to previously shown results (mitoribosome sedimentation profiles in Figure 11), stronger signals for MRPs of both subunits were detected in disassembled mitoribosomes (+ 5 mM EDTA). Results indicate stronger binding to the mtSSU whereas binding to the mtLSU seemed to be reduced. However, MRPs co-precipitating with CS raised the question whether these interactions are real. In the experiment shown constant salt concentrations (50 mM

NH₄Cl) were used during lysis as well as in all washing steps. Increasing salt concentrations in washing steps would disrupt unphysiological interactions and thereby verify specificity of observed interactions.

Probing with endogenous antibodies confirmed previous described results that ICT1 and MGPX do not co-precipitate [113]. Stable expression of all probed proteins is shown in cell lysates. Double bands for ICT1 and MGPX are caused by the presence of FLAG-tagged and endogenous proteins (Figure 12, B).

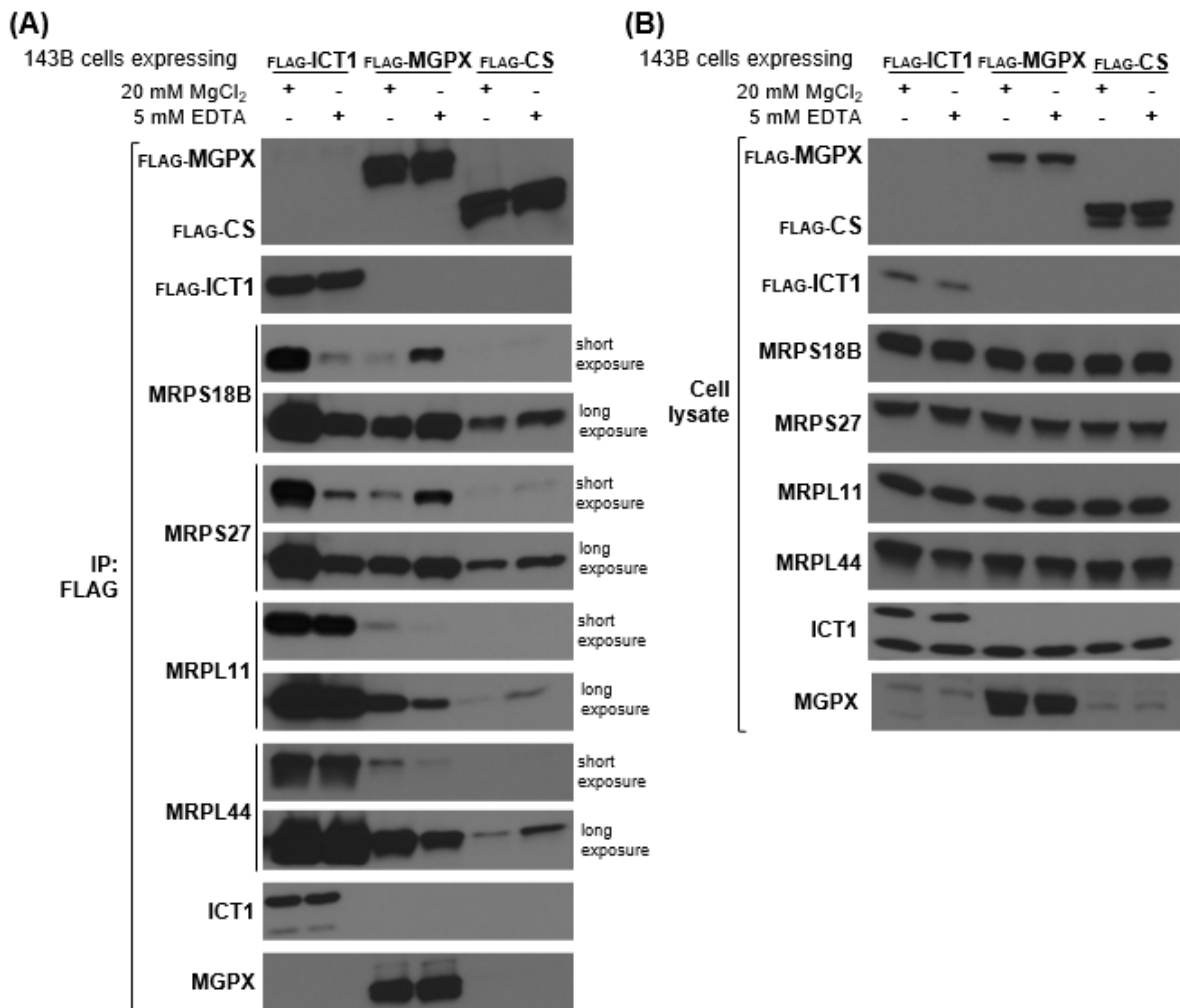


Figure 12: MGPX binding to the mtSSU is enhanced by inhibition of monosome formation.

143B cells stably expressing FLAG-tagged ICT1, FLAG-MGPX and FLAG-CS were analyzed for co-precipitation with MRPs in conditions of assembled (20 mM MgCl₂) and separated (5 mM EDTA) mitoribosomes. FLAG-immunoprecipitates **(A)** and lysates **(B)** were analyzed by immunoblotting for the indicated proteins. All cells were cultivated in DMEM galactose prior to the experiment. Protein expression in cells expressing FLAG-MGPX was induced by addition of DOX (10 ng/mL). **(A)** Successful mitoribosome splitting was confirmed by cells expressing FLAG-ICT1. CS was used as negative control. Short and long exposure indicate relative blot exposure times.

In addition to testing interaction of MGPX with MRPs in cells stably expressing the protein, transfected HEK293T cells were analyzed in similar experiments. Cells in these experiments transiently expressed FLAG-tagged DDX28, MGPX, CS, ICT1 and MRPS27. In contrast to the experiment shown in Figure 12, MgCl₂ (20 mM) was exchanged by EDTA (5 mM) in buffers only during washing steps. CS was included as negative control. ICT1 and MRPS27 were used as representatives of the mtLSU and mtSSU, respectively. Furthermore, DDX28, an RNA helicase proposed to act during mtLSU assembly [33] and claimed to interact with MGPX [39] was transfected into HEK293T cells.

Co-precipitation of proteins with the FLAG-tagged bait would indicate binding. In case of successful disassembly of mitoribosomes, signals for mtLSU and mtSSU proteins would be reduced in MRPS27 and ICT1 precipitates respectively.

Including EDTA only during washing steps was shown to be sufficient to induce ribosome separation, as confirmed by reduced binding of MRPs from the opposite subunit in cells transiently expressing FLAG-tagged ICT1 and MRPS27. Only in one of the two experiments shown, faint bands for MRPS18B, MRPS27 and MRPL44 were detected in IPs of CS (Figure 13, A). As previously mentioned, specificity of observed interactions would have to be further verified by increasing salt concentrations during washing steps.

Both DDX28 as well as MGPX co-precipitated with MRPs of both subunits in both treatments. Bands for MRPL11 were very faint throughout all analyzed samples, which could be related to lower endogenous expression of the protein in cells or the specificity of the used antibody. Immunoprecipitation as well as protein interactions for MGPX seemed to be not affected by EDTA treatment, whereas precipitation of DDX28 appeared to be reduced, which might correlate with lower signal intensities of interaction partners. Surprisingly, expression of DDX28 and MGPX seemed to be decreased compared to other transfected cDNAs, although cells in panel A were transfected with 150 ng DNA for the protein of interest whereas in panel B only 100 ng DNA were used. Errors during the cloning process can be excluded since all plasmids were verified by diagnostic digests and sequencing before usage in transfections.

In the experiments shown no interaction of DDX28 with MGPX could be detected. In fact, none of the transfected proteins co-purified with MGPX or ICT1. However, the used endogenous MGPX antibody showed unspecific bands and weak signals in cell lysates in panel A and B and in multiple other unrelated experiments. Signal detection could be improved by using a monoclonal antibody or using epitope-tagged versions of the protein. Double bands for FLAG-MGPX suggest the presence of variants of the protein still carrying the mitochondrial targeting sequence. Double bands in samples probed for endogenously expressed MGPX, represent the presence of endogenous as well as FLAG-tagged versions of the protein (seen in cells transfected with FLAG-tagged ICT1 and MRPS27; Figure 13, B). Low molecular weight bands detected for endogenous ICT1, in MRPS27 and CS cell lysates are artefacts related to inefficient membrane stripping (Figure 13, B).

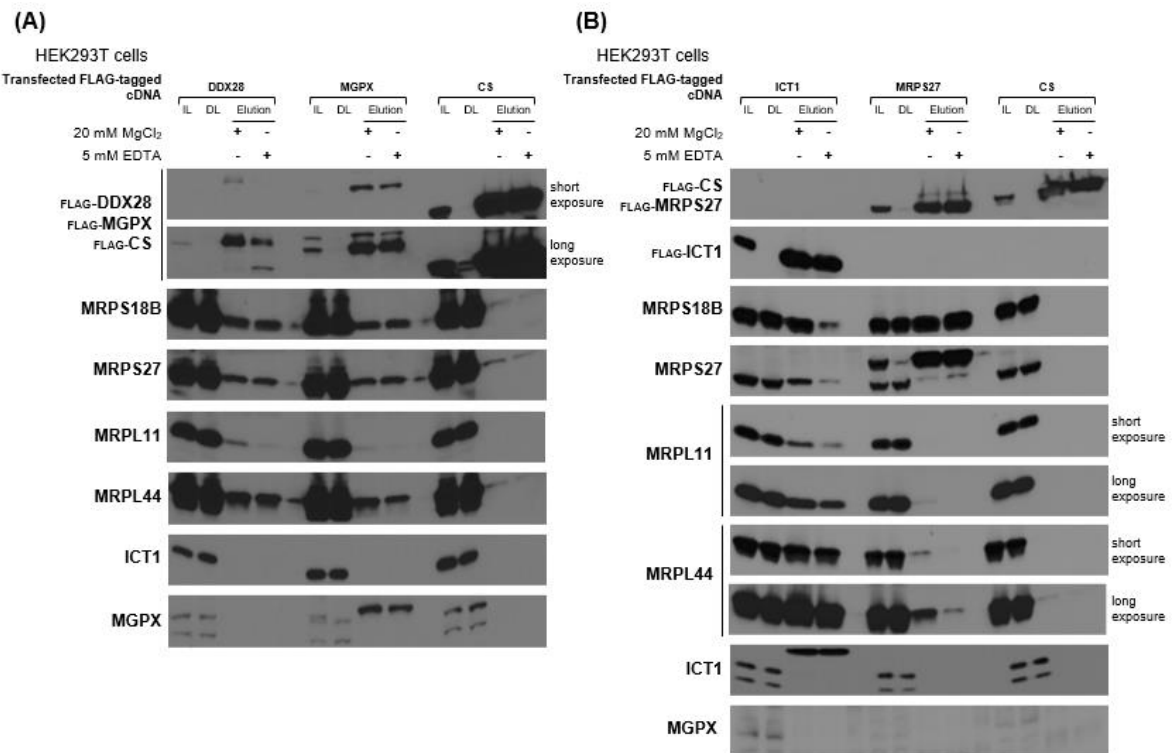


Figure 13. MGPX co-precipitates with MRPs of both mitoribosomal subunits. HEK293T cells were transfected with 150 ng **(A)** and 100 ng **(B)** DNA to express FLAG-tagged DDX28, MGPX, CS, ICT and MRPS27. During the IP, MgCl₂ (20 mM) was exchanged for EDTA (5 mM) in corresponding samples to induce ribosome splitting. Samples were analyzed by immunoblotting for indicated proteins. **(B)** Successful monosome disassembly was confirmed by ICT1 and MRPS27. **(A)** Weak precipitation of MRPs with FLAG-CS was observed. Panels **(A)** and **(B)** show results of two separate experiments performed under the same conditions. Short and long exposure indicate relative blot exposure times. Abbr.: IL = input lysate, DL = depleted lysate.

3.3 TRMT61B is a potential binding partner of MGPX

Mass spectrometry can be used to identify proteins. In the process, proteins are first digested by proteases, usually trypsin which cleaves peptide bonds at carboxyl groups of arginine and lysine. Digested peptides are further separated, fragmented and ionized. The mass spectrometer captures peaks which represent individual peptide fragments, enabling generation of a protein specific mass spectrum. Comparison of this data with established protein databases enables identification of the protein [114].

In the analysis shown here, 143B rho0 cells expressing FLAG-tagged MGPX, IARS2 and LARS2 (both mitochondrial tRNA-synthetases) and 143B WT cells expressing FLAG-tagged MGPX were immunoprecipitated and sent for mass spectrometry. IARS2 and LARS2 represented controls, which have to be included to verify detected binding interactions between proteins, since not all co-purified proteins are real binding partners. Enrichment in

peptide counts from cells expressing the tagged protein of interest compared to the control verifies protein binding to MGPX.

A fraction of the obtained data can be found in the appendix (Supplemental table 2). Peptide counts were normalized to corresponding total spectrum counts and molecular weights (shown as log₁₀), in order to establish a ranking of identified proteins. The ranking shown in Supplemental table 2, was created related to peptide counts in 143B rho0 cells.

Top hits within this ranking were the 3xFLAG-tag used for protein precipitation, the bait (MGPX) and HSPD1, a common chaperone present within mitochondria. As expected, the bait was absent in control cells. Proteins colored in light grey were neglected as they were also detected in control cells. However, MGPX showed a tendency to bind ribosomal proteins, not exclusively of mitochondrial origin. Especially in 143B WT cells expressing FLAG-MGPX, many MRPLs were co-purified. Lack of mt-DNA and thereby mitoribosomes in 143B rho0 cells could be the reason why compared to 143B WT cells reduced amounts of MRPs were co-purified with this sample. Although, missing control cells for FLAG-tagged MGPX 143B WT cells, question detected binding interactions.

In 143B rho0 cells expressing FLAG-tagged MGPX, two interesting proteins were identified as potential binding partners: TRMT61B and YBX1. TRMT61B is a mitochondrial methyltransferase, mentioned before as being involved in mtLSU maturation. Additionally, to this function the protein is responsible for the formation of 1-methyadenosine at position 58 in human mt-tRNAs [115]. YBX1 is a DNA- and RNA-binding protein with various functions, including RNA stabilization, translation repression and transcription regulation. However, it is described to predominantly localize to the cytosol [116].

Since TRMT61B represented the most promising interaction partner for MGPX identified by mass spectrometry, next experiments focused on confirming this interaction. One possibility to investigate such interactions is to perform immunoblotting on IPs of cells expressing both proteins with epitope tags. Using tagged versions of the proteins facilitates detection. If the two co-transfected proteins bind each other both of them would be detected in IPs. Experimental conditions were similar to IPs performed for mass spectrometry to enable comparison of obtained results (4% Digitonin in lysis buffer, 125 mM KCl in lysis and wash buffer).

We cloned FLAG- and HA-tagged versions of TRMT61B, MGPX, DDX28 and CS. Those plasmids were used to co-transfect HEK293T cells in a 1:1 ratio. Co-immunoprecipitations were detected by immunoblotting using epitope-tag specific antibodies as well as endogenous antibodies for MRPs. MRPs were included to assess interactions between TRMT61B and the mitoribosome. Specificity for binding of HA-tagged versions to the FLAG-tagged precipitated baits was verified by including controls, where FLAG-CS was co-transfected with HA-TRMT61B and HA-MGPX, respectively. If the HA-tag would bind used beads on its own, the protein would be detected in the IPs of cells expressing FLAG-tagged

CS, which was not the case in our experiments. Moreover, CS did not co-precipitate with any of the probed MRPs (Figure 14, A).

TRMT61B and MGPX were co-immunoprecipitated using either of the two proteins as bait, indicating specific binding of the two proteins. Both proteins as well as FLAG-tagged DDX28 also showed interactions with endogenous MRPs, which was observed previously for MGPX and DDX28.

In this experiments MGPX co-immunoprecipitated with DDX28, which correlates with results presented by Maiti *et al.* but disagrees with what we saw in cells transiently expressing FLAG-DDX28 alone [39]. Prior mentioned results might be biased by the specificity of the used endogenous MGPX antibody. However, DDX28 was not detected in the mass spectrum of MGPX.

General low signal intensity for cells expressing FLAG-tagged TRMT61B, can be explained by reduced amounts of input protein, also seen by band intensities in cell lysates (Figure 14, B). This might be related to biological variation during cultivation of transfected cells. Cells transfected with FLAG-tagged TRMT61B and HA-tagged MGPX, were overgrown and started to detach from the cell culture plate at the time the experiment was performed. In comparison with other samples less cells were therefore collected, lysed and immunoprecipitated. For all other samples, equal loading as well as comparable transient protein expression and endogenous expression levels for MRPs could be confirmed in cell lysates (Figure 14, B).

Taken together, mass spectrometry analysis of MGPX suggested interactions with MRPs of the mtLSU and identified TRMT61B as a potential binding partner of the GTPase. Interaction of the two proteins was confirmed by co-immunoprecipitation in using FLAG-tagged proteins as baits. However, salt concentrations in performed experiments were rather low (125 mM KCl), which has to be considered concerning the specificity of this interaction.

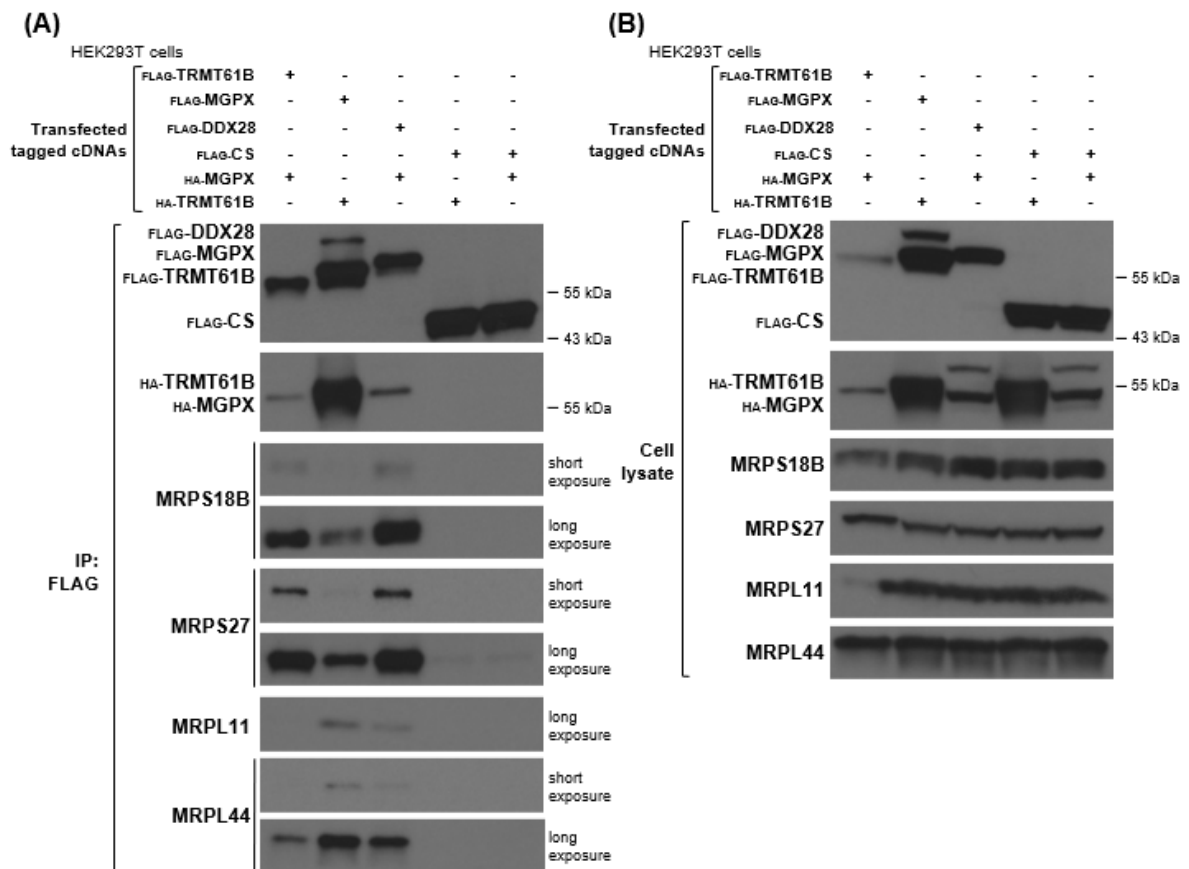


Figure 14. MGPX interacts with TRMT61B and DDX28. (A) MGPX co-immunoprecipitated with TRMT61B and vice versa. DDX28 co-immunoprecipitated with MGPX as well. MGPX, TRMT61B and DDX28 show binding to MRPs of both subunits. CS was added as negative control. FLAG-IPs were prepared from HEK293T cells transiently expressing the indicated tagged cDNA (A) and were analyzed together with cell lysates (B) by immunoblotting, probing for indicated proteins. A ratio of 1:1 was used for transfection aiming for a total of 100 ng DNA. Proteins carrying epitope-tags varied in their molecular weight. Reference marks are given for those proteins and annotations are ordered according to molecular weight. Short and long exposure refer to relative blot exposure times.

3.4 MGPX is essential for mitochondrial translation and mutations in its G-domain affect its ability to restore cellular respiration

In order to determine which of MGPX's protein domains is essential for its functionality, variants of the protein carrying point mutations within the four different G-motifs of the GD of MGPX were cloned and transduced into 143B MGPX KO cells. Locations of these mutations were chosen related to a study published by Huang *et al.*, focusing on BGPX in *Sulfolobus solfataricus* [105]. Six mutations were introduced corresponding to this work within the P-

loop (G1) (N304P; T308N), the switch I (G2) (T329V) and the switch II (G3) (G352P, G352S, F353P) motif. The last three mutations were located in the conserved DxxGF sequence of the BGPX protein family, which corresponds to the DxxGQ motif in Ras-like GTPases [105]. Additionally, a mutation within the G4-motif was generated (D421N). G4 determines the nucleotide specificity of GTPases and the corresponding mutation D119N in Ras-like proteins was described to affect nucleotide affinity [38], [117].

In Figure 15, relevant parts of the amino acid sequences of MGPX and BGPX (*Sulfolobus solfataricus*) are aligned. G-motifs 1-4 are highlighted as well as locations of introduced point mutations. The main question for those mutants was if they were able to restore mitochondrial translation and thereby cellular respiration in cells where MGPX has been knocked out.

	G1		G2		G3														
MGPX 295	PVISVVG	YTCGK	TLIKAL	TGDAAI	QPRDQL	FALD	VTAHAG	TLPSR	MTVLY	VDTI	GFL	354							
BGPX 180	PSIGIV	GYTSGK	SLFN	SLTGL	TQKV	-DTKL	FTM	SPKRY	AIF-	INNR	KIML	VDTV	237						
		G4																	
MGPX 411	DSMV	-----	EVH	NKV	LV	PGY	----	SPTE	PNV	VPV	SAL	RGH	GLQEL	KAE	LDA	AVL	KAT	459	
BGPX 297	VTLN	KIDK	INGD	LYK	KLDL	VEK	LSK	ELYS	PIF	DV	IP	SAL	KRTN	LELL	LRD	KI	YQ	-----	350

Figure 15. Localization of introduced point mutations within the four different G-motifs of MGPX. The amino acid sequence of MGPX (*Homo sapiens*) and BGPX (*Sulfolobus solfataricus*) are aligned and G-motifs are highlighted in grey. Highlighted in red are six point mutations introduced within G-motif 1-3, corresponding to the bacterial homolog BGPX (N304P, T308N, T329V, G352P, G352S, F353P). Numbering refers to MGPX. One mutation was generated in the G4-motif (D421N) highlighted in green. Depicted are relevant sections of the amino acid sequences.

After lentiviral transduction of 143B MGPX KO cells with MGPX mutants, expression of MGPX was validated by immunoblotting and probing for FLAG-tagged MGPX. MGPX expression was stimulated by addition of DOX (10 ng/mL). In case of successful host cell transduction, FLAG-MGPX would be detected at ~55 kDa, similar to protein expression in MGPX AB cells and no signal would be detected in 143B WT cells (negative control).

As expected, no signal and stable expression for FLAG-tagged MGPX was validated in 143B WT cells and MGPX AB cells, respectively. However, signals detected for FLAG-tagged mutated versions of MGPX were very faint compared to MGPX AB and BGPX (Figure 16). One possible explanation is that the generated mutant variants of MGPX are more prone to misfolding and degradation than wild-type MGPX, although no such effects were observed by Huang *et al.* for similar mutations in BGPX [105]. Another explanation may be variability of expression in response to DOX, since DOX inducible expression tends to be more variable than expression from a constitutive promoter. Strong signals for MGPX and BGPX confirmed the used concentration of DOX (10 ng/mL) as sufficient for those plasmids. Equal sample loading was confirmed by probing for Golgin 97.

A heavier version of the protein was faintly detected for N304P and the shape of the band for BGPX might indicate the presence of a double band, including a heavier version of the protein as well. Such an effect can be explained by the presence of the protein not only at mitochondria but rather throughout the whole cell. In this case, a subpopulation of the protein still carries the mitochondrial targeting sequence at the N-terminus, which increases the molecular weight of the protein by ~4 kDa.

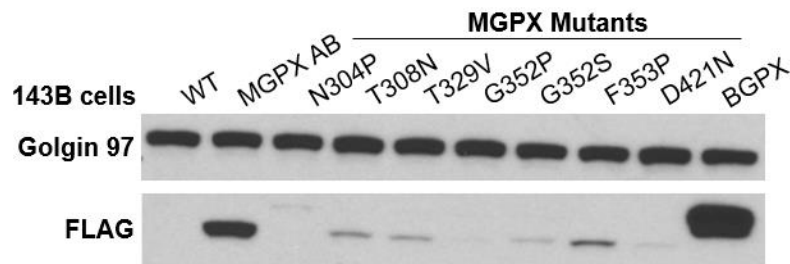
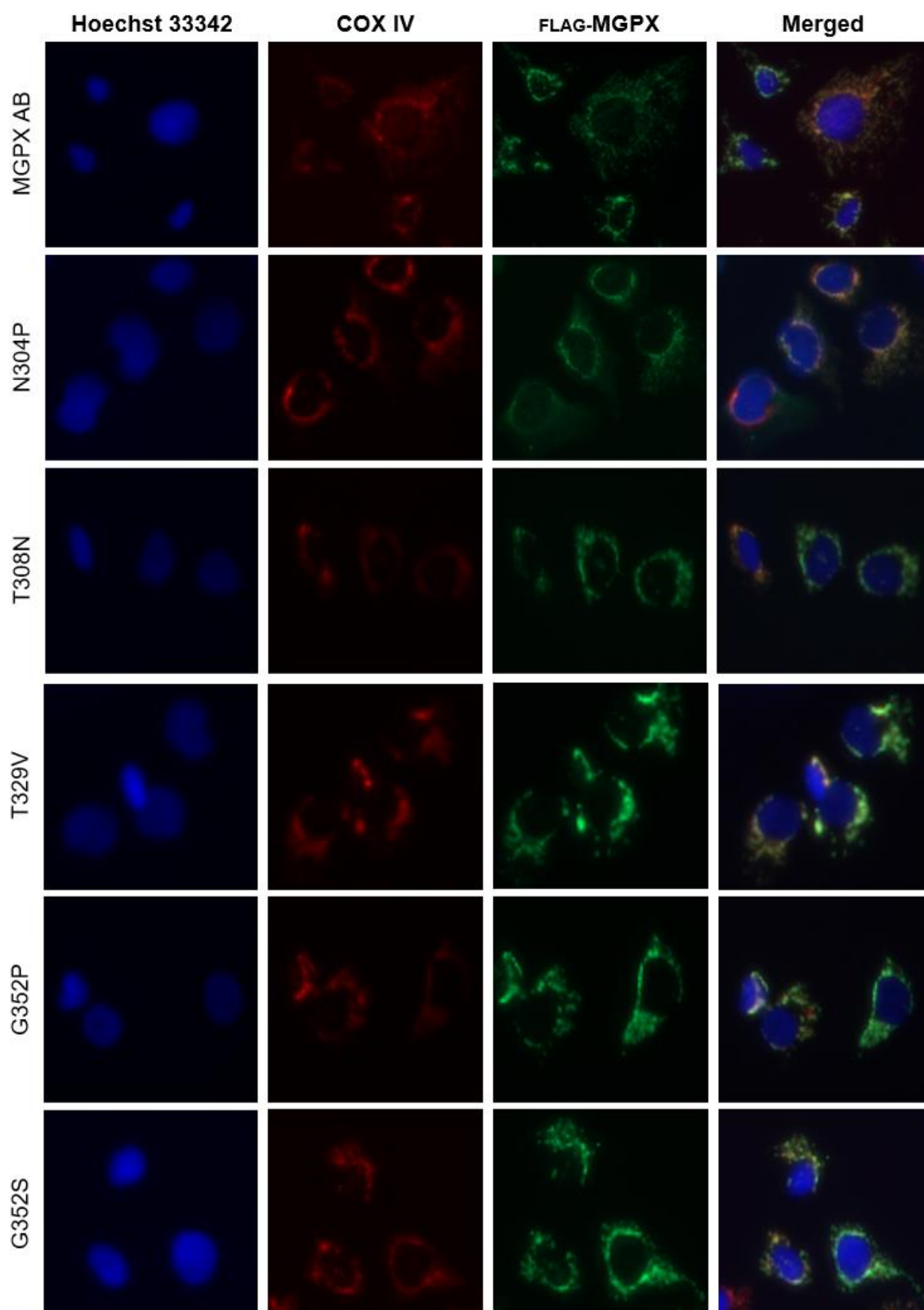


Figure 16. Expression of FLAG-tagged MGPX in generated MGPX mutants. After lentiviral transduction, protein expression in 143B MGPX KO cells expressing aforementioned point mutations was assessed by immunoblotting for the FLAG-tagged MGPX. In addition, the bacterial homolog (BGPX) was induced into 143B MGPX KO cells. Cells were pretreated with DOX (10 ng/mL) and lysed in 1% Triton X-100 buffer. Golgin 97 was used as loading control. MGPX AB cells were used as positive control and 143B WT cells as negative control.

As a verification for translocation of MGPX mutants to mitochondria, IF staining of cells stably expressing the proteins was performed. Using this method, it could be ensured that failure of a mutant to restore cellular respiration was not due to mislocation of the protein. As mitochondrial loading control COX IV, binding to the cytochrome c oxidase (Complex IV) located at the mitochondrial inner membrane, was used (shown in red). The FLAG-tag included in MGPX mutants enabled detection with the corresponding antibody (shown in green). MGPX expression was induced by addition of DOX (100 ng/mL). Cell nuclei were stained with Hoechst 33342. Mitochondria localize around the nucleus in the cytosol. For correctly localized versions of MGPX, the FLAG-MGPX signal would overlap with the signal for COX IV in these areas. Indeed, this phenotype was observed for all seven MGPX mutants and translocation to mitochondria was thereby confirmed for all of them (Figure 17).



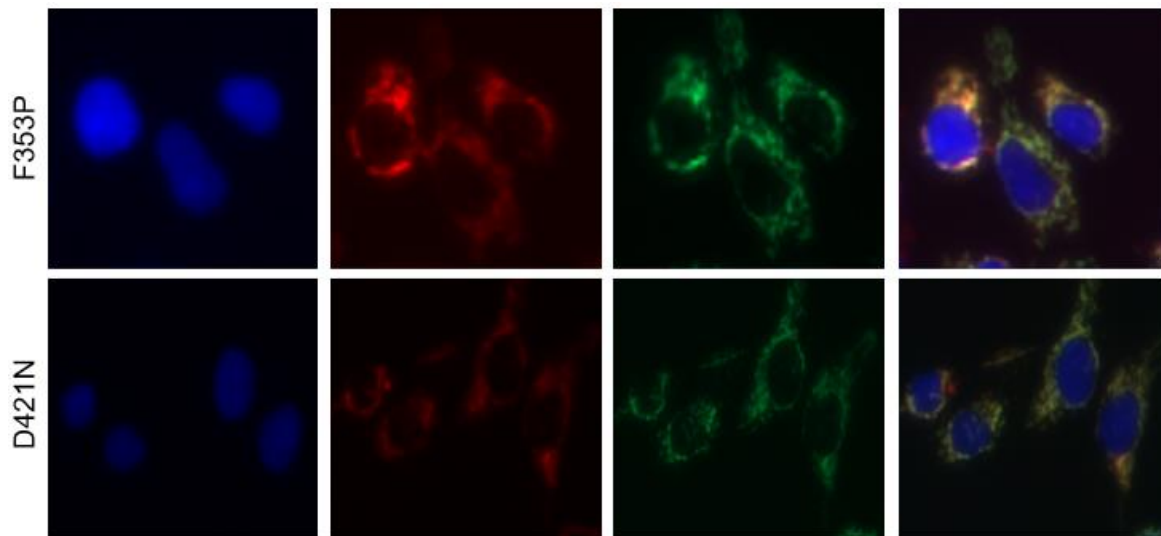


Figure 17. Translocation of MGPX mutants to mitochondria confirmed by IF staining. Prior to fixation cells were treated with DOX (100 ng/mL) for app. 12 h. Shown are 143B MGPX KO cells transduced with generated MGPX mutant plasmids. Localization of proteins to mitochondria was assessed by co-localization with the cytochrome c subunit 4 (COX IV) stained with AlexaFluor® 568. FLAG-MGPX was detected with AlexaFluor® 488 and nuclear staining was conducted with Hoechst 33342. Pictures were taken at the Zeiss Observer.Z1 microscope at a magnification of 40x and were edited with the software Zen.pro 2012.

Once protein expression and translocation to mitochondria was validated, experiments to answer the main question rather MGPX carrying mentioned point mutations is still able to restore cellular respiration, were performed.

In the first experiment, 143B MGPX KO cells transduced with FLAG-tagged MGPX and MGPX mutants expressed by a DOX inducible promoter and were switched from standard DMEM complete to DMEM galactose + 10% DMEM with glucose + DOX (10 ng/mL). Reducing glucose in the culture medium simultaneously reduces the amount of ATP generated by glycolysis, since galactose is metabolized significantly slower. Cells therefore rely on ATP from mitochondria, produced through OXPHOS, for their survival. OXPHOS and ATP synthesis both involve mitochondrial translated proteins, making a functional protein biosynthesis system within the organelle absolutely essential. As mentioned before, knock-out of MGPX affects mitochondrial protein biosynthesis to an extent that makes cell survival impossible without addition of uridine (200 µg/mL). Cellular synthesis of uridine requires a functional electron transport chain, which is not the case in cells lacking MGPX. Without uridine, cells cannot replicate and will therefore stop proliferating. Previous experiments already showed that the MGPX AB is able to restore cellular respiration and thereby ensure survival of 143B MGPX KO cells. MGPX mutants not affecting the GTPase's functionality in mitochondria would be expected to likewise rescue cell growth.

Only two MGPX mutants (F353P and D421N) showed similar cell growth to MGPX AB cells. All other mutations failed to restore cellular respiration, verified by similar cell counts to 143B MGPX KO cells in the performed experiments (Figure 18).

Rescue of F353P correlates with the phenotype of the corresponding mutation in the bacterial homolog BGPX, described by Huang *et al.* [105]. Replacing MGPX with the BGPX in human mitochondria (143B cells) failed to restore cellular respiration, suggesting a rather species-specific function for the two homologs.

The mutation D119N in Ras-like GTPases is described as a constitutively active (GTP bound) mutant due to its reduced affinity for nucleotides and enhanced affinity for its GEF [117]. The results obtained for the corresponding MGPX mutant (D421N) suggest that MGPX is still active in this state, but there is no known GEF for MGPX and further study would be needed to determine whether this mutation locks MGPX in an active state as in the case of RAS.

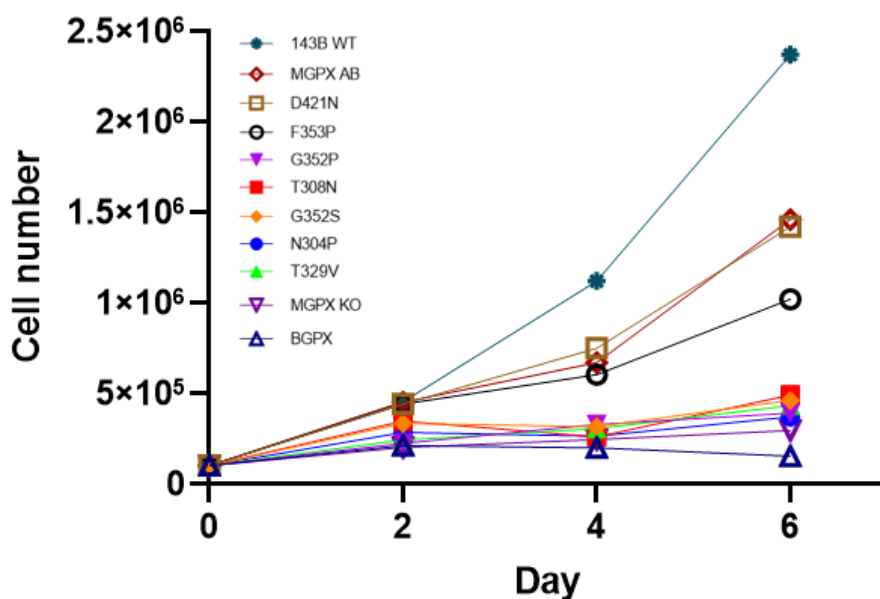


Figure 18. Ability of MGPX AB and MGPX mutants to restore proliferation in 143B MGPX KO cells. On day 0, 100,000 cells were seeded into 6-well cell culture plates (100,000 cells/well) and switched to DMEM galactose + 10% DMEM glucose + DOX (10 ng/mL). Every other day, cell growth was validated by counting total cell numbers. Mutants able to restore mitochondrial translation and ensure cell proliferation were F353P and D421N. One sample was counted per time point (n=1). Shown is a representative for experiments performed of this type, with slightly different medium and DOX conditions as well as time points. Labels of the samples are ordered according to their cell numbers.

Cellular respiration of 143B MGPX KO cells stably expressing MGPX, MGPX mutants and BGPX was further assessed by performing a mitochondrial stress test via Seahorse assay. Protein expression was induced by addition of DOX (20 ng/mL).

The assay enables to distinguish whether cells use glycolysis or mitochondrial respiration as their source of energy. Glycolytic ATP production results in lactate secretion, which acidifies the media, and respiration or OXPHOS converts oxygen to water. Thus, the Seahorse apparatus measures changes in pH to indicate glycolysis and changes in oxygen tension to indicate respiration. During the stress test assay, four defined metabolic modulators are added. The first one is Oligomycin, which blocks activity of the ATPase synthase. The respiratory chain transports electrons to oxygen and couples this transport to the pumping of protons across the inner mitochondrial membrane to maintain an electrochemical potential, while the ATP synthase allows protons to flow back across the membrane, which dissipates the membrane potential to generate ATP. Addition of oligomycin thus causes hyperpolarization of the membrane potential and prevents flow of electrons to oxygen. Oligomycin is added after 20 min and its effects can be seen in decreased OCR of 143B WT, MGPX AB and F353P cells (Figure 19, A). To depolarize the membrane again, FCCP is added. The modulator acts as a carrier of protons across the mitochondrial inner membrane. This proton flow leads to increased oxygen consumption and respiratory rate. This maximal OCR can be observed after the 40 min mark. Addition of the two inhibitors Antimycin A and Piericidin at the 60 min mark rapidly inhibits the respiratory chain itself. Any remaining OCR after this point is thus unrelated to mitochondrial respiration. Figure 19 (A) shows the OCR over the time of the Seahorse assay for 143B WT, MGPX KO and MGPX AB cells as well as for all constructed mutants of MGPX and BGPX. Figure 19 (B) shows the basal oxygen consumption of all cell lines.

The ability of F353P to restore cellular respiration previously observed was further confirmed by Seahorse assay. Basal respiration capacity of those cells was significantly higher than values measured in 143B MGPX KO cells (p -value < 0.0001). However, levels for cells expressing MGPX AB and 143B WT cells could not be reached (p -value < 0.0001 / p -value = 0.079, respectively).

Rescue by D421N was not predominantly obvious in the OCR time course (Figure 19, A). Nevertheless, measured basal respiration capacity was significantly higher compared to 143B MGPX KO (Figure 19, B; p -value = 0.0002).

Values for MGPX AB cells measured in the Seahorse assay were significantly higher than basal respiration capacity measured for 143B WT cells (p -value = 0.0015), which is not in correlation with results observed in rescue experiments in DMEM galactose (Figure 18). Though robust respiration is required for growth in galactose, it is not certain whether differences in respiration levels would always correlate with differences in growth in galactose. Another possible reason for the discrepancy is variation in density of cells plated for the Seahorse assay.

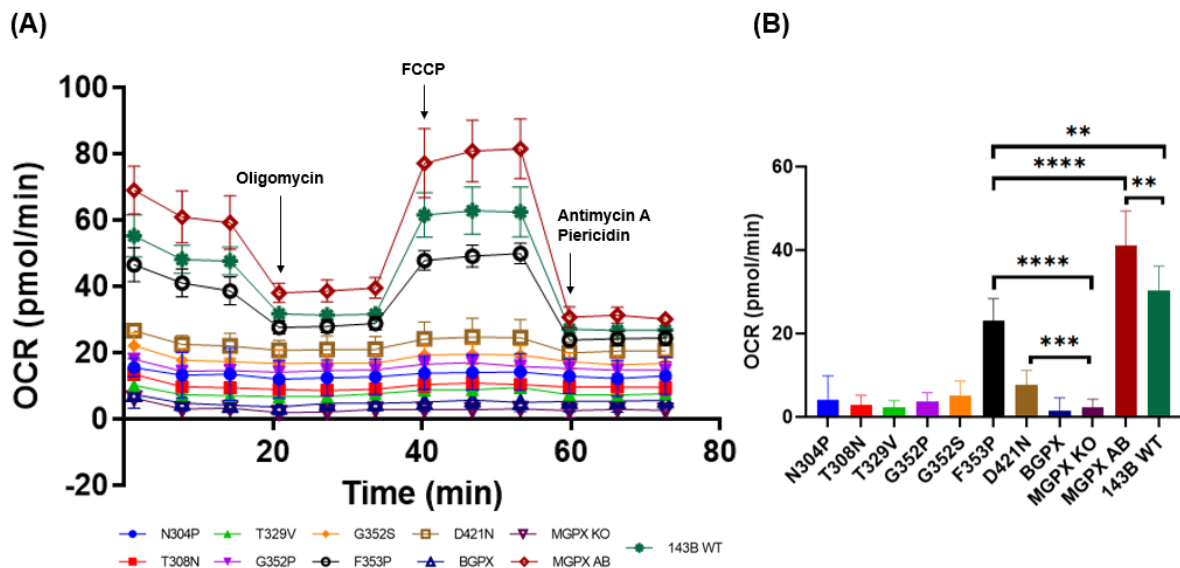


Figure 19. Restoration of cellular respiration by MGPX AB and MGPX mutants F353P and D421N in 143B MGPX KO cells confirmed in mitochondrial stress tests. A mitochondrial stress test was performed via Seahorse assay, which enabled real-time measurement of OCR in cells. 15,000 cells/well were seeded into a Seahorse XFp Cell Culture Miniplate 96-well plate. MGPX protein expression was induced by addition of DOX (20 ng/mL). Error bars show standard deviation (SD). **(A)** OCR measured over the time of the experiment affected by addition of four metabolic modulators (Oligomycin, FCCP, Antimycin A and Piericidin) is shown as the mean of four biological replicates. Time points for addition of the modulators are annotated. Outliers were excluded. For better visual presentation of individual curves all values were similar nudged. **(B)** Basal respiration capacity was calculated as the mean of the first three OCR measurements. Values shown are therefore the mean of 12 individual measurements per group (4 biological replicates per group, 3 measurements per replicate). Statistical significance was validated by unpaired t-test with Welch's correction after testing data sets for normal distribution using D'Agostino & Pearson test (p-values: ** < 0.01; *** < 0.001; **** < 0.0001).

Performed experiments where MGPX was added back into 143B MGPX KO cells confirmed the essentiality of the protein in mitochondrial protein translation and thereby for cell proliferation. BGPX failed to rescue cells. Only two out of seven mutations introduced in MGPX's GD maintained its ability to restore cellular respiration, highlighting the importance of a functional GD for its function. However, protein expression in cell lines stably expressing FLAG-tagged MGPX and MGPX mutants strongly depended on DOX addition and showed varying results related to used DOX concentrations.

4 Discussion

Previous genetic screens and bioinformatic analyses performed in the David M. Sabatini Laboratory, identified the mitochondrial GTPase MGPX (name pseudonymized) and proved it to be an essential factor for mitochondrial protein biosynthesis. GTPases are molecular switches which are involved in several cellular processes including mitochondrial translation. Conformational changes related to nucleotide interactions affect their affinity to effector molecules and thereby regulate and control cellular processes.

No effector molecules, interaction partners or biochemical activities have been described for MGPX so far, which drove the aim of this project to investigate the role of this essential protein in human mitochondria. Attempts to answer this question focused on three main approaches: (1) Analysis of mitoribosomal sedimentation profiles in relation to MGPX, (2) identifying potential binding partners of MGPX and (3) determining which protein domain of MGPX is responsible for its function.

Mitoribosomal sedimentation was analyzed using sucrose density gradients and ultracentrifugation. Within the gradient, ribosomes are expected to sediment according to their sedimentation coefficients, generating a cell line specific sedimentation profile with defined peaks for all three ribosomal subpopulations (SSU, LSU and monosome).

143B cells, where MGPX was knocked out, showed a sedimentation profile different from WT cells. Detection for the mtLSU was reduced and no assembled monosomes were detected (Figure 11, A). Effects mainly focusing on the mtLSU suggest a defect during its maturation, but in order to truly determine the step where this knock-out effects mitoribosome assembly, further investigation would be needed.

One possibility to identify where the process is stopped, would be ribosome profiling. For this approach, cell lysates are treated with RNase before loading on gradients which digests all mRNA not protected by ribosomes. Hence, this procedure requires presence of intact assembled ribosomal monosomes. After centrifugation and immunoblotting for MRPs, fractions enriched for mitoribosomal subunits are pooled and digested with proteinase to reveal mRNA bound by ribosomes. Digested mRNA fragments can be gel-purified and identified by sequencing, enabling determination of the step where ribosomes stalled by specific mRNA sequences [118]. However, monosome formation is inhibited in cells lacking MGPX, making described ribosome profiling likely unfeasible for this cell line.

Potentially cells could be treated with antibiotics (e.g. chloramphenicol or cycloheximide) before RNase treatment to stop translation, but this treatment might bias sedimentation profiles due to general effects of antibiotics on mitochondria. Our collaboration partner for these experiments (L. Stirling Churchman Laboratory at Harvard Medical School) recommended complete abandonment of antibiotics, due to potential biasing effects. In our experiments, we used DOX to induce protein expression in MGPX AB cells. DOX is a known inhibitor for mitochondrial protein translation and therefore could also affect our results. We

used rather low concentrations (10 ng/mL) but the duration of the treatment (up to one week) could potentially affect mitochondria [119].

Moreover, not all cells were treated equal during the experiment. 143B WT cells and 143B MGPX AB cells were cultivated in DMEM galactose, whereas 143B MGPX KO cells were cultivated in DMEM complete containing glucose. Cells lacking MGPX cannot respire and are thereby unable to survive in DMEM galactose. In order to minimize potential biasing related to these differences in culture conditions, all cells should be cultivated with glucose and pretreated with DOX similarly to 143B MGPX AB cells, if DOX treatment is not omitted in future experiments.

Another interesting experiment would be to assess mitochondrial translation and how efficiency of the process is affected by MGPX knock-out, by labeling newly synthesized mitochondrial protein using radioisotopes, like ³⁵S-Methionine/Cysteine. Mitochondrial protein biosynthesis is largely absent in cells where MGPX is missing. Nonetheless, any residual protein biosynthesis remaining in those cells, would be revealed by this assay.

Described changes in sedimentation profiles were observed in the presence of Mg²⁺ ions. Mg²⁺ is an essential factor for ribosome assembly, ribosome-protein-interactions and activity of GTPases. Addition of the metal chelator EDTA sequesters Mg²⁺ ions and thereby initiates ribosomes splitting. Interestingly, those conditions seemed to enhance binding of MGPX to the mitoribosome, observed by co-sedimentation of MGPX with MRPs of both subunits (Figure 11, B).

Co-sedimentation of MGPX with separated mitoribosomal subunits, encouraged follow-up experiments related to the second approach: identifying potential interaction partners of MGPX. Indeed, MGPX was shown to co-immunoprecipitate with proteins of both mitoribosomal subunits in cells stably (Figure 12) as well as transiently expressing (Figure 13) the protein. Strength of these interactions seemed to be increased by EDTA treatment and thereby ribosome dissociation. Binding to the mtSSU appeared stronger. However, signals for probed MRPSs (MRPS27, MRPS18B) were stronger throughout all performed experiments compared to MRPL44 and especially MRPL11. Hence, this observation might be an artificial effect related to qualities of used antibodies.

In general, additional experiments would be needed to verify binding interactions. In all experiments rather low salt concentrations were used and, in some experiments, MRPs were co-precipitated with the negative control CS.

Protein interactions as well as protein stability are strongly affected by salt concentrations in their environment. Concentrations chosen for experiments must be high enough to disrupt unphysiological interactions, but simultaneously should not disrupt specific protein interaction or initiate protein aggregation. The best way to meet all these requirements is to perform IPs with increasing salt concentrations, while assessing if interactions remain.

Similar to, what we show for MGPX, BGPX was described to bind both ribosomal subunits related to nucleotide binding states at its two nucleotide binding domains [104]. Presence of two nucleotide binding domains is a feature shared with MGPX and the bacterial GTPase Der, which is known to regulate its ribosome interactions by GTP-hydrolysis at the two domains [41]. This hydrolysis is strongly depending on the presence of Mg^{2+} ions [38], [104]. MGPX binding to MRPs was observed in absence of Mg^{2+} . Hence, it remains to be clarified if the GTPase is still active under these conditions.

Cells transiently expressing ICT1 (also called MRPL58) or MRPS27 did not precipitate with endogenous MGPX. At least for ICT1, observed results were expected given published data by Busch *et al.* [113]. However, it is surprising given the fact that MGPX showed binding with other MRPLs. Endogenous MRPS27 co-precipitated with MGPX, if MGPX was used as bait. As previously mentioned, missing expression bands might be related to the used endogenous MGPX antibody, which showed unsatisfying specificity and sensitivity throughout multiple experiments.

Encouraged by a study from Maiti *et al.*, mentioning co-precipitation of the RNA-helicase DDX28 and MGPX [39], we tested co-immunoprecipitation in cells transiently expressing one of the two proteins individually, but could not detect binding of the two proteins (Figure 13). Also, in performed mass spectrometry analysis for MGPX, DDX28 was not detected (Supplemental table 2). However, in HEK293T cells co-transfected with DDX28 and MGPX, (Figure 14) co-immunoprecipitation was confirmed. In general, detection of protein interactions by IP and immunoblotting is more sensitive, indicating that this could be a real interaction. In the aforementioned study, binding was confirmed up to physiological salt concentrations of 150 mM (KCl) [39]. We used slightly lower concentrations (125 mM KCl). To fully verify the interaction, salt concentrations should be increased in follow up experiments. Protein overexpression can also cause non-physiological binding interactions. To mitigate this possibility, one can use endogenous antibodies for IP or engineer cell lines with epitope-tagged proteins expressed at endogenous levels.

One specific mitochondrial protein identified in MGPX's interactome caught our attention: the methyltransferase TRMT61B. Similar to MGPX, a homolog of TRMT61B is missing in fungi and the potential bacterial homolog RImN is not essential. However, the protein itself also did not score as an essential factor for cellular respiration in the genetic screen performed by the supervisor, which differs from phenotypes described for MGPX and DDX28 (both essential factors). Co-transfection experiments confirmed the interaction of the two proteins, and TRMT61B co-precipitated with endogenous MRPs as well. It would be interesting to test if the interaction remains when mitoribosomes are separated, which could be tested by IP of cells stably expressing the proteins and removal of Mg^{2+} ions by EDTA treatment. Both TRMT61B and DDX28 are described to localize to mitochondrial RNA granules, where they are involved in RNA maturation and ribosome assembly, respectively. So far five modification

of the 16S mt-rRNA have been described. Given observed interaction with TRMT61B, MGPX might be involved in the 1-methyladenosine modification catalyzed by TRMT61B [27], [42].

Furthermore, MGPX appears to interact with many MRPs, especially of the mtLSU. MRPs probed in IPs (MRPS27, MRPL11, MRPL44) were identified in mass spectrometry analysis as well. However, stronger interaction with the mtLSU disagrees with results of performed IPs, where stronger signals for MRPSs were detected, but these results might be biased by specificity and sensitivity of used endogenous antibodies against MRPs. MRPs were mainly identified in the mass spectrum of 143B WT cells expressing MGPX, which can be explained by the fact that 143B rho0 cells lack mtDNA and thereby mt-rRNA, making mitoribosome formation impossible.

Nevertheless, the IP mass spectrometry generated a list of potential interactors of MGPX. Potential interactors can be assessed based on their attributes in literature and validated by IP with immunoblotting. Ideally IP mass spectrometry data for an identically-prepared control protein, which is not available in this case, would also help identify true versus false positive interactions.

In first confirmation experiments of mass spectrometry data, YBX1 has been excluded, due to it being predominantly expressed in the cytosol. However, potential presence of the protein in mitochondria has been described in literature [120]. Further investigations of the identified interaction with MGPX should therefore be considered, albeit localization of YBX1 to mitochondria should be confirmed prior, by e.g. IF staining.

Finally, to focus on the question of which protein domain is responsible for MGPX's function, mutations were introduced into MGPX's GD and analyzed for their ability to restore cellular respiration. Out of seven cloned mutants, we identified two variants of MGPX that maintained this ability. This was verified by rescue of cell proliferation in DMEM galactose (Figure 18) and mitochondrial stress tests (Figure 19). Failed translocation as a causing factor can be excluded, since localization to mitochondria was confirmed (Figure 17), but instability of the protein caused by introduced mutation could be the case given observed protein expression patterns (Figure 16).

F353P was one of those mutants. Mutations at the neighboring amino acid G352 (G352P and G352S) did not restore cell proliferation or show cellular respiration at similar levels. Corresponding mutations in BGPX were described as being important for alignment of a nucleophilic water molecule, a step necessary for GTP hydrolysis, and showed similar results. Albeit in bacteria, G235S (corresponding to G352S in MGPX) showed significantly higher GTPase activity than exchange of glycine with proline at the same position (G235P). G235S retained the backbone amino group needed for aforementioned nucleophilic water molecule alignment and thereby GTP hydrolysis [105]. Potential lack of GTPase activity for both mutants in MGPX could be related to reduced backbone flexibility, assuming a similar mechanism for nucleophilic water molecule alignment in MGPX. Based on these

assumptions and maintained rescue function of the F353P mutant, the amino acid present at position G352 seems to be more relevant for GTP hydrolysis and the previous step of nucleophilic water molecule alignment.

Besides these three mutations in the G3-motif, mutations in the G1- (N304P) and G2-motif (T308N; T329N) were introduced. All of them failed to restore cellular respiration, correlating with results for similar mutations in BGPX [105]. The mutations seem to interfere with the G-motifs to an extent not compatible with domain functionality or potentially stability of the protein.

D421N (G4-motif) represented the second MGPX mutant able to restore cell proliferation in DMEM galactose. Cellular respiration (basal respiration capacity) measured in Seahorse assay, was not as high as in WT cells or MGPX AB cells but still significantly higher than in 143B MGPX KO cells (Figure 19, B). Depending on performed assays and used expression systems, the corresponding mutation in Ras-like GTPases was described as constitutively activated and with primary negative effects [117]. In our system the mutation appeared to be active.

Within all performed experiments including MGPX mutants, protein expression seemed to be strongly affected by used DOX concentrations, which could present a biasing factor for results obtained. In order to determine DOX concentrations sufficient to induce protein expression but not affecting any other cellular processes or initiating overexpression of the target protein, a DOX titration experiment could be performed. One might also consider complete elimination this influencing factor, by cloning MGPX mutants into a constitutive expression vector.

It would be interesting to test whether how different MGPX mutants affect mitochondria sedimentation profiles and assess their effects on ribosome binding in IP. Usage of constitutive expression vectors for used plasmids would be beneficial in this approach as well, due to the inhibiting effect of DOX on mitochondrial translation.

Next steps could include purification of F353P and D421N mutants and analysis of their effects on MGPX activity *in-vitro*. One method to assess this is differential scanning fluorimetry (DSF). By mixing the purified protein with a ligand, (in our case GTP) and a fluorescent dye, protein folding and stability can be assessed. During the assay, the mixture is gradually heated while fluorescence is monitored. A spike in fluorescence indicates protein unfolding. Binding of the ligand to the target protein stabilizes it, allowing it to remain folded at higher temperature. Prior mentioned identified binding partners of MGPX (TRMT61B and DDX28) may have a similar effect and could be tested using this technique as well.

Further investigations could focus on truncated versions of MGPX and their effects on protein stability and function. First attempts for this approach showed that the protein is still stable, after truncation of the C-terminal, N-terminal or both terminal domains (data not shown). Next experiments could assess cellular respiration of those variants. IF staining should be performed in advance to verify that the protein still localizes to mitochondria.

In addition to mutated variants of MGPX, BGPX was transduced into 143B MGPX KO cells. The protein was not able to restore cellular respiration, suggesting that the two homologs are not interchangeable. Taken into account species-specific differences and actual similarity of the homologs (~30%), this observation is not surprising [101]. However, possible failure due to mislocation has to be excluded, especially since immunoblotting for the protein indicated expression of two versions of the protein, with and without mitochondrial targeting sequence (Figure 16). The shown IF staining (Figure 17) was performed before drug selection of 143B MGPX KO cells stably expressing FLAG-tagged BGPX was completed, which is why those cells were not included.

In conclusion, the presented work revealed effects on mitoribosome assembly in cells lacking MGPX, indicating a potential involvement of the protein in this step or prior during mtLSU maturation. Interactions with MRPLs as well as enzymes (TRMT61B and DDX28) known to be involved in these processes, could be verified. Binding of MGPX to the mitoribosome appeared to be enhanced when the monosome is dissociated by EDTA treatment, consistent with the possibility that MGPX functions as a mitoribosome assembly factor.

Bibliography

- [1] M. Ott, A. Amunts, and A. Brown, "Organization and Regulation of Mitochondrial Protein Synthesis," *Annu. Rev. Biochem.*, vol. 85, no. 1, pp. 77–101, Jun. 2016.
- [2] L. Sagan, "On the origin of mitosing cells," *J. Theor. Biol.*, vol. 14, no. 3, 1967.
- [3] B. E. Christian and L. L. Spremulli, "Mechanism of protein biosynthesis in mammalian mitochondria.," *Biochim. Biophys. Acta*, vol. 1819, no. 9–10, pp. 1035–54, 2012.
- [4] L. Vara, A. A. Kane, J. L. Cahill, E. S. Rasche, and G. F. Kutty Everett, "Complete genome sequence of *Caulobacter crescentus* siphophage Sansa," *Genome Announc.*, vol. 3, no. 5, 2015.
- [5] A. Uzman, H. Lodish, A. Berk, L. Zipursky, and D. Baltimore, "Molecular Cell Biology (4th edition) New York, NY, 2000, ISBN 0-7167-3136-3," *Biochem. Mol. Biol. Educ.*, vol. 29, p. Section 1.2The Molecules of Life, 2000.
- [6] T. M. Schmeing and V. Ramakrishnan, "What recent ribosome structures have revealed about the mechanism of translation," *Nature*, vol. 461, no. 7268. Nature Publishing Group, pp. 1234–1242, 29-Oct-2009.
- [7] B. J. Greber and N. Ban, "Structure and Function of the Mitochondrial Ribosome," *Annu. Rev. Biochem.*, vol. 85, no. 1, pp. 103–132, Jun. 2016.
- [8] E. O. Van Der Sluis *et al.*, "Parallel Structural Evolution of Mitochondrial Ribosomes and OXPHOS Complexes."
- [9] G. Yusupova and M. Yusupov, "High-Resolution Structure of the Eukaryotic 80S Ribosome," *Annu. Rev. Biochem.*, vol. 83, no. 1, pp. 467–486, Jun. 2014.
- [10] B. J. Greber *et al.*, "The complete structure of the 55S mammalian mitochondrial ribosome," *Science (80-.)*, vol. 348, no. 6232, pp. 303–308, Apr. 2015.
- [11] A. Brown *et al.*, "Structures of the human mitochondrial ribosome in native states of assembly," *Nat. Struct. Mol. Biol.*, vol. 24, no. 10, pp. 866–869, Oct. 2017.
- [12] R. Zeng, E. Smith, and A. Barrientos, "Yeast Mitoribosome Large Subunit Assembly Proceeds by Hierarchical Incorporation of Protein Clusters and Modules on the Inner Membrane," *Cell Metab.*, vol. 27, no. 3, pp. 645–656.e7, Mar. 2018.
- [13] J. D. Dinman, "5S rRNA: Structure and Function from Head to Toe.," *Int. J. Biomed. Sci.*, vol. 1, no. 1, pp. 2–7, Jun. 2005.
- [14] A. Brown *et al.*, "Structure of the large ribosomal subunit from human mitochondria," *Science (80-.)*, vol. 346, no. 6210, pp. 718–722, Nov. 2014.
- [15] B. J. Greber *et al.*, "The complete structure of the large subunit of the mammalian mitochondrial ribosome," *Nature*, vol. 515, no. 7526, pp. 283–286, Nov. 2014.
- [16] D. E. Handy and J. Loscalzo, "Redox regulation of mitochondrial function," *Antioxidants and Redox Signaling*, vol. 16, no. 11. Mary Ann Liebert, Inc., pp. 1323–1367, 01-Jun-2012.
- [17] R. J. Mailloux, X. Jin, and W. G. Willmore, "Redox regulation of mitochondrial function with emphasis on cysteine oxidation reactions," *Redox Biology*, vol. 2, no. 1. Elsevier

B.V., pp. 123–139, 2014.

- [18] M. R. Sharma, E. C. Koc, P. P. Datta, T. M. Booth, L. L. Spremulli, and R. K. Agrawal, “Structure of the mammalian mitochondrial ribosome reveals an expanded functional role for its component proteins,” *Cell*, vol. 115, no. 1, pp. 97–108, Oct. 2003.
- [19] A. Amunts *et al.*, “Structure of the yeast mitochondrial,” *Science (80-.)*, vol. 343, no. 6178, pp. 1485–1489, 2014.
- [20] B. J. Greber *et al.*, “The complete structure of the large subunit of the mammalian mitochondrial ribosome,” *Nature*, vol. 515, no. 7526, pp. 283–286, Nov. 2014.
- [21] D. De Silva, Y. T. Tu, A. Amunts, F. Fontanesi, and A. Barrientos, “Mitochondrial ribosome assembly in health and disease,” *Cell Cycle*, vol. 14, no. 14. Taylor and Francis Inc., pp. 2226–2250, 01-Jan-2015.
- [22] S. Fung, T. Nishimura, F. Sasarman, and E. A. Shoubridge, “The conserved interaction of C7orf30 with MRPL14 promotes biogenesis of the mitochondrial large ribosomal subunit and mitochondrial translation,” 2013.
- [23] M. Liu and L. Spremulli, “Interaction of mammalian mitochondrial ribosomes with the inner membrane,” *J. Biol. Chem.*, vol. 275, no. 38, pp. 29400–29406, Sep. 2000.
- [24] R. A. Z. Al-Faresi, R. N. Lightowlers, and Z. M. A. Chrzanowska-Lightowlers, “Mammalian mitochondrial translation-revealing consequences of divergent evolution,” *Biochemical Society Transactions*, vol. 47, no. 5. Portland Press Ltd, pp. 1429–1436, 24-Sep-2019.
- [25] Z. Shajani, M. T. Sykes, and J. R. Williamson, “Assembly of Bacterial Ribosomes,” *Annu. Rev. Biochem.*, vol. 80, no. 1, pp. 501–526, Jul. 2011.
- [26] C. T. Madsen, J. Mengel-Jørgensen, F. Kirpekar, and S. Douthwaite, “Identifying the methyltransferases for m⁵U747 and m⁵U1939 in 23S rRNA using MALDI mass spectrometry.”
- [27] D. Bar-Yaacov *et al.*, “Mitochondrial 16S rRNA Is Methylated by tRNA Methyltransferase TRMT61B in All Vertebrates,” *PLoS Biol.*, vol. 14, no. 9, Sep. 2016.
- [28] S. M. Toh, L. Xiong, T. Bae, and A. S. Mankin, “The methyltransferase YfgB/RlmN is responsible for modification of adenosine 2503 in 23S rRNA,” *RNA*, vol. 14, no. 1, pp. 98–106, Jan. 2008.
- [29] L. Huang *et al.*, “Identification of two Escherichia coli pseudouridine synthases that show multisite specificity for 23S RNA,” *Biochemistry*, vol. 37, no. 45. pp. 15951–15957, 10-Nov-1998.
- [30] N. Mai, Z. M. A. Chrzanowska-Lightowlers, and R. N. Lightowlers, “The process of mammalian mitochondrial protein synthesis,” *Cell and Tissue Research*, vol. 367, no. 1. Springer Verlag, pp. 5–20, 01-Jan-2017.
- [31] Y. Itoh, A. Naschberger, N. Mortezaei, J. Herrmann, and A. Amunts, “Analysis of translating mitoribosome reveals functional characteristics of protein synthesis in mitochondria of fungi,” *bioRxiv*, p. 2020.01.31.929331, May 2020.
- [32] I. Dalla Rosa *et al.*, “MPV17L2 is required for ribosome assembly in mitochondria,” *Nucleic Acids Res.*, vol. 42, no. 13, pp. 8500–8515, 2014.

- [33] Y. T. Tu and A. Barrientos, "The Human Mitochondrial DEAD-Box Protein DDX28 Resides in RNA Granules and Functions in Mitoribosome Assembly," *Cell Rep.*, vol. 10, no. 6, pp. 854–864, Feb. 2015.
- [34] D. De Silva, F. Fontanesi, and A. Barrientos, "The DEAD box protein Mrh4 functions in the assembly of the mitochondrial large ribosomal subunit," *Cell Metab.*, vol. 18, no. 5, pp. 712–725, Nov. 2013.
- [35] T. Kotani, S. Akabane, K. Takeyasu, T. Ueda, and N. Takeuchi, "Human G-proteins, ObgH1 and Mtg1, associate with the large mitochondrial ribosome subunit and are involved in translation and assembly of respiratory complexes."
- [36] S. Goto, A. Muto, and H. Himeno, "JB Review GTPases involved in bacterial ribosome maturation."
- [37] M. Gulati, N. Jain, B. Anand, B. Prakash, and R. A. Britton, "Mutational analysis of the ribosome assembly GTPase RbgA provides insight into ribosome interaction and ribosome-stimulated GTPase activation."
- [38] N. Verstraeten, M. Fauvart, W. Versees, and J. Michiels, "The Universally Conserved Prokaryotic GTPases," *Microbiol. Mol. Biol. Rev.*, vol. 75, no. 3, pp. 507–542, Sep. 2011.
- [39] P. Maiti, H.-J. Kim, Y.-T. Tu, and A. Barrientos, "Human GTPBP10 is required for mitoribosome maturation," *Nucleic Acids Res.*, vol. 46, pp. 11423–11437, 2018.
- [40] L. Wang, "Biological Functions of Novel Mitochondrial Proteins." 2019.
- [41] S. Kumar Tomar, N. Dhimole, M. Chatterjee, and B. Prakash, "Distinct GDP/GTP bound states of the tandem G-domains of EngA regulate ribosome binding," *Nucleic Acids Res.*, vol. 37, no. 7, pp. 2359–2370, 2009.
- [42] S. F. Pearce, P. Rebelo-Guiomar, A. R. D'Souza, C. A. Powell, L. Van Haute, and M. Minczuk, "Regulation of Mammalian Mitochondrial Gene Expression: Recent Advances," *Trends in Biochemical Sciences*, vol. 42, no. 8. Elsevier Ltd, pp. 625–639, 01-Aug-2017.
- [43] L. Van Haute *et al.*, "METTL15 introduces N4-methylcytidine into human mitochondrial 12S rRNA and is required for mitoribosome biogenesis," *Nucleic Acids Res.*, vol. 47, pp. 10267–10281, 2019.
- [44] C. A. Powell and M. Minczuk, "TRMT2B is responsible for both tRNA and rRNA m 5 U-methylation in human mitochondria," *bioRxiv*, p. 797472, Oct. 2019.
- [45] I. M. Moustafa, A. Uchida, Y. Wang, N. Yennawar, and C. E. Cameron, "Structural models of mammalian mitochondrial transcription factor B2," *Biochim. Biophys. Acta - Gene Regul. Mech.*, vol. 1849, no. 8, pp. 987–1002, Aug. 2015.
- [46] H. Chen *et al.*, "The human mitochondrial 12S rRNA m 4 C methyltransferase METTL15 is required for mitochondrial function Downloaded from," 2020.
- [47] J. Rorbach, "YbeY is required for ribosome small subunit assembly and tRNA processing in human mitochondria," *bioRxiv Mol. Biol.*, p. 2019.12.12.874305, Dec. 2019.
- [48] J. S. Tscherne, K. Nurse, P. Popienick, and J. Ofengand, "Purification, cloning, and

characterization of the 16 S RNA m2G1207 methyltransferase from *Escherichia coli*,” *J. Biol. Chem.*, vol. 274, no. 2, pp. 924–929, Jan. 1999.

- [49] Y. Park and J. S. Bader, “How networks change with time,” vol. 28, pp. 40–48, 2012.
- [50] A. Rozanska *et al.*, “The human RNA-binding protein RBFA promotes the maturation of the mitochondrial ribosome,” *Biochem. J.*, vol. 474, no. 13, pp. 2145–2158, Jul. 2017.
- [51] J. He *et al.*, “Human C4orf14 interacts with the mitochondrial nucleoid and is involved in the biogenesis of the small mitochondrial ribosomal subunit.”
- [52] A. Jeganathan, A. Razi, B. Thurlow, and J. Ortega, “The C-terminal helix in the YjeQ zinc-finger domain catalyzes the release of RbfA during 30S ribosome subunit assembly,” *RNA*, vol. 21, no. 6, pp. 1203–1216, Jun. 2015.
- [53] H. Himeno *et al.*, “A novel GTPase activated by the small subunit of ribosome.”
- [54] S. Goto, S. Kato, T. Kimura, A. Muto, and H. Himeno, “RsgA releases RbfA from 30S ribosome during a late stage of ribosome biosynthesis,” *EMBO J.*, vol. 30, no. 1, pp. 104–114, Jan. 2011.
- [55] M. R. Sharma *et al.*, “Interaction of Era with the 30S ribosomal subunit: Implications for 30S subunit assembly,” *Mol. Cell*, vol. 18, no. 3, pp. 319–329, Apr. 2005.
- [56] S. Dennerlein, A. Rozanska, M. Wydro, Z. M. A. Chrzanowska-Lightowlers, and R. N. Lightowlers, “Human ERAL1 is a mitochondrial RNA chaperone involved in the assembly of the 28S small mitochondrial ribosomal subunit,” *Biochem. J.*, vol. 430, pp. 551–558, 2010.
- [57] E. C. Koc and L. L. Spremulli, “Identification of Mammalian Mitochondrial Translational Initiation Factor 3 and Examination of Its Role in Initiation Complex Formation with Natural mRNAs*,” 2002.
- [58] D. L. Rudler *et al.*, “Fidelity of translation initiation is required for coordinated respiratory complex assembly,” *Sci. Adv.*, vol. 5, no. 12, p. eaay2118, Dec. 2019.
- [59] I. V. Chicherin, M. V. Baleva, S. A. Levitskii, E. B. Dashinimaev, I. A. Krashennnikov, and P. Kamenski, “Initiation Factor 3 is Dispensable For Mitochondrial Translation in Cultured Human Cells,” *Sci. Rep.*, vol. 10, no. 1, pp. 1–11, Dec. 2020.
- [60] A. Kuzmenko *et al.*, “Aim-less translation: Loss of *Saccharomyces cerevisiae* mitochondrial translation initiation factor mIF3/Aim23 leads to unbalanced protein synthesis,” *Sci. Rep.*, vol. 6, no. 1, pp. 1–9, Jan. 2016.
- [61] K. Korla and C. K. Mitra, “Kinetic modelling of mitochondrial translation,” *J. Biomol. Struct. Dyn.*, vol. 32, no. 10, pp. 1634–1650, Oct. 2014.
- [62] M. V. Rodnina, “Translation in prokaryotes,” *Cold Spring Harbor Perspectives in Biology*, vol. 10, no. 9. Cold Spring Harbor Laboratory Press, p. a032664, 01-Sep-2018.
- [63] A. Kuzmenko *et al.*, “Mitochondrial translation initiation machinery: Conservation and diversification,” *Biochimie*, vol. 100, no. 1. Elsevier, pp. 132–140, 2014.
- [64] S. Anderson *et al.*, “Sequence and organization of the human mitochondrial genome,”

Nature, vol. 290, no. 5806, pp. 457–465, Apr. 1981.

- [65] N. Desai, A. Brown, A. Amunts, and V. Ramakrishnan, “The structure of the yeast mitochondrial ribosome,” *Science* (80-.), vol. 355, no. 6324, pp. 528–531, Feb. 2017.
- [66] E. H. Williams, C. A. Butler, N. Bonnefoy, and T. D. Fox, “Translation Initiation in *Saccharomyces cerevisiae* Mitochondria: Functional Interactions Among Mitochondrial Ribosomal Protein Rsm28p, Initiation Factor 2, Methionyl-tRNA-Formyltransferase and Novel Protein Rmd9p.”
- [67] O. Rackham and A. Filipovska, “Supernumerary proteins of mitochondrial ribosomes,” *Biochimica et Biophysica Acta - General Subjects*, vol. 1840, no. 4. Elsevier, pp. 1227–1232, 2014.
- [68] E. J. Tucker *et al.*, “Mutations in MTFMT underlie a human disorder of formylation causing impaired mitochondrial translation,” *Cell Metab.*, vol. 14, no. 3, pp. 428–434, Sep. 2011.
- [69] Y. Li, W. B. Holmes, D. R. Appling, and U. L. RajBhandary, “Initiation of protein synthesis in *Saccharomyces cerevisiae* mitochondria without formylation of the initiator tRNA,” *J. Bacteriol.*, vol. 182, no. 10, pp. 2886–2892, May 2000.
- [70] S. Haag *et al.*, “NSUN 3 and ABH 1 modify the wobble position of mt-t RNA Met to expand codon recognition in mitochondrial translation ,” *EMBO J.*, vol. 35, no. 19, pp. 2104–2119, Oct. 2016.
- [71] J. L. Miller, H. Koc, and E. C. Koc, “Identification of phosphorylation sites in mammalian mitochondrial ribosomal protein DAP3,” *Protein Sci.*, vol. 17, no. 2, pp. 251–260, Feb. 2008.
- [72] B. S. Laursen, H. P. Sørensen, K. K. Mortensen, H. Uffe, and S.- Petersen, “Initiation of Protein Synthesis in Bacteria,” *Microbiol. Mol. Biol. Rev.*, vol. 69, no. 1, pp. 101–123, 2005.
- [73] V. L. Worliax, J. M. Bullard, L. Ma, T. Yokogawa, and L. L. Spremulli, “Mechanistic studies of the translational elongation cycle in mammalian mitochondria,” *Biochim. Biophys. Acta - Gene Struct. Expr.*, vol. 1352, no. 1, pp. 91–101, May 1997.
- [74] M. G. Jeppesen, T. Navratil, L. L. Spremulli, and J. Nyborg, “Crystal structure of the bovine mitochondrial elongation factor Tu·Ts complex,” *J. Biol. Chem.*, vol. 280, no. 6, pp. 5071–5081, Feb. 2005.
- [75] P. Bieri, B. J. Greber, and N. Ban, “High-resolution structures of mitochondrial ribosomes and their functional implications,” *Current Opinion in Structural Biology*, vol. 49. Elsevier Ltd, pp. 44–53, 01-Apr-2018.
- [76] S. Chiron, A. Suleau, and N. Bonnefoy, “Mitochondrial Translation: Elongation Factor Tu Is Essential in Fission Yeast and Depends on an Exchange Factor Conserved in Humans but Not in Budding Yeast,” 2005.
- [77] Y. C. Cai, J. M. Bullard, N. L. Thompson, and L. L. Spremulli, “Interaction of mitochondrial elongation factor Tu with aminoacyl-tRNA and elongation factor Ts,” *J. Biol. Chem.*, vol. 275, no. 27, pp. 20308–20314, Jul. 2000.
- [78] G. Hernández and R. Jagus, “Evolution of the Protein Synthesis Machinery and Its Regulation.”

- [79] B. G. Barrell, A. T. Bankier, and J. Drouin, "A different genetic code in human mitochondria," *Nature*, vol. 282, no. 5735, pp. 189–194, 1979.
- [80] T. Martin Schmeing, K. S. Huang, S. A. Strobel, and T. A. Steitz, "An induced-fit mechanism to promote peptide bond formation and exclude hydrolysis of peptidyl-tRNA," *Nature*, vol. 438, no. 7067, pp. 520–524, Nov. 2005.
- [81] R. Temperley, R. Richter, S. Dennerlein, R. N. Lightowers, and Z. M. Chrzanowska-Lightowers, "Hungry codons promote frameshifting in human mitochondrial ribosomes," *Science*, vol. 327, no. 5963. American Association for the Advancement of Science, p. 301, 15-Jan-2010.
- [82] I. Duarte, S. B. Nabuurs, R. Magno, and M. Huynen, "Evolution and Diversification of the Organellar Release Factor Family."
- [83] M. G. Gagnon, S. V. Seetharaman, D. Bulkley, and T. A. Steitz, "Structural basis for the rescue of stalled ribosomes: Structure of YaeJ bound to the ribosome," *Science (80-.)*, vol. 335, no. 6074, pp. 1370–1372, Mar. 2012.
- [84] A. Amunts, A. Brown, J. Toots, S. H. W. Scheres, and V. Ramakrishnan, "The structure of the human mitochondrial ribosome," *Science (80-.)*, vol. 348, no. 6230, pp. 95–98, Apr. 2015.
- [85] S. A. Ayyub, F. Gao, R. N. Lightowers, and Z. M. Chrzanowska-Lightowers, "Rescuing stalled mammalian mitoribosomes - what can we learn from bacteria?," *Journal of cell science*, vol. 133, no. 1. NLM (Medline), 02-Jan-2020.
- [86] E. Scolnick, R. Tompkins, T. Caskey, and M. Nirenberg, "Release factors differing in specificity for terminator codons.," *Proc. Natl. Acad. Sci. U. S. A.*, vol. 61, no. 2, pp. 768–774, 1968.
- [87] C. C. Lee, K. M. Timms, C. N. Trotman, and W. P. Tate, "Isolation of a rat mitochondrial release factor. Accommodation of the changed genetic code for termination.," *J. Biol. Chem.*, vol. 262, no. 8, pp. 3548–3552, 1987.
- [88] S. Adio *et al.*, "Dynamics of ribosomes and release factors during translation termination in *E. coli*," 2018.
- [89] F. Peske, S. Kuhlkoetter, M. V. Rodnina, and W. Wintermeyer, "Timing of GTP binding and hydrolysis by translation termination factor RF3."
- [90] M. Tsuboi *et al.*, "EF-G2mt Is an Exclusive Recycling Factor in Mammalian Mitochondrial Protein Synthesis."
- [91] C. Guyomar and R. Gillet, "When transfer-messenger RNA scars reveal its ancient origins," *Ann. N. Y. Acad. Sci.*, vol. 1447, no. 1, pp. 80–87, Jul. 2019.
- [92] S. Ude, J. Lassak, A. L. Starosta, T. Kraxenberger, D. N. Wilson, and K. Jung, "Translation elongation factor EF-P alleviates ribosome stalling at polyproline stretches," *Science (80-.)*, vol. 339, no. 6115, pp. 82–85, Jan. 2013.
- [93] N. Caliskan, I. Wohlgemuth, N. Korniy, M. Pearson, F. Peske, and M. V. Rodnina, "Conditional Switch between Frameshifting Regimes upon Translation of dnaX mRNA," *Mol. Cell*, vol. 66, no. 4, pp. 558-567.e4, May 2017.
- [94] M. R. Gibbs, K.-M. Moon, M. Chen, R. Balakrishnan, L. J. Foster, and K. Fredrick,

“Conserved GTPase LepA (Elongation Factor 4) functions in biogenesis of the 30S subunit of the 70S ribosome.”

- [95] P. Zhu *et al.*, “Human elongation factor 4 regulates cancer bioenergetics by acting as a mitochondrial translation switch,” *Cancer Res.*, vol. 78, no. 11, pp. 2813–2824, Jun. 2018.
- [96] H. R. Bourne, D. A. Sanders, and F. McCormick, “The GTPase superfamily: conserved structure and molecular mechanism,” *Nature*, vol. 349, no. 6305. Nature Publishing Group, pp. 117–127, 1991.
- [97] K. Karbstein, “Role of GTPases in ribosome assembly,” *Biopolymers*, vol. 87, no. 1, pp. 1–11, Sep. 2007.
- [98] S. R. Sprang, “G proteins, effectors and GAPs: Structure and mechanism,” *Curr. Opin. Struct. Biol.*, vol. 7, no. 6, pp. 849–856, Dec. 1997.
- [99] M. Paduch, F. Jeleń, and J. Otlewski, “Structure of small G proteins and their regulators.”
- [100] D. D. Leipe, Y. I. Wolf, E. V. Koonin, and L. Aravind, “Classification and evolution of P-loop GTPases and related ATPases,” *J. Mol. Biol.*, vol. 317, no. 1, pp. 41–72, Mar. 2002.
- [101] K. Srinivasan, S. Dey, and J. Sengupta, “Structural modules of the stress-induced protein HflX: an outlook on its evolution and biological role,” *Current Genetics*, vol. 65, no. 2. Springer Verlag, pp. 363–370, 05-Apr-2019.
- [102] T. Morimoto *et al.*, “Six GTP-binding proteins of the Era/Obg family are essential for cell growth in *Bacillus subtilis*,” *Microbiology*, vol. 148, no. 11. Microbiology Society, pp. 3539–3552, 01-Nov-2002.
- [103] S. Y. Gerdes *et al.*, “Experimental determination and system level analysis of essential genes in *Escherichia coli* MG1655,” *J. Bacteriol.*, vol. 185, no. 19, pp. 5673–5684, Oct. 2003.
- [104] N. Jain, N. Vithani, A. Rafay, and B. Prakash, “Identification and characterization of a hitherto unknown nucleotide-binding domain and an intricate interdomain regulation in HflX-a ribosome binding GTPase.”
- [105] B. Huang *et al.*, “Functional study on GTP hydrolysis by the GTP-binding protein from *Sulfolobus solfataricus*, a member of the HflX family.”
- [106] L. A. Kelley, S. Mezulis, C. M. Yates, M. N. Wass, and M. J. E. Sternberg, “The Phyre2 web portal for protein modeling, prediction and analysis,” *Nat. Protoc.*, vol. 10, no. 6, pp. 845–858, Jun. 2015.
- [107] Y. Zhang *et al.*, “HflX is a ribosome-splitting factor rescuing stalled ribosomes under stress conditions,” *Nat. Struct. Mol. Biol.*, vol. 22, no. 11, pp. 906–913, Nov. 2015.
- [108] M. L. Coatham, H. E. Brandon, J. J. Fischer, T. Schümmer, S. Schümmer, and H.-J. Wieden, “The conserved GTPase HflX is a ribosome splitting factor that binds to the E-site of the bacterial ribosome,” *Nucleic Acids Res.*, vol. 44, no. 4, pp. 1952–1961, 2016.
- [109] S. Dey, C. Biswas, and J. Sengupta, “The universally conserved GTPase HflX is an

RNA helicase that restores heat-damaged Escherichia coli ribosomes,” 2519 *J. Cell Biol.*, vol. 217, p. 2519, 2018.

- [110] E. B. Warren, A. E. Aicher, J. P. Fessel, and C. Konradi, “Mitochondrial DNA depletion by ethidium bromide decreases neuronal mitochondrial creatine kinase: Implications for striatal energy metabolism,” *PLoS One*, vol. 12, no. 12, Dec. 2017.
- [111] D. G. Gibson, L. Young, R. Y. Chuang, J. C. Venter, C. A. Hutchison, and H. O. Smith, “Enzymatic assembly of DNA molecules up to several hundred kilobases,” *Nat. Methods*, vol. 6, no. 5, pp. 343–345, Apr. 2009.
- [112] D. A. Clayton and G. S. Shadel, “Isolation of mitochondria from tissue culture cells,” *Cold Spring Harb. Protoc.*, vol. 2014, no. 10, pp. 1109–1111, Oct. 2014.
- [113] J. D. Busch *et al.*, “MitoRibo-Tag Mice Provide a Tool for In Vivo Studies of Mitochondrial Ribosome Composition,” *Cell Rep.*, vol. 29, no. 6, pp. 1728–1738.e9, Nov. 2019.
- [114] P. Wang and S. R. Wilson, “Mass spectrometry-based protein identification by integrating de novo sequencing with database searching,” *BMC Bioinformatics*, vol. 14 Suppl 2, no. Suppl 2, p. S24, 2013.
- [115] T. Chujo and T. Suzuki, “Trmt61B is a methyltransferase responsible for 1-methyladenosine at position 58 of human mitochondrial tRNAs,” *RNA*, vol. 18, no. 12, pp. 2269–2276, Dec. 2012.
- [116] U. Raffetseder *et al.*, “Splicing factor SRp30c interaction with Y-box protein-1 confers nuclear YB-1 shuttling and alternative splice site selection,” *J. Biol. Chem.*, vol. 278, no. 20, pp. 18241–18248, May 2003.
- [117] R. H. Cool, G. Schmidt, C. U. Lenzen, H. Prinz, D. Vogt, and A. Wittinghofer, “The Ras Mutant D119N Is Both Dominant Negative and Activated,” *Mol. Cell. Biol.*, vol. 19, no. 9, pp. 6297–6305, Sep. 1999.
- [118] K. Rooijers, F. Loayza-Puch, L. G. Nijtmans, and R. Agami, “Ribosome profiling reveals features of normal and disease-associated mitochondrial translation,” *Nat. Commun.*, vol. 4, no. 1, pp. 1–8, Dec. 2013.
- [119] K. B. Wallace, V. A. Sardão, and P. J. Oliveira, “Mitochondrial determinants of doxorubicin-induced cardiomyopathy,” *Circulation Research*. Lippincott Williams and Wilkins, pp. 926–941, 27-Mar-2020.
- [120] N. C. de Souza-Pinto *et al.*, “Novel DNA mismatch-repair activity involving YB-1 in human mitochondria,” *DNA Repair (Amst.)*, vol. 8, no. 6, pp. 704–719, Jun. 2009.

List of Figures

Figure 1. Structural comparison of mammalian and yeast mitochondrial ribosomes and bacterial ribosomes	12
Figure 2. Ribosome assembly line – Large subunit (LSU)	16
Figure 3. Ribosome assembly line – Small subunit (SSU)	19
Figure 4. Translation initiation	22
Figure 5. Translation elongation.	24
Figure 6. Translation termination	27
Figure 7. Translation complex recycling.	28
Figure 8. Rescue mechanisms for stalled ribosomes	30
Figure 9. Structural models of BGPX and MGPX	33
Figure 10. EDTA induces ribosome splitting	51
Figure 11. MGPX KO affects the sedimentation profile of mitoribosomes in 143B cells	53
Figure 12: MGPX binding to the mtSSU is enhanced by inhibition of monosome formation	55
Figure 13. MGPX co-precipitates with MRPs of both mitoribosomal subunits.	57
Figure 14. MGPX interacts with TRMT61B and DDX28.	60
Figure 15. Localization of introduced point mutations within the four different G-motifs of MGPX.	61
Figure 16. Expression of FLAG-tagged MGPX in generated MGPX mutants.	62
Figure 17. Translocation of MGPX mutants to mitochondria confirmed by IF staining.	64
Figure 18. Ability of MGPX AB and MGPX mutants to restore proliferation in 143B MGPX KO cells	65
Figure 19. Restoration of cellular respiration by MGPX AB and MGPX mutants F353P and D421N in 143B MGPX KO cells confirmed in mitochondrial stress tests	67

List of Tables

Table 1. Composition of mammalian, bacterial and yeast ribosomes.	11
Table 2. List of cloned plasmids.	36
Table 3. Reaction mix plasmid fragment generation PCR.	37
Table 4. Protocol plasmid fragment generation PCR.	37
Table 5. Primers for fragment generation PCR.	37
Table 6. Reaction mix for backbone linearization.	38
Table 7. GoTaq Master Mix for colony PCR	39
Table 8. Protocol colony PCR.	40
Table 9. Transfection mix for virus production	41
Table 10. Used antibodies for Western blot.	43
Table 11. Components 1% Triton X-100 buffer	44
Table 12. Used antibodies for IF staining.	44
Table 13. Concentrations supplements for Seahorse XF DMEM medium pH 7.4	45
Table 14. Drug concentrations used for Seahorse assay.	45
Table 15. Buffer compositions for mitochondria isolation	46
Table 16. Components potassium lysis buffer	47
Table 17. Components Lauryl Maltoside lysis buffer	47

List of Abbreviations

10-formyl-THF	10-formyltetrahydrofolate
aa-tRNA	Aminoacyl-tRNA
AB	Add-back
Arf	Alternative rescue factor
ATP	Adenosine triphosphate
BGPX	Bacterial GTPase X
bp	Base pairs
BSA	Bovine serum albumin
CP	Central protuberance
CS	Citrate synthase
CTD	C-terminal domain
DSF	Differential scanning fluorimetry
DL	Depleted lysate
DMEM	Dulbecco's Modified Eagle's Medium
DOX	Doxycycline
DTT	Dithiothreitol
ECL	Enhanced chemiluminescence
EF	Elongation factor
ERAL1	Era-like 1
EtBr	Ethidium bromide
FACS	Fluorescence activated cell sorting
FBS	Fetal bovine serum
fMet-tRNA ^{Met}	Aminoacylated and formylated initiator tRNA
FwdP	Forward primer
GAP	GTPase-activating protein
GEF	Guanine nucleotide exchange factor
GDI	Guanine nucleotide dissociation inhibitor
GDP	Guanosine diphosphate
GTP	Guanosine triphosphate
GTPBP	GTP-binding protein
HEK	Human embryonic kidney cells
ICT1	Immature colon carcinoma transcript 1
IF	Immunofluorescence
IL	Input lysate
IP	Immunoprecipitation
kb	Kilobases
kDa	Kilodalton
KO	Knock-out
LB	Lysogeny broth

LSU	Large ribosomal subunit
MGPX	Mitochondrial GTPase X
mRNA	Messenger RNA
MRP	Mitoribosomal protein
MRPL	Mitoribosomal large-subunit protein
MRPS	Mitoribosomal small-subunit protein
mt	Mitochondrial
mtFMT	Methionyl-tRNA formyltransferase
Mtg	Mitochondrial GTPases
RRF	Ribosome recycling factor
NTD	N-terminal domain
NTP	Nucleotide triphosphate
OCR	Oxygen consumption rate
ORF	Open reading frame
OXPPOS	Oxidative phosphorylation
PBS	Phosphate Buffered Saline
PEI	Polyethylenimine
PTC	Peptidyl transferase center
PVDF	Polyvinylidene fluoride
RevP	Reverse primer
RF	Release factors
r-proteins	Ribosomal proteins
rRNA	Ribosomal RNA
R-state	Rotated state
RT	Room temperature
SDS-PAGE	Sodium dodecyl sulfate polyacrylamide gel electrophoresis
SIMIBI	Signal recognition particle, MinD and BioD class
SSU	Small ribosomal subunit
TAE	Tris-Acetate-EDTA
TBST	Tris Buffered Saline with Tween
THF	Tetrahydrofolate
TRAFAC	Translation factors class
tRNA	Transfer RNA
UTR	Untranslated regions
WT	Wild-type

Appendix

Supplemental table 1. Cloned mutants of MGPX

Mutation	Primers
N304P	<i>Fragment 1</i>
	FwdP: CACTTCCTACCCTCGTAAAGTCGACACCGgccaccATGTGGGCCCTGCGGGCCGCCGTAC
	RevP: tggctttccgcaAGGgtataccccaccacggagatcacg
	<i>Fragment 2</i>
FwdP: gtgatctccgtgggggtatacaCCTtgcggaaagaccacgctg	
RevP: ttcacaaatgtgtaatccagaggttgattgatCTTATTACTTGTATCATCGTCATCCTTG	
T308N	<i>Fragment 1</i>
	FwdP: CACTTCCTACCCTCGTAAAGTCGACACCGgccaccATGTGGGCCCTGCGGGCCGCCGTAC
	RevP: cagtgcttgatcagcgtGTTctttccgcaattgtatac
	<i>Fragment 2</i>
FwdP: gtatacaaatgcggaaagAACacgctgatcaaggcactg	
RevP: ttcacaaatgtgtaatccagaggttgattgatCTTATTACTTGTATCATCGTCATCCTTG	
T329V	<i>Fragment 1</i>
	FwdP: CACTTCCTACCCTCGTAAAGTCGACACCGgccaccATGTGGGCCCTGCGGGCCGCCGTAC
	RevP: cgtgggccgtgacgtccagCACggcaaacagctggtcccgt
	<i>Fragment 2</i>
FwdP: acgggaccagctgttggcGTGctggacgtcacggcccacg	
RevP: ttcacaaatgtgtaatccagaggttgattgatCTTATTACTTGTATCATCGTCATCCTTG	
G352P	<i>Fragment 1</i>
	FwdP: CACTTCCTACCCTCGTAAAGTCGACACCGgccaccATGTGGGCCCTGCGGGCCGCCGTAC
	RevP: gtgcggcagctgggagaggaaTGGgatggtgtccacgtacaggac
	<i>Fragment 2</i>
FwdP: gtcctgtacgtggacaccatcCCAAtcctctcccagctgccgcac	
RevP: ttcacaaatgtgtaatccagaggttgattgatCTTATTACTTGTATCATCGTCATCCTTG	
G352S	<i>Fragment 1</i>
	FwdP: CACTTCCTACCCTCGTAAAGTCGACACCGgccaccATGTGGGCCCTGCGGGCCGCCGTAC
	RevP: gtgcggcagctgggagaggaaTGAgatggtgtccacgtacaggac
	<i>Fragment 2</i>
FwdP: gtcctgtacgtggacaccatcTCAAtcctctcccagctgccgcac	
RevP: ttcacaaatgtgtaatccagaggttgattgatCTTATTACTTGTATCATCGTCATCCTTG	
F353P	<i>Fragment 1</i>
	FwdP: CACTTCCTACCCTCGTAAAGTCGACACCGgccaccATGTGGGCCCTGCGGGCCGCCGTAC
	RevP: cgtgcggcagctgggagagTGGgccgatggtgtccacgtac
	<i>Fragment 2</i>
FwdP: gtacgtggacaccatcggcCCAAtcctctcccagctgccgcacg	
RevP: ttcacaaatgtgtaatccagaggttgattgatCTTATTACTTGTATCATCGTCATCCTTG	
D421N	<i>Fragment 1</i>
	FwdP: CACTTCCTACCCTCGTAAAGTCGACACCGgccaccATGTGGGCCCTGCGGGCCGCCGTAC
	RevP: gctgtaccgggacagagGTTgactttattgtgaacctcac
	<i>Fragment 2</i>
FwdP: gaggtcacaataaagtcAACctcgtgccgggtacagc	
RevP: ttcacaaatgtgtaatccagaggttgattgatCTTATTACTTGTATCATCGTCATCCTTG	

Supplemental table 2. Mass spectrometry data for MGPX

Identified Protein	Accession Number	Alternate ID	Molecular weight (kDa)	Total Spectrum Counts:					
				MGXP	IARS2	LARS2	Rank	MGPX	
3xFLAG-MCS-3xFLAG [Expression vector nQF]	AGU98855.1	NA	8	1,9668	1,8444	2,0131	1	1,5424	1543
MGPX [Homo sapiens]	NP_036359.3	MGPX	57	1,4008	0	0	11	0,7526	
60 kDa heat shock protein, mitochondrial [Homo sapiens]	NP_855472.1	HSPD1	61	1,0633	1,385	1,2512	8	0,7837	
Cluster of actin, cytoplasmic 1 [Homo sapiens] [NP_001092.1]	NP_001092.1 [8]	ACTB	42	0,9897	0,3284	0,3051	2	1,3332	
annexin A2 isoform 1 [Homo sapiens]	NP_001002858.1 (+1)	ANXA2	40	0,9308	0,7785	0,8597	12	0,7231	
49S ribosomal protein S3 isoform 1 [Homo sapiens]	NP_001243731.1	RPS3	27	0,9082	0,1846	0,2202	49	0,3863	
49S ribosomal protein S14 [Homo sapiens]	NP_001020242.1	RPS14	16	0,8616	0,203	0,2768	182	0	
49S ribosomal protein L12 [Homo sapiens]	NP_000867.1	RPL12	18	0,8501	0,3962	0,2025	78	0,2837	
Cluster of 60S acidic ribosomal protein P2 [Homo sapiens] [NP_000905.1]	NP_000905.1 [2]	RPLP2	12	0,8179	0,6775	0,5989	23	0,6757	
Cluster of polyadenylate-binding protein 1 [Homo sapiens] [NP_002559.2]	NP_002559.2 [7]	PABPC1	71	10	0,7468	0	0,191	39	0,4578
49S ribosomal protein S19 isoform 1 [Homo sapiens]	NP_001308413.1	RPS19	16	11	0,7144	0	0,2768	183	0
Cluster of Y-box-binding protein 1 [Homo sapiens] [NP_004550.2]	NP_004550.2 [7]	YBX1	36	12	0,7109	0	0	184	0
Cluster of tRNA (adenine(58)-N(1))-methyltransferase, mitochondrial isoform X1 [Homo sapiens] [XP_005264450.1]	XP_005264450.1 [2]	TRMT61B	52	13	0,6706	0	0	185	0
28S ribosomal protein S22, mitochondrial isoform 2 [Homo sapiens]	NP_001350786.1 (+2)	MRPS22	37	51	0,2605	0	0,1103	203	0
28S ribosomal protein S27, mitochondrial isoform 1 [Homo sapiens]	NP_002940.2	MRPL12	21	80	0,1587	0	0	33	0,4923
38S ribosomal protein L12, mitochondrial isoform 1 [Homo sapiens]	NP_001273877.1 (+1)	MRPS27	49	138	0,0508	0	0,0857	155	0,0884
38S ribosomal protein L11, mitochondrial isoform a [Homo sapiens]	NP_067134.1	MRPL11	21	179	0	0	0	10	0,7589
38S ribosomal protein L24, mitochondrial isoform X1 [Homo sapiens]	XP_011508284.1	MRPL24	25	180	0	0	0	14	0,6776
38S ribosomal protein L1, mitochondrial precursor [Homo sapiens]	NP_064621.3	MRPL1	37	184	0	0	0	32	0,5108
38S ribosomal protein L38, mitochondrial isoform a [Homo sapiens]	NP_059142.3 (+1)	MRPL38	39	186	0	0	0	35	0,4749
38S ribosomal protein L28, mitochondrial isoform X1 [Homo sapiens]	XP_011520563.1	MRPL28	30	194	0	0	0	41	0,4538
38S ribosomal protein L19, mitochondrial isoform 1 [Homo sapiens]	NP_055578.2	MRPL19	34	199	0	0	0	48	0,3916
38S ribosomal protein L50, mitochondrial isoform 1 [Homo sapiens]	NP_061924.1	MRPL50	18	200	0	0	0	58	0,3481
38S ribosomal protein L49, mitochondrial isoform a [Homo sapiens]	NP_004918.1	MRPL49	19	201	0	0	0	60	0,3353
38S ribosomal protein L47, mitochondrial isoform a [Homo sapiens]	NP_065142.2	MRPL47	29	207	0	0	0	62	0,3312
38S ribosomal protein L4, mitochondrial isoform a [Homo sapiens]	NP_057040.2 (+2)	MRPL4	35	208	0	0	0	68	0,3234
38S ribosomal protein L45, mitochondrial isoform 1 [Homo sapiens]	NP_115727.5	MRPL45	35	212	0	0	0	77	0,2896
38S ribosomal protein L43, mitochondrial isoform X2 [Homo sapiens]	XP_008718098.1 (+1)	MRPL43	18	223	0	0	0	80	0,2837
38S ribosomal protein L13, mitochondrial isoform 1 [Homo sapiens]	NP_054797.2	MRPL13	21	224	0	0	0	88	0,2528
28S ribosomal protein S23, mitochondrial isoform 1 [Homo sapiens]	NP_057154.2	MRPS23	22	226	0	0	0	90	0,244
38S ribosomal protein L9, mitochondrial isoform 1 [Homo sapiens]	NP_113508.1	MRPL9	30	227	0	0	0	91	0,2369
38S ribosomal protein L46, mitochondrial isoform 1 [Homo sapiens]	NP_071446.2	MRPL46	32	229	0	0	0	96	0,2282
38S ribosomal protein L27, mitochondrial isoform 1 [Homo sapiens]	NP_057588.1	MRPL27	16	269	0	0	0	97	0,2282
38S ribosomal protein L15, mitochondrial isoform 1 [Homo sapiens]	NP_054894.1	MRPL15	33	271	0	0	0	98	0,2228
28S ribosomal protein S7, mitochondrial isoform 1 [Homo sapiens]	NP_057055.2	MRPS7	28	273	0	0	0	105	0,2021
38S ribosomal protein L44, mitochondrial isoform b [Homo sapiens]	NP_075066.1 (+1)	MRPL44	38	275	0	0	0	107	0,1992
38S ribosomal protein L55, mitochondrial isoform 1 [Homo sapiens]	NP_852127.2 (+1)	MRPL55	19	278	0	0	0	108	0,1992
38S ribosomal protein L14, mitochondrial isoform c [Homo sapiens]	NP_001305699.1	MRPL14	22	278	0	0	0	122	0,1769
38S ribosomal protein L38, mitochondrial precursor [Homo sapiens]	NP_115867.2	MRPL38	45	282	0	0	0	124	0,1736
38S ribosomal protein L3, mitochondrial isoform 1 [Homo sapiens]	NP_009139.1	MRPL3	39	300	0	0	0	129	0,1539
Cluster of 38S ribosomal protein L37, mitochondrial isoform 2 [Homo sapiens] [NP_057575.2]	NP_057575.2 [2]	MRPL37	48	235	0	0	0	137	0,1289